International Scientific-Technical and Production Journal

The Paton WELDING JOURNAL

March
2007
3

English translation of the monthly «Avtomaticheskaya Svarka» (Automatic Welding) journal published in Russian since 1948

Founders: *E.O. Paton Electric Welding Institute of the NAS of Ukraine*
International Association «Welding»

Publisher: *International Association «Welding»*

Address:
E.O. Paton Electric Welding Institute,
International Association «Welding»,
11, Bozhenko str., 03680, Kyiv, Ukraine
Tel.: (38044) 287 67 57
Fax: (38044) 528 04 86
E-mail: journal@paton.kiev.ua
http://www.nas.gov.ua/pwj

State Registration Certificate
KV 4790 of 09.01.2001

Subscriptions:
$324, 12 issues per year,
postage and packaging included.
Back issues available.

CONTENTS

INFLUENCE OF THE WIDTH OF STAINLESS STEEL INSERT ON PERFORMANCE OF JOINTS OF RAILWAY FROGS WITH RAIL ENDS

S.I. KUCHUK-YATSENKO[1], **Yu.V. SHVETS**[1], **A.V. KAVUNICHENKO**[1], **V.I. SHVETS**[1], **S.D. TARANENKO**[2] and **V.A. PROSHCHENKO**[2]
[1]E.O.Paton Electric Welding Institute, NASU, Kiev, Ukraine
[2]OJSC «Dnepropetrovsky Strelochny Zavod», Dnepropetrovsk, Ukraine

Determined is the effect of the width of an insert of stainless steel 08Kh18N10T in pulsed flash-butt welding of steel 110G13L to M76 on the structural strength and wear resistance of the joints. It is shown that variation of insert width in the range from 10 to 40 mm hardly has any effect on performance of railway frogs.

K e y w o r d s : flash-butt welding, pulsed flashing, high-manganese steel, rail steel, austenitic steel, insert width

PWI developed the technology and equipment for resistance flash-butt welding of railway frogs. Reference [1] sets forth the main principles of this technology and establishes the welding mode parameters. The technology is based on the process of pulsed flash-butt welding [2], which allows producing joints of high-manganese steel 110G13L (GOST 7432--87) with rail steel M76 (GOST 8161--75) through an insert from chromium-nickel austenitic steel (GOST 5632--72).

Technology of pulsed flash-butt welding developed at PWI, and K924 welding machine made at OJSC «Kakhovka Plant of Electric Welding Equipment», were successfully introduced in OJSC «Dnepropetrovsky Strelochny Zavod» plant.

Experience of operation of welded frogs in the railways of Ukraine showed that the width of the austenitic insert should be optimized to reduce metal consumption. The purpose of this study was to determine the influence of insert width on structural strength (in particular, wear resistance) of butt joints and frog performance.

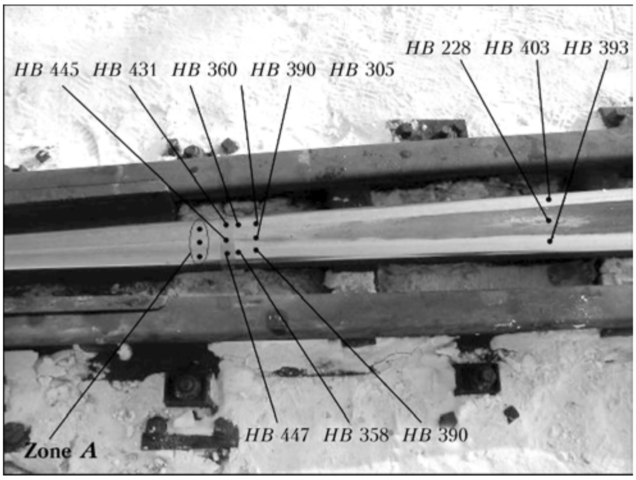

Figure 1. Appearance of a welded frog laid at Verkhovtsevo station of Pridneprovsky Railway, and results of hardness measurement on the rolling surface after passage of 65.2 mln t of traffic

When selecting the optimum width of the insert, it is necessary to take into account its increased wear, as of the softest element of the frog, influence of repeated heating on structural changes in the HAZ metal of the first weld in welding of the second weld, and influence of insert ductility on the joint properties.

To determine the influence of the insert width welded frogs of different types were studied, which differed by the quantity of transported tonnage. Frogs were made at OJSC «Dnepropetrovsky Strelochny Zavod», and were under the field supervision of the plant.

Wear level was evaluated by deviation from linearity on the rolling surface in the insert zone (depression), and degree of metal work hardening –– by the value of its hardness. Hardness measurement was performed by TDM-2 hardness meter with upper measurement level of *HB* 450. Indents were made on the insert in its center, on the rail end at the distance of 8, 50 and 550 mm from the rail–insert weld and 50 mm distance from the core--insert weld.

Figure 1 shows the indent locations and averaged results of five hardness measurements. It is seen from the Figure that hardness of zone *A* of the core is higher than *HB* 450.

The Table gives the results of measurement of frog wear in the insert zone, conducted on three frogs, laid in different sections of Pridneprovsky Railway, as well as average hardness values in the insert center. As is seen from the Table, maximum deviation of the rolling surface profile from the initial condition (wear) was equal to 0.5–0.8 mm at not more than 100 mm width of the depression. No local wear in the insert zone was observed.

Comparative analysis of hardness distribution in the frog showed (Figure 2) an increase of hardness of both the manganese and rail steel and chromium-nickel steel from which the insert is made during operation. In this case the insert hardness is higher than that of rail steel.

Obtained results are in agreement with published data [3]. Chromium-nickel austenitic steel is prone to

Frog wear in the insert zone

Track section of Pridneprovsky Railway	Passed tonnage, mln t	Insert width, mm	Frog wear (depression), mm	*HB* hardness in the insert center
Verkhovtsevo st.	65.20	18--22	0.75	441
Varvarovka st.	48.37	40--42	0.80	420
Samojlovka st.	48.57	18--20	0.50	410

deformation strengthening similar to manganese austenitic steels, although strengthening of the latter is more intensive at the same degree of deformation.

Frog wear in the insert zone is attributable to different degrees of initial deformation, required for work hardening at the start of operation in rail steel M76, chromium-nickel austenitic steel 08Kh18N10T and high-manganese steel 110G13L.

The above-said leads to the conclusion that the insert width of 10–40 mm is not critical in terms of increased wear of the welded frog. Insert width can influence the HAZ metal structure of the first weld at reheating which occurs when the second weld is made.

For welding of frog cores to rail ends using the insert, it is very important to select the most favourable welding sequence.

Two variants are possible, namely the first consists in welding an insert to the high-manganese core (first butt joint), the insert being cut to the required length and welding the rail end to it (second butt joint); the second is welding the insert to the rail end (first butt joint), cutting the insert to the required length, and welding the core to it (second butt joint).

In the first variant at insert width of 10--25 mm the metal of the HAZ of 110G13L steel butt joint is reheated to 500–700 °C, this leading to additional carbide formation, and, consequently, to lowering of the joint ductile properties [4].

Making the welds by the second variant is more favourable, as it is known that reheating of rail steel to 700–900 °C does not have any adverse influence on its sorbite structure.

At mechanical testing of welded items by static bending, their fracture runs in the rail steel at 2--3 mm distance from the joint line at strength values exceeding the requirements of standards [5].

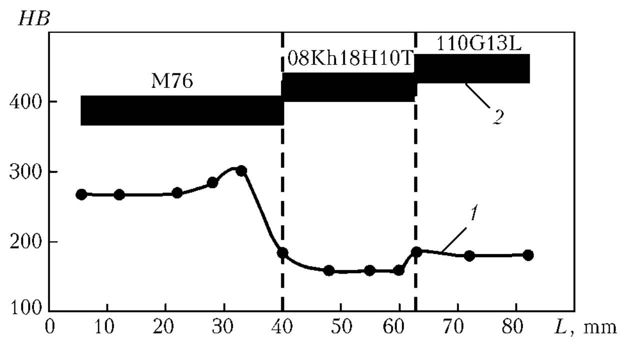

Figure 2. Hardness distribution in a welded frog after welding (*1*) and in operation (*2*)

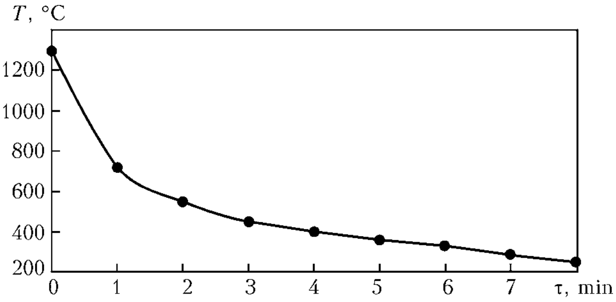

Figure 3. Experimental temperature curve of ISC zone cooling obtained after making the first weld

Microstructural studies of the joints showed that in the near-contact layer of rail steel, having a sorbite structure, a light-coloured structural component forms between the grain blocks, namely the interblock structural component (ISC). This is austenite, sometimes with martensite inclusions [6]. Joint fracture runs through ISC.

Carbon content in ISC is equal to 0.978–1.193, manganese –– 1.125--1.389, nickel — 1.774–2.047, chromium — 2.631–5.277 wt.%. As is known, steels of such a composition are quenched in oil and even in air, while remaining austenitic [7]. In the case of tempering at the temperature of 400–600 °C carbides can precipitate in metastable austenite.

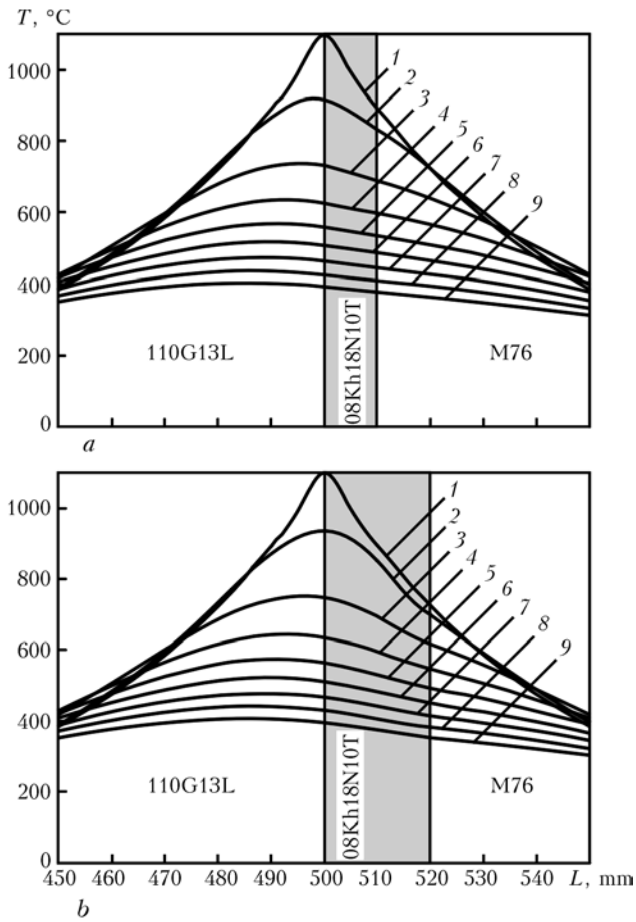

Figure 4. Calculated temperature fields produced at cooling of welded joint after making the second butt weld at insert width of 10 (*a*) and 20 (*b*) mm: *1* — τ = 0; *2* — 10; *3* — 50; *4* — 100; *5* — 150; *6* — 200; *7* — 250; *8* — 300; *9* — 350 s

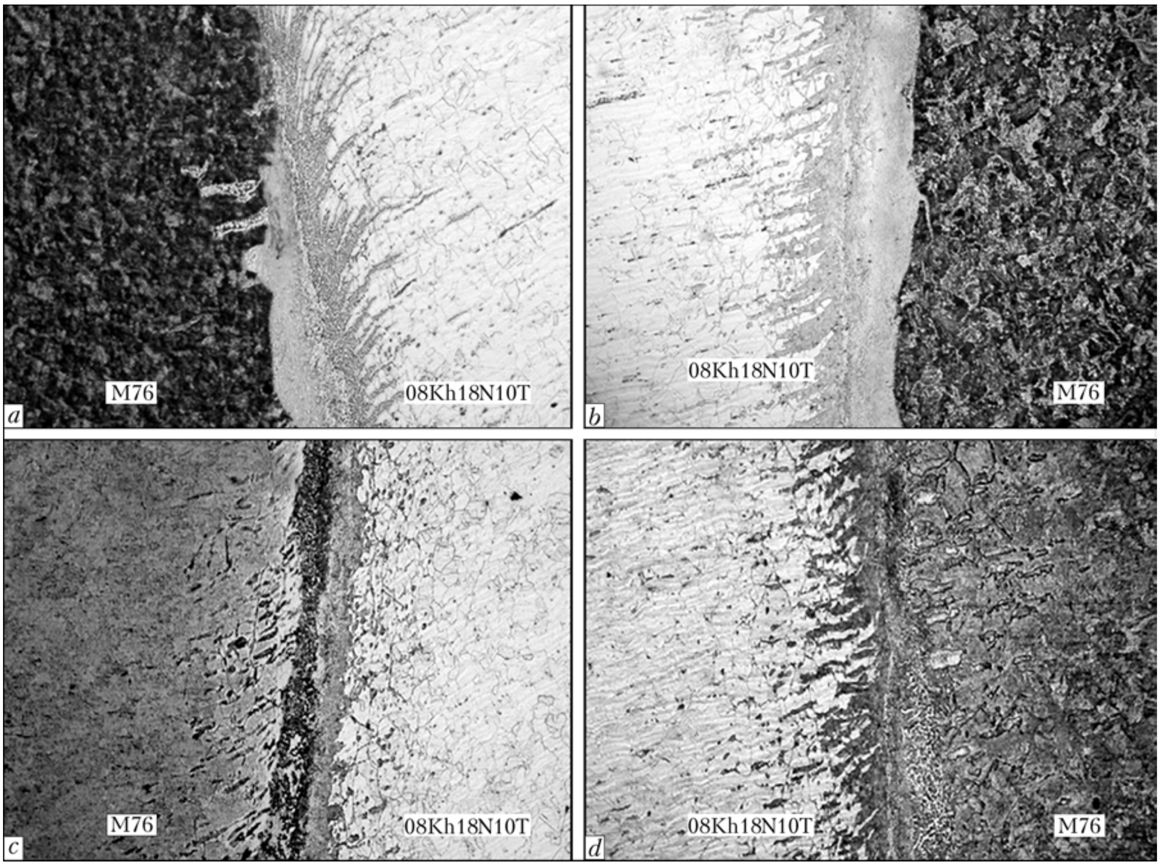

Figure 5. Microstructure of the transition zone metal of the first (*a, c*) and second (*b, d*) butt weld of M76 + 08Kh18N10T + M76 joint produced at insert width of 10--12 (*a, b*) and 20--22 (*c, d*) mm (×50)

According to calculations by an empirical formula given in [7], the cooling rate of this item in air is equal to 0.3 and in oil — to 3.0 °C / s.

In keeping with the experimental curve derived by us (Figure 3), the cooling rate in the zone with ISC in the temperature range of 1250–550 °C is equal to approximately 6 °C / s. At such a cooling rate ISC quenching with formation of metastable austenite should take place [8].

Time of ISC staying in the carbide precipitation range was equal to 2–3 min. This is insufficient for subsequent development of the carbide formation process, which was confirmed by the result of microstructural analysis.

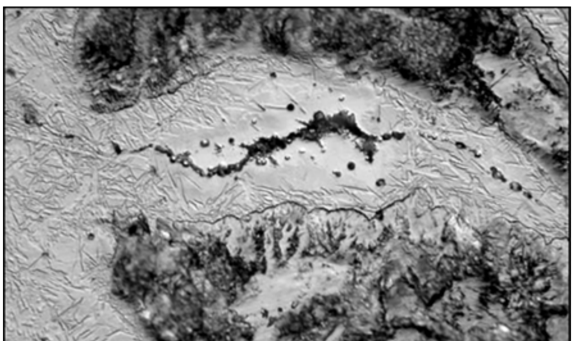

Figure 6. Carbide precipitations in ISC of the first butt weld of M76 steel joint after reheating (×1000)

To study the possible structural transformation in ISC at reheating PWI used the method of mathematical simulation to calculate the temperature fields present at cooling of the welded joint after welding the second butt joint (Figure 4) [9]. It is established that the time of the ISC zone staying in the temperature range of carbide formation with insert of 10 and 20 mm width is practically the same, and is $\tau \approx 200$ s. This gives rise to the assumption that reheating at insert width of 10–20 mm does not influence the structure of ISC metal.

Experimental studies of the influence of insert width on structural transformations at reheating were

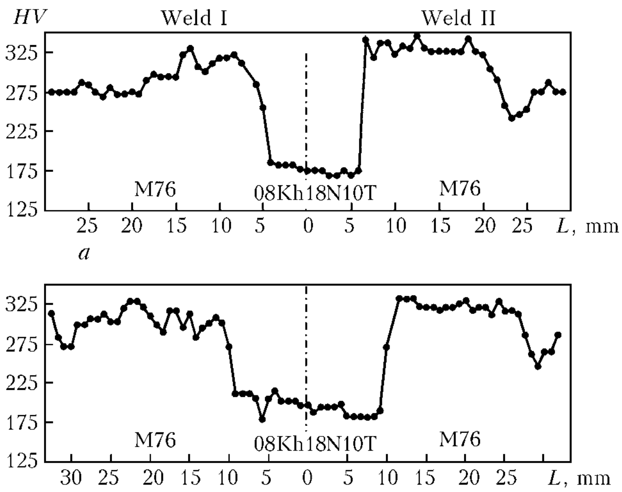

Figure 7. Hardness distribution in M76 + 08Kh18N10T + M76 welded joint produced at insert width of 10–12 (*a*) and 20–22 (*b*) mm

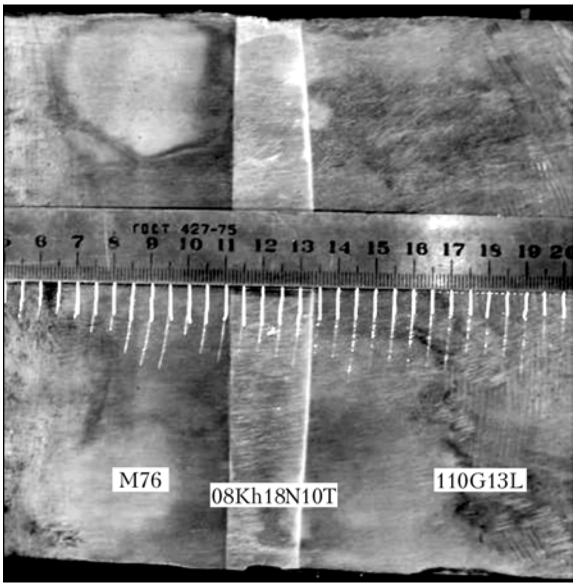

Figure 8. Appearance of a welded sample before testing for static bending

also conducted. For this purpose welded samples of M76 + 08Kh18N10T + M76 type with insert width of 10–12 and 20–22 mm were prepared. It is established that the metal microstructure in the transition zones of the first and second butt joints of steels M76 and 08Kh18N10T is similar and independent on the insert width in the established ranges (Figure 5). A slight precipitation of carbides was observed in the metal microstructure of the ISC zone of the first butt joint subjected to reheating (Figure 6).

Vickers hardness distribution in the welded joint at insert width of 10–12 mm is shown in Figure 7. A slight increase of insert hardness is observed (from *HV* 175 to 185 in the first case, and from *HV* 185 to 210, in the second case), as well as a certain non-uniformity of hardness distribution in steel M76, which has a tendency for lowering after reheating.

Thus, reheating of M76 + 08Kh18N10T joint in welding of the second butt joint through an insert of 10–22 mm width does not have any significant influence on the structure of the joint metal.

A sample with an insert of 10–13 mm width was welded to study the distribution of the degree of plastic deformation in the joint zone at testing for static bending. Marks were made on its toe (R65 profile) approximately every 5 mm before testing (Figure 8).

Testing was conducted in keeping with the requirements described in [5], at loading of the sample head. The sample was brought to fracture and by the photos taken using the tool measuring microscope, the distance between the marks was measured before and after fracture. The degree of plastic deformation was determined as the ratio of the difference to the initial mark spacing.

Figure 9 shows the distribution of plastic deformation along the sample length after its fracture at loading in the insert center at the breaking force of 1180 kN and deflection of 26 mm.

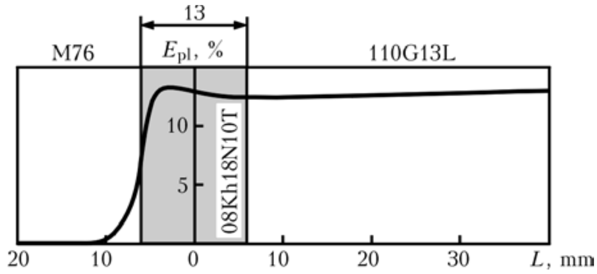

Figure 9. Distribution of relative plastic deformation E_{pl} along the sample length after its fracture at loading in the center of 10–13 mm wide insert

At sample testing for static bending it was found that the deflection due to elastic deformations is equal to not less than 11 mm at the breaking force of 900 kN (R65 profile), higher deflection values are found due to plastic deformation running mainly in the high-manganese steel, and the insert width does not have any essential influence on the welded joint ductility.

CONCLUSIONS

1. Conducted studies showed that work hardening of 08Kh18N10T steel insert, 110G13L steel core and rail end of M76 steel occurs during operation of welded railway frogs, the core and insert metal having a higher hardness than the metal of the rail end.
2. At static testing by bending change of the insert width within 10–40 mm does not have any essential influence on the item performance and welded joint ductility.
3. Item wear in the insert zone develops at the initial stage of operation, and practically does not increase afterwards.
4. Reducing insert width to 10 mm will allow reducing the cost of rolling 08Kh18N10T steel by 30 %, and thus lowering the cost of the item.
5. Application of an insert of less than 10 mm width is inadmissible. This is related to the fact that in welding the insert width changes around the rail perimeter because of non-uniform melting in different sections, and its actual width varies within ±3 mm of the calculated value.

1. Kuchuk-Yatsenko, S.I., Shvets, Yu.V., Dumchev, E.A. et al. (2005) Flash-butt welding of railway frogs with rail ends using an intermediate insert. *The Paton Welding J.*, **1**, 2–4.
2. Kuchuk-Yatsenko, S.I., Didkovsky, O.V., Bogorsky, M.V. et al. *Method of flash butt welding*. Pat. 46820 Ukraine. Publ. 17.06.2002.
3. Bogachev, I.N., Rozhkova, S.B. (1963) Strengthening of austenitic steels in cold plastic deformation. *Izvestiya Vuzov. Chyorn. Metallurgiya*, **7**, 162–168.
4. Davydov, N.G. (1979) *High-manganese steel*. Moscow: Metallurgiya.
5. *TU U 27.3-26524137-1342:2006*. Frogs and cores with welded rail ends of types P65, P50 UIC60. UkrDNTTs Energostal. Valid from 12.05.2006.
6. Kuchuk-Yatsenko, S.I., Shvets, V.I., Gordan, G.N. et al. (2006) Features of formation of structure of joints of rail steel M76 to steel 110G13L made by flash-butt welding. *The Paton Welding J.*, **1**, 2–8.
7. Blanter, M.E. (1984) *Theory of heat treatment*. Moscow: Metallurgiya.
8. Goudremont, E. (1969) *Special steels*. Moscow: Chyorn. i Tsvet. Metallurgiya.
9. Makhnenko, V.I. (1976) *Computational methods of investigation of kinetics of welding stresses and strains*. Kiev: Naukova Dumka.

ENERGY CONDITIONS OF EXPLOSION WELDING OF LAYERED COMPOSITE MATERIALS

V.A. CHUVICHILOV, S.V. KUZMIN and **V.I. LYSAK**
Volgograd State Technical University, Volgograd, Russia

Energy conditions of formation of joints in layered composite materials by explosion welding using stack and plane-parallel collision schemes are analysed. It is established that the stack cladding scheme is indicated in terms of cost and technology, starting from a certain thickness of target plate.

Keywords: explosion welding, composite materials, plane-parallel and stack welding schemes, energy conditions, formation of joint

Among a wide variety of the explosion welding process schemes [1–3], the widest acceptance for manufacture of three-layer composite materials of plane configuration has been received by the stack (with simultaneous two-sided symmetric cladding) (Figure 1) and plane-parallel (Figure 2) schemes of explosion welding.

Despite certain advantages of the stack scheme of welding, its application is limited by a number of factors associated, first of all, with the issue of energy conditions of formation of a joint, which remains unstudied until now.

The purpose of this study was to investigate energy conditions of formation of joints by explosion welding of metals using the stack and plane-parallel collision schemes.

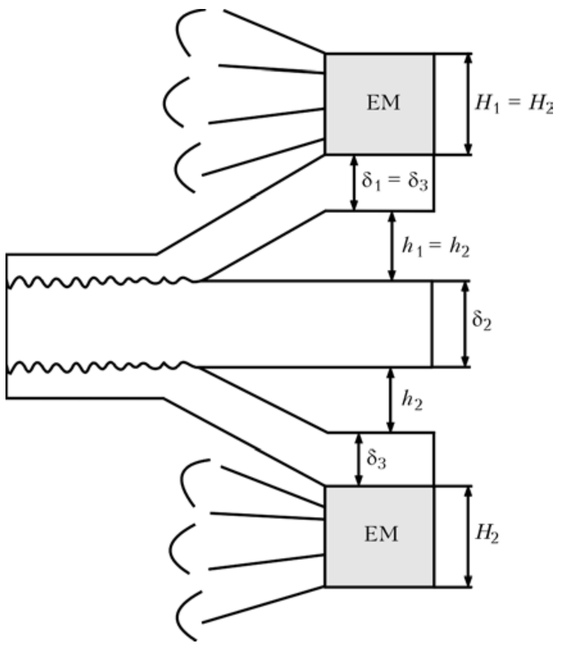

Figure 1. Stack scheme of explosion welding of layered composite materials [2]: EM — explosive material; H_1 and H_2 — heights of EM at the first and second interfaces of composite material; δ_1 and δ_3 — thickness of the flyer plates; δ_2 — thickness of the target plate; h_1 and h_2 — welding gaps at the first and second interfaces of composite material

Formal analysis of energy conditions of formation of joints by using different schemes of explosion welding (see Figures 1 and 2), but identical kinematic parameters of collision shows that in a general case the amount of specific kinetic energy W of a flyer plate at its collision with a target plate is consumed for the following items [4]:

$$W = W_1 + W_2 + W_3, \tag{1}$$

where W_1 is the specific residual kinetic energy of the system of the plates welded; W_2 and W_3 are the specific energies consumed, respectively, for plastic deformation of metal and cumulation.

In this case, W for both plane-parallel (superscript «p») and stack (superscript «s») (per interface of a joint) schemes of explosion welding is determined by mass and velocity of the flyer plate:

$$W^{\rm p} = W^{\rm s} = \frac{m_1 v_{\rm col}^2}{2}. \tag{2}$$

The energy consumed for plastic deformation of metal, $W_2^{\rm p}$, which determines final properties of a welded joint [5], can be calculated as follows, according to [4]:

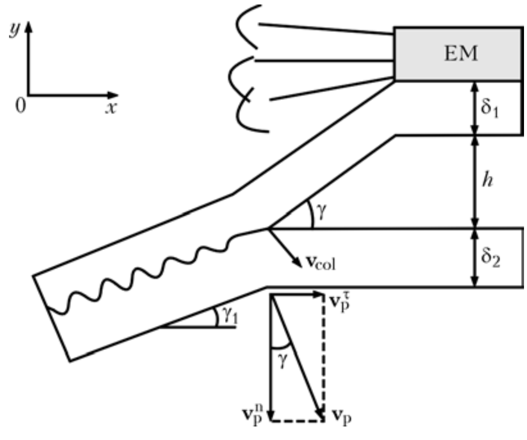

Figure 2. Typical pattern of collision using plane-parallel scheme of explosion welding [1]: $\mathbf{v}_{\rm p}$ — resultant vector of velocity of two-layer pack; $\mathbf{v}_{\rm p}^{\rm n}$ and $\mathbf{v}_{\rm p}^{\tau}$ — normal and tangential components of velocity vector $\mathbf{v}_{\rm p}$; $\mathbf{v}_{\rm col}$ — collision velocity vector; γ — collision angle; γ_1 — plate pack turning angle

$$W_2^p = \frac{m_1 m_2}{(m_1 + m_2)} \frac{v_{col}^2}{2} [1 - (v_{con}/c_0)^2], \quad (3)$$

$$W_3^p = W_3^s = \tilde{m} \frac{v_{col}^2}{2} \left(\frac{v_{con}}{c_0}\right)^2, \quad (4)$$

where $m_1 = \rho_1\delta_1$ and $m_2 = \rho_2\delta_2$ are the specific masses of the flyer and target plates, respectively; ρ_1 and ρ_2 are the densities of the metals welded; v_{col} is the collision velocity; v_{con} is the contact point velocity; $\tilde{m} = m_1 m_2 / (m_1 + m_2)$ is the averaged mass of two colliding plates; and c_0 is the velocity of sound in metal.

It follows from expression (1) that

$$W_2^p = W^p - W_1^p - W_3^p; \quad W_2^s = W^s - W_1^s - W_3^s. \quad (5)$$

It should be noted that during the explosion welding process using the plane-parallel scheme, after the flyer plate has collided with the target plate, the pack can go on moving at velocity v_p determined from the law of conservation of momentum, $\mathbf{v}_p = m_1\mathbf{v}_{col} / (m_1 + m_2)$ [6]. Expansion of resultant vector $\mathbf{v}_p$ into normal and tangential components, $\mathbf{v}_p^n$ and $\mathbf{v}_p^\tau$ (see Figure 2), yields

$$\mathbf{v}_p^n = \mathbf{v}_p \cos \gamma_1; \quad \mathbf{v}_p^\tau = \mathbf{v}_p \sin \gamma_1.$$

Given that collision angle γ in the majority of cases of explosion welding of metal is not in excess of 10–12°, it is evident that tangential component $\mathbf{v}_p^\tau$ is much lower than $\mathbf{v}_p^n$. Thus, ignoring $\mathbf{v}_p^\tau$ because of its low value (more so that $\gamma_1 << \gamma$), the following can be written down for the case of explosion welding using the plane-parallel scheme [4]:

$$W_1^p \approx \frac{m_1^2 v_p^{n2}}{2(m_1 + m_2)}. \quad (6)$$

In explosion welding using the stack scheme, the flyer pates collide with the target plate simultaneously and symmetrically on two sides. In this case, normal components $\mathbf{v}_{cool\ i}^n$ of vector $\mathbf{v}_{cool\ i}$ move strictly towards each other from opposite directions, thus preventing the three-layer pack from movement along axis y, which inevitably leads to $W_1^s \approx 0$.

Differences in energy conditions of formation of joints with the plane-parallel and stack schemes of explosion welding are illustrated in Figure 3. It can be seen from the Figure that in the latter case (stack scheme), independently of the ratio of δ_1 to δ_2, the energy consumed for plastic deformation (at identical collision parameters) exceeds W_2 with the plane-parallel scheme (to a higher degree at $\delta_1 > \delta_2$), which should inevitably lead to increase in parameters of the wave profile and mass of molten metal within the zone of a joint produced by explosion welding using the stack scheme.

The calorimetry method [7] was used to experimentally estimate energy W_2 consumed for plastic deformation of metal of the weld zone (WZ) in explosion welding using both schemes. The choice of this method is based on the fact that, as follows from [8], up to 90–95 % of the total energy consumed for plastic deformation of metal is released in welded specimens in the form of heat. We used the following expression [4] to determine the amount of heat Q introduced into a specimen during explosion welding:

$$Q = A(T_e - T_b) + m_{sp}c_{sp}(T_e - T_a), \quad (7)$$

where A is the water equivalent of the calorimeter, which is determined experimentally (it was 1.358 J / deg in our experiments); T_a, T_b and T_e are the temperature of a specimen before the experiment, equal to the temperature of ambient air and water at the beginning and end of the experiment, respectively; m_{sp} is the mass of the welded specimen; and c_{sp} is the specific heat of the specimen.

In the experiments conducted on similar aluminium plates AD0, the collision parameters were kept constant: v_{col} = 630 m / s and v_{con} = 2700 m / s. Thickness of the target plate, δ_2, was varied from an experiment to an experiment from 2 to 16 mm for both collision schemes. In the experiments the explosion and calorimetry systems were arranged separately from each other, the time of transportation of a specimen to the calorimeter being not more than 20 s, and water temperature measured with a mercurial thermometer at an accuracy of 0.1 °C being not in excess of 50 °C.

Figure 4 shows experimental dependencies $W_2 = f(\delta_2)$ derived for the stack and plane-parallel schemes of welding. To make their analysis more convenient, for the stack scheme the values of W_2 per interface were considered.

Analysis of the derived dependencies $W_2 = f(\delta_2)$ shows that at a relatively small value of thickness δ_2 there is a substantial difference in numerical values of energies $W_2^s / 2$ and W_2^p, which are realised, respectively, with the stack and plane-parallel welding schemes. For example, at δ_2 = 2 mm the value of $W_2^s / 2$ is almost two times as high as W_2^p (curves *1* and *2* in Figure 4). As δ_2 increases, the difference in the values of energies $W_2^s / 2$ and W_2^p decreases due to redistribution of W between the energy consumption items (see Figure 3, *a*) (with the plane-parallel scheme, according to dependence (6), component W_1 decreases), whereas at $\delta_2 \geq 10$ mm the values of W_2 become approximately equal to each other, i.e. starting from certain thickness $\delta_2 \geq \delta_{2cr}$ (δ_{2cr} is the critical thickness of the target plate), the value of which, as reported in [9], depends upon collision velocity v_{col},

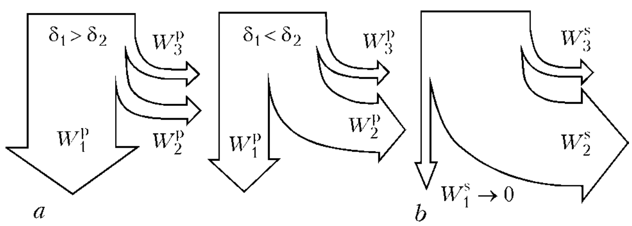

Figure 3. Structure of energy balances in explosion welding using plane-parallel (*a*) and stack (*b*) schemes

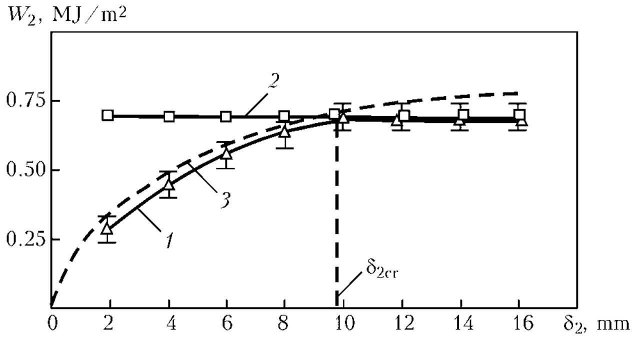

Figure 4. Dependence of W_2 on target plate thickness δ_2 in explosion welding of aluminium plates (δ_1 = 2 mm, v_{col} = 670 m/s, v_{con} = = 2700 m/s) using plane-parallel (Δ) and stack (❐) schemes: *1*, *2* — experimental curves $W_2^p/2 = f(\delta_2)$ and $W_2^s/2 = f(\delta_2)$, respectively; *3* — calculation curve $W_2^p = f(\delta_2)$

the energy conditions of formation of joints with both welding schemes under consideration become identical.

Apparently, at $\delta_2 < \delta_{2cr}$ the high values of energy W_2^s consumed for plastic deformation of the WZ metal in the case of stack welding scheme are attributable, according to [9], to increase in deformation pressure pulse I_{pr}, which is an integrated parameter that allows for the values of pressure within the collision zone and time of its effect. This value, being proportional to W_2, additionally activates the processes of plastic deformation of the WZ metal. Besides, the lower the δ_2 value, the higher is the value of plastic deformation pressure pulse I_{pr}, and the more intensive is the development of the processes of plastic deformation of the WZ metal.

Therefore, it can be considered proved that at $\delta_2 \geq$ $\geq \delta_{2cr}$ the energy and deformation-time conditions of formation of joints at both interfaces of the three-layer joint in explosion welding using the stack scheme are identical to those taking place with the plane-parallel scheme. The situation is different at $\delta_2 \leq \delta_{2cr}$. In this case, as shown by the experimental data (see Figure 4), energy W_2^s consumed for plastic deformation of the WZ metal using the stack scheme is higher than W_2^p, thus causing growth of the parameters of wave profiles and amount of molten metal (strength of the resulting joint decreases, and transient resistance increases). That is, properties of the joint produced by explosion welding using the stack scheme will differ from those of the joint produced by the traditional scheme.

To ensure identical conditions for formation of explosion welded joints using both schemes, it is necessary to decrease heat input at each interface of a composite material or decrease the deformation pulse on the interfaces when using the stack scheme, which can be achieved, at least, by two methods. The first method provides for the possibility of formation of a joint at each interface between the layers of a composite produced by the stack scheme, independently of each other. This requires increase in thickness of the target plate, $\delta_2 > \delta_{2cr}$, which is far from being always acceptable, as the values of δ_2 are usually strictly limited. The second method provides for a corresponding change in the conditions of collision of the flyer plates with the target one (e.g. decrease in collision velocity v_{col}).

Consider this variant by a specific example. In cladding of steel plate 2 mm thick with a copper layer 1 mm thick, the optimal value of W_2 providing a full-strength and defect-free weld is roughly 0.45–0.50 MJ/m^2. At a preset combination of thickness of the materials welded, this level of the energy consumed for plastic deformation can be achieved at $v_{col} \approx$ $\approx$ 470 m/s (for ammonite 6ZhV, H = 11 mm, h = = 1.5 mm). If we try to produce a three-layer composite under the same conditions by the stack scheme, energy input W_2 at each of its interfaces will be about 0.9 MJ/m^2, which is proved by the calorimetry results. Parameters of the wave profile will grow accordingly. Given that W_2 is in squared relationship with v_{col}, the values of the latter should be decreased, at least, approximately 1.4 times, i.e. to 330–340 m/s.

The values of v_{col} can be decreased also by two methods, i.e. by decreasing the height of the explosive charge, H, and keeping the size of the gap, h, at a constant level; or by decreasing h and keeping H unchanged.

As shown by the calculations, in the first variant the values of H should be decreased approximately to 7 mm, which is critical for ammonite 6ZhV [10], and in the second variant the values of h should be decreased to 0.5–0.7 mm, which is also unacceptable, as at such value of h (phase of intensive acceleration of the flyer plate) its insignificant accidental deviation from the calculated one to this side or the other will lead to a substantial change in v_{col} (the $h \pm 0.3$ deviation leads to a corresponding change of ±70 m/s in the value of calculated collision velocity v_{col}^{cal}), as well as to violation of the collision geometry, which causes focusing of the cumulative jet [11].

All this taken together may cause defects of both internal (local lacks of penetration, excessive amount of fusion, etc.) and external (burns-through, blue holes) character.

Therefore, as experimentally proved, in explosion welding using the stack and plane-parallel schemes the energy conditions of formation of metal joints will be substantially different, if thickness of the target plate is $\delta_2 < \delta_{2cr}$. For example, in explosion welding of similar aluminium plates (v_{col} = 630 m/s, v_{con} = = 2700 m/s) at target plate thickness δ_2 = 2 mm, energy W_2^s consumed for plastic deformation of the WZ metal by using the stack scheme of explosion welding is more than twice as high as the corresponding value of W_2^p by using the plane-parallel scheme. In this case, to produce a three-layer composite with symmetric cladding, the preferable scheme is that of successive cladding of the base metal using the traditional plane-parallel scheme. Starting from a certain thickness of the target plate ($\delta_2 \geq \delta_{2cr}$) the energy conditions of formation of joints become identical for both welding schemes considered. Therefore, to produce three-layer composite materials, the stack scheme is indicated in terms of cost and technology. If it is possible to increase thickness of the target plate to $\delta_2 \geq \delta_{2cr}$ followed by rolling of a composite to the required thickness, the preference in selection of the process scheme to produce three-layer composites should be given to the stack scheme of explosion welding.

1. Sedykh, V.S., Kazak, N.N. (1971) *Explosion welding and properties of welded joints*. Moscow: Mashinostroenie.
2. Lysak, V.I., Kuzmin, S.V. (2002) Classification of process schemes of explosion welding of metals. *Svarochn. Proizvodstvo*, **9**, 33–39.
3. Kobelev, A.G., Lysak, V.I., Chernyshov, V.N. et al. (2002) *Production of layered composites*. Moscow: Intermet Engineering.
4. Sedykh, V.S., Sonnov, A.P. (1970) Calculation of energy balance of explosion welding process. *Fizika i Khimiya Obrab. Materialov*, **2**, 6–13.
5. Sedykh, V.S. (1985) Classification, evaluation and relationship of main explosion welding parameters. In: *Transact. on Explosion Welding and Properties of Welded Joints*. Volgograd: VPI, 3–30.
6. Aleksandrov, E.V., Sokolinsky, V.B. (1969) *Applied theory and calculations of impact systems*. Moscow: Nauka.
7. (1971) *Laboratory works on welding*. Ed. by G.A. Nikolaev. Moscow: Vysshaya Shkola.
8. McLean, D. (1965) *Mechanical properties of metals*. Moscow: Metallurgiya.
9. Kuzmin, S.V., Chuvichilov, V.A., Lysak, V.I. (2005) Time conditions of formation of joint in explosion welding. *Perspektiv. Materialy*, **1**, 85–91.
10. Lysak, V.I., Trykov, Yu.P. (1984) *Detonation characteristics of explosives for processing of metals*. Volgograd: VPI.
11. Kriventsov, A.N., Sedykh, V.S., Baluev, A.V. et al. (1998) Peculiarities of explosion welding process in zones of technological bending of elements being welded. *Svarochn. Proizvodstvo*, **2**, 6–10.

STRUCTURE AND PROPERTIES OF POWDERS FOR PRODUCTION OF BIO-CERAMIC COATINGS BY THE PLASMA SPRAYING METHOD

Yu.S. BORISOV, A.L. BORISOVA, A.Yu. TUNIK, M.V. KARPETS, V.G. BOBRIK, S.G. VOJNAROVICH and **E.K. KUZMICH-YANCHUK**

E.O. Paton Electric Welding Institute, NASU, Kiev, Ukraine

Structure and properties of domestic and foreign hydroxyapatite powders were studied by the method of differential thermal analysis. Phase transformations occurring in the powders during heating in neutral environment were investigated. Applicability of the powders for deposition of coatings on medical-application parts by microplasma spraying was determined.

Keywords: bio-ceramic materials, hydroxyapatite powders, plasma spraying, coating

Bio-ceramic materials in the form of coatings on implants of titanium and stainless steel have received wide acceptance in medical practice in the last years. Hydroxyapatite (HAP) $Ca_{10}(PO_4)_6(OH)_2$ is most often applied as a material for deposition of such coatings, as it coincides in chemical composition with a mineral base of live bones. Interlayer of a bio-ceramic material provides strong bond between the bone tissues and implant material, and prevents formation of a soft fibrous interlayer that deteriorates the quality of fixation of an implant in living organism.

One of the methods for deposition of coatings of HAP or similar bio-ceramic materials is plasma spraying [1–6]. Parameters of initial powders are known to be a decisive factor in the technology of plasma spraying of coatings, including bio-ceramic ones. Conditions of formation of coatings are related primarily to the kinetic and thermal energy of spraying particles, i.e. to the stored energy they acquire in interaction with the plasma jet. The time of dwelling of the particles within the plasma jet zone is determined by their velocity, which in turn is a function of such properties of the particles as size, shape and density.

Phase and structural transformations changing composition and properties of the material that forms a coating may occur during the process of plasma spraying under the effect of heating with a high-temperature gas flow. The degree of this effect depends upon the spraying conditions and characteristics of a powder (size and shape of powder particles, thermal conductivity, etc.) [1].

The E.O. Paton Electric Welding Institute is active in deposition of bio-ceramic coatings using microplasma spraying. The use of argon instead of the $Ar + H_2$ mixture as a plasma gas allows the temperature gradient across the section of particles to be decreased, and risk of their overheating and decomposition of HAP to be avoided. In addition, the method of microplasma spraying, providing an insignificant size of the spraying spot (1–5 mm), allows deposition of coatings on small-size parts, as well as saving of a consumable [7, 8].

Such a property of powders as flowability, which determines the possibility and stability of feeding them to the plasma jet due to their own weight without the use of a transportation gas, is of a special significance under microplasma spraying conditions.

To compare HAP powders from different manufacturers, the investigations described in this article

Table 1. Comparative content of hard metal impurities in HAP powders

Metal	Requirements of ASTM F1185–88, ppm	Synthesised HAP powders, ppm
Arsenic	3	2.00
Cadmium	5	< 0.02
Mercury	5	< 0.15
Lead	30	< 0.45
Total of hard metals	50	< 4.00

were conducted to study their properties, which may be important for the conditions of microplasma spraying of coatings (pycnometric and apparent density, flowability), and examine morphology and microstructure of particles of the powders, their phase composition and behaviour in heating.

Four types of powders manufactured by the «Technimed» (France), KAM (the Netherlands), «Kergap» (Ukraine) and «Tomita» (Japan) companies were investigated. The investigations were carried out by the methods of scanning electron microscopy, metallography, X-ray phase analysis (XPA), X-ray microanalysis (XMA) and differential thermal analysis (DTA), as well as by the standard procedures for evaluation of technological properties of the powders (pycnometric and apparent density, flowability).

Properties and structure of the HAP powders depend in many respects upon the methods used to produce them. The key methods among them are the liquid-phase ones, as well as solid-phase and hydrothermal synthesis, each having advantages and drawbacks.

Requirements imposed on medical-application HAP powders are best met by using the method of liquid-phase chemical synthesis, which is implemented through interaction of soluble salts in alkaline environment. Powders produced by chemical deposition have a large surface area and consist of particles with homogeneous chemical and phase composition, and with regulated sizes (starting from micrometer units). Chemical purity of synthesised HAP is much superior to that of the reagents employed. Moreover, this eliminates the use of numerous mechanical operations leading to contamination of a synthesised material [9–11].

The domestic HAP powder investigated in this study was produced by the Kergap Company using the technology covered by the patent of Ukraine, which is based on the targeted utilisation of the powder, i.e. microplasma spraying of coatings on medical-application parts (metal implants). The method for production of this powder comprises synthesis of HAP by chemical deposition of calcium nitrate and ammonium hydrophosphate from aqueous solutions, ageing, washing, separation and drying of the formed deposit followed by its crushing, spinning, separation of fine particles and baking [12].

Foreign powders (except for those produced by Technimed) after synthesis by chemical deposition are subjected to extra treatment, i.e. agglomeration of the deposit by atomisation drying or plasma spheroidisation.

According to certificates, all the powders investigated meet requirements of standard ASTM F1185–88 as to the content of hard metal impurities (Table 1). Appearance and microstructure of the HAP powder particles are shown in Figure 1, results of DTA are shown in Figure 2, and technological properties and phase composition are given in Tables 2 and 3.

Particles of the Technimed HAP powder have a fragmented shape, and their sizes substantially differ along the axes (Figure 1, *a*, *b*). The particles can be subdivided into two groups as to their sizes: with d_p = = 30–50 and 50–80 μm. Powders with d_p = 50–80 μm are characterised by flowability of 120–124 s / 50 g, have apparent density of 1.07 g / cm^3 and pycnometric density of their particles equal to 2.99 g / cm^3 (Table 2). Powders with finer particles (30–50 μm) do not differ in flowability and are prone to formation of lumps. Their microhardness is *HV* 0.02 (5.20 ± ± 0.10) GPa.

The Tomita HAP powder consists of particles of a spherical shape, which are conglomerates of finer particles (Figure 1, *c*, *d*). Most of its particles are 10–40 μm in size, the content of particles with d_p ≤ ≤ 5 μm is no more than 10 %, and their pycnometric density is 3.08 g / cm^3. Structure of such particles is loose and weak. They fracture in attempts made to measure microhardness.

The Kergap HAP powder, like the Tomita one, consists mostly of particles of a fragmented shape (Figure 1, *e*, *f*). However, the spinning operation leads to smoothing of angles of many particles, which pro-

Table 2. Characteristics of HAP powders produced by different methods

Manufacturing company	d_p, μm	Flowability, s / 50 g (GOST 20899–75)	Apparent density, g / cm^3 (GOST 19440–74)	Pycnometric density, g / cm^3	*HV* 0.02, GPa	Ñà / Ð, at.%
Technimed	30–50	No flow	0.95 ± 0.001	2.98	5.20 ± 0.10	1.67
	50–80	120–124	1.07 ± 0.001	2.99		1.67
Tomita	≤ 40	–	–	3.08	--	1.68
Kergap	63–80	70–80	–	–	5.40 ± 0.16	1.67
	≤ 63	68–75	1.30 ± 0.001	3.10		1.66
KAM	≤ 50	No flow	1.25 ± 0.001	3.20	5.00 ± 0.12	1.67

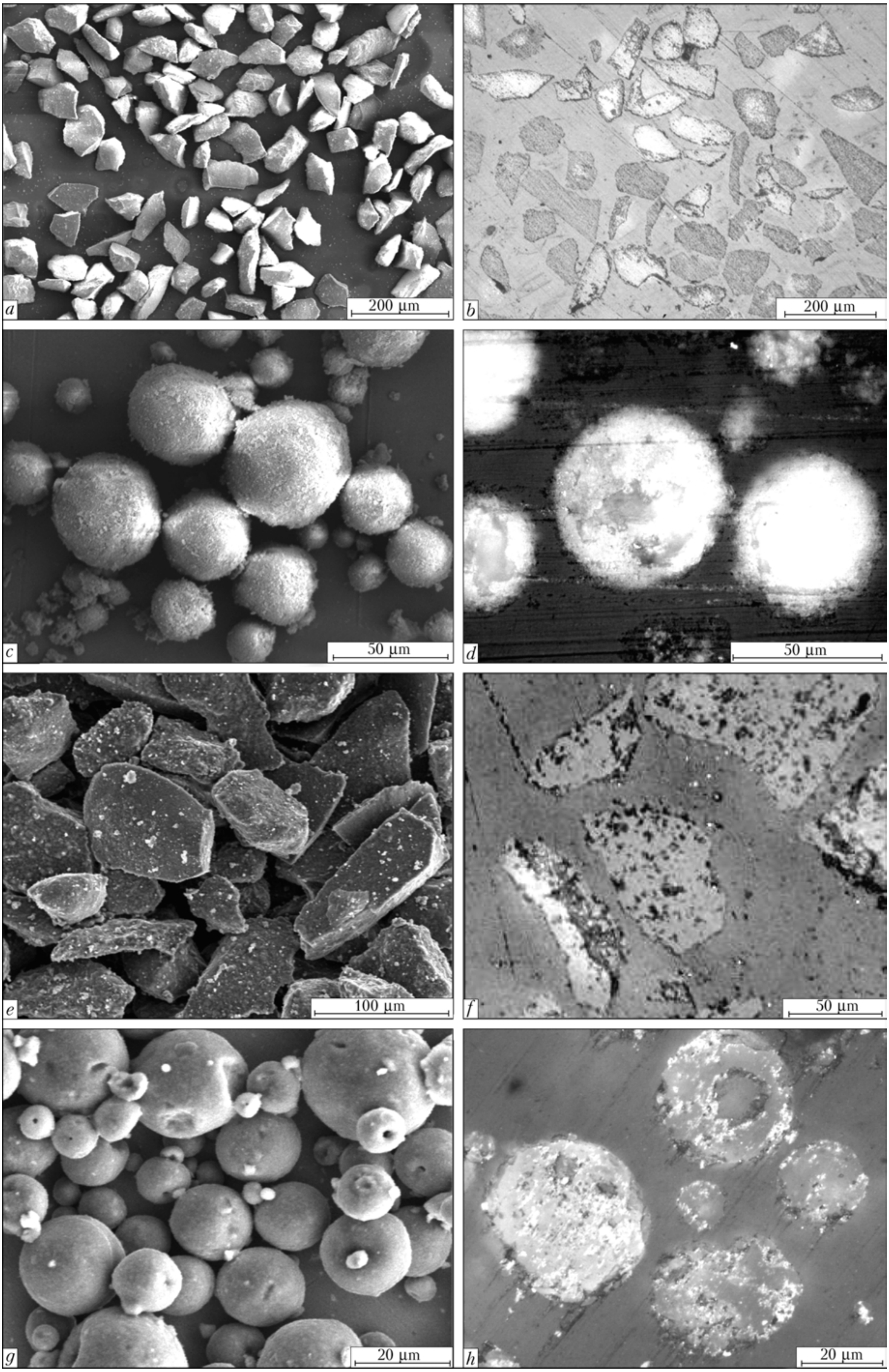

Figure 1. Appearance (*a, c, e, g*) and microstructure (*b, d, f, h*) of HAP powders produced by Technimed (d_p = 50–80 μm) (*a, b*), Tomita ($d_p \leq 40$ μm) (*c, d*), Kergap(d_p = 63–80 μm) (*e, f*) and KAM ($d_p \leq 50$ μm) (*g, h*)

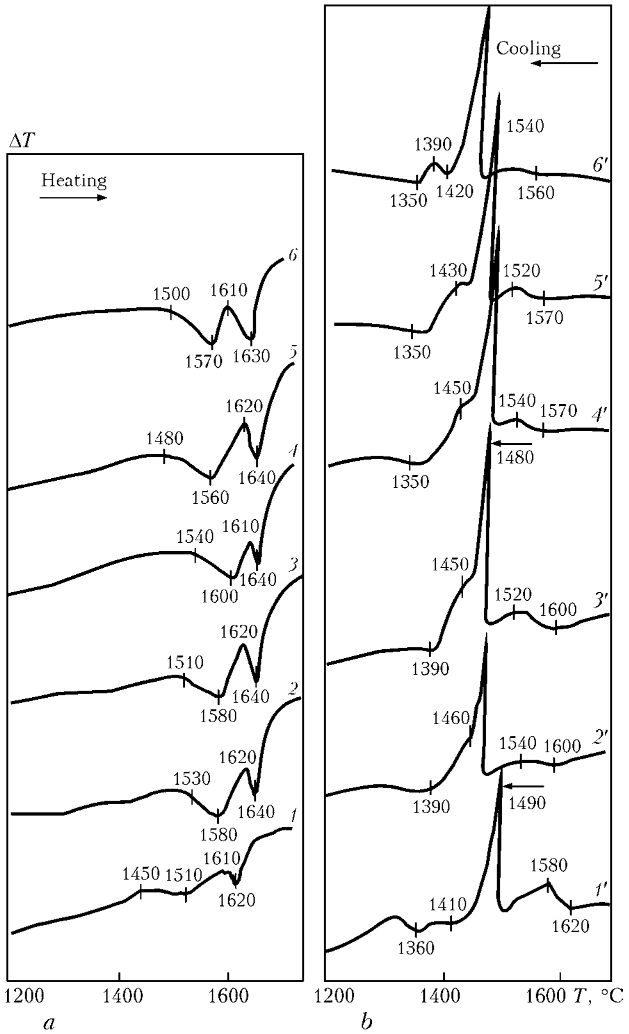

Figure 2. Differential thermal curves of heating (*a*) and cooling (*b*) of HAP powders produced by Tomita with $d_p \le 40$ μm (*1, 1′*), Kergap with $d_p = 63–80$ (*2, 2′*) and 63 μm (*3, 3′*), Technimed with $d_p = 50–80$ (*4, 4′*) and 30–50 μm (*5, 5′*), and KAM with $d_p \le 50$ μm (*6, 6′*)

vides increased flowability (68–75 s / 50 g) and apparent density (1.30 g / cm^3) (Table 2). Pycnometric density of the particles is 3.10 g / cm^3, and microhardness is *HV* 0.02 (5.40 ± 0.16) GPa.

The KAM HAP powder (Figure 1, *g*, *h*) consists of spherical particles with $d_p < 50$ μm. It does not flow; although, according to the certificate, its content of particles with $d_p < 15$ μm (which, as a rule, affects flowability) is low (≤ 10 %). At the same time, particles of this powder are characterised by the highest pycnometric density (3.20 g / cm^3), which is close to the theoretical density of HAP (3.219 g / cm^3). Apparent density of the KAM powder particles is 1.25 g / cm^3, and microhardness of its particles is (5.00 ± 0.12) GPa.

X-ray phase analysis was conducted in monochromatic CuK_α-radiation using diffractometer DRON-UM1. Graphite single crystal mounted on the diffracted beam was used as a monochromator. Diffraction patterns were taken by step scanning in an inter-

Table 3. Structure parameters and crystalline phase content of HAP powders

Manufacturing company	Lattice parameters		Cell volume *V*, nm^3	Content of crystalline phase $Ca_5(PO_4)_3OH$, wt.%
	à, nm	ñ, nm		
Technimed	0.9420	0.6880	0.5287	100
Tomita	0.9412	0.6875	0.5275	99
Kergap	0.9418	0.6881	0.5286	100
KAM	0.9409	0.6881	0.5251	100

Note. Coefficient of texture along crystallographic direction [001] *t* = 1.

val of angles 2θ = 10–120°. The scanning step was 0.05°, and time of exposure was 3–9 s. In addition to determination of phase composition (content of crystalline phase $Ca_5(PO_4)_3OH$ and its lattice parameters, as well as impurities of other crystalline and amorphous phases), analysis of the diffraction patterns allowed also detection of the presence of texture along different crystallographic directions*, which may affect the processes of resorption of HAP under conditions of a living organism [10].

Analysis of the data in Table 3 shows that all the specimens made from initial powders by the compaction method are not textured (*t* = 1), and are a single-phase crystalline product $Ca_5(PO_4)_3OH$. Traces of CaO (≤ 0.1 wt.%) were detected only in the powder produced by Tomita. Lattice parameters *a* and *c*, as well as volume *V* of the elementary cell of the HAP powders differ but insignificantly. At the same time, lattice parameters of the Kergap powder correspond to the highest degree to stoichiometric composition (*a* = 0.9418 nm, *c* = 0.6878 nm) at a content of Ca equal to 39.90 wt.%, P equal to 18.5 wt.%, and OH equal to 3.38 wt.% [13].

According to certificates, all the powders investigated meet requirements of standards ASTM F1185–88 as to the content of harmful impurities (not more than 50 ppm). According to the data of X-ray microanalysis, the Ca / P ratio was 1.68 (Tomita powders), 1.67 (Technimed powders), 1.66–1.67 (Kergap powders), and 1.67 at.% (KAM powders).

As shown by testing of flowability of the HAP powders under conditions of feeding them using a powder feeder that is a part of the microplasma system MPN-004, in the case of using a vibrator all the HAP powders, except for that supplied by KAM, were characterised by very stable feeding using the above powder feeder.

DTA was conducted to evaluate behaviour of the HAP powders in heating. Heating was performed in the atmosphere of helium under a pressure of 5 MPa, temperature of 20 to 1750 °C and rate of 80 °C / min. Results are shown in Figure 5. The character of dif-

*Texture along direction [001] was found to be formed in live bones.

ferential thermal curves for all the types of the powders investigated, except for the Tomita powder, was almost identical. Heating curves *2–6* (Figure 2) show two endothermic effects in close temperature ranges where they take place, and cooling curves *2′–6′* show the exothermic crystallisation effects with the following peaks: precipitation of CaO occurs at 1520–1540 °C, α-$Ca_3(PO_4)_2$ forms at 1480 °C, and β-$Ca_5(PO_4)_2$ forms at a temperature below 1460 °C. The DTA data on the Tomita powders (curves *1* and *1′* in Figure 2) differ to some extent from the above ones both in heating and in cooling, which suggests the presence of some peculiarities in structural-phase composition of this material. For example, the first endothermic effect in heating is considerably smoothed, and the second effect is less pronounced and shifted by 20 °C towards lower (1620 °C) temperatures. The exothermic effect is absent in the cooling curve at a temperature of 1460 °C. The DTA products of the HAP powders also differ in composition. In the first case they contain α-$Ca_3(PO_4)_2$ and β-$Ca_3(PO_4)_2$, and in the second case — α-$Ca_3(PO_4)_2$ only for the Tomita powder. Differences in these characteristics may affect structure and phase composition of spray coatings.

CONCLUSIONS

1. The technology developed by the «Kergap» Company for production of the HAP powders intended for microplasma spraying conditions provides increased flowability of 70–80 s / 50 g, which leads to stability of feeding of the powders using the MNP-004 system feeder.

2. Powders produced by the «Technimed», «Tomita», «Kergap» and KAM companies have a HAP content of not less than 99 % at Ca / P = 1.66–1.68 at.%, and a low content of harmful impurities, which meets requirements imposed on the composition of the HAP powders intended for production of bioceramic coatings.

3. Flowability of the Technimed powders (d_p = = 50–80) and Kergap powders (d_p = 63–80 and ≤ 63 μm) is 70–124 s / 50 g. The rest of the powders do not flow under the above conditions. Tests of the HAP powders when using the MPN-004 system powder feeder with vibration proved the possibility of applying them for microplasma spraying.

1. Khor, K.A., Cheang, P. (1994) Effect of powder feedstock on thermal sprayed hydroxyapatite coatings. In: *Proc. of 7th Nat. Thermal Spray Conf*. (Boston, USA, June 20–24, 1994), 147–152.
2. Gross, K.A., Berndt, C.C. (1998) Thermal processing of hydroxyapatite for coating production. *J. Biomed. Mater. Res.*, 39(**4**), 580–587.
3. Gross, K.A., Berndt, C.C., Herman, H.A. (1998) Amorphous phase formation in plasma-sprayed hydroxyapatite coating. *Ibid*., 39(**3**), 407–411.
4. Oh, K.T., Park, Y.S. (1998) Plasma-sprayed coating of hydroxyapatite on superaustenitic stainless steel. *Surface and Coatings Technology*, **110**, 4–12.
5. Kalita, V.I. (2000) Physics and chemistry of formation of bio-inert and bio-active surfaces on implants. *Fizika i Khimiya Obrab. Metallov*, **5**, 28–45.
6. Xue, W., Tao, S., Liu, X. et al. (2004) In vivo evaluation of plasma sprayed hydroxyapatite coating having different crystallinity. *Biomaterials*, **25**, 415–421.
7. Borisov, Yu.S., Vojnarovich, S.G., Bobrik, V.G. et al. (2000) Microplasma spraying of bio-ceramic coatings. *The Paton Welding J*., **12**, 62–66.
8. Borisov, Yu.S., Vojnarovich, S.G., Ulianchich, N.V. et al. (2002) Investigation of bio-ceramic coatings produced by microplasma spraying. *Ibid*., **9**, 4–6.
9. Cheang, P., Khor, K.A. (1995) Bioceramic powders and coatings by thermal spray techniques. In: *Proc. of ITSC'95* (Kobe, August 1995), Vol. 2, 181–186.
10. Kanazava, T. (1998) *Inorganic phosphate materials*. Kiev: Naukova Dumka.
11. LeGerous, R.Z., LeGerous, J.P. (1995) Calcium phosphate biomaterials: preparation, properties and biodegradation. In: *Encyclopedic handbook of biomaterials and bioengineering*, Vol. 2, 1429–1463.
12. Dubok, V.A., Ulianchich, N.V., Kryuchkov, Yu.M. et al. *Method for production of hydroxyapatite powder for plasma spraying*. Pat. 19491 UA. Int. Cl. A, C01 F 11 / 02; A 61 K 6 / 033. Publ. 23.12.93.
13. Shpak, A.P., Karbovsky, V.L., Trachevsky, V.V. (2002) *Apatites*. Kiev: Akademperiodika.

DESIGN WHILE INVENTING

A.A. MOZZHUKHIN
E.O. Paton Electric Welding Institute, NASU, Kiev, Ukraine

March, 2007 will mark the 90th anniversary of the birth of Vladimir Evgenievich Paton, Merited Inventor of Ukraine, prominent designer of welding equipment. The memory of this remarkable person retains the wonderful diversity of the traits of his character, which were a harmonious combination of professional talent and personal charm and a vivid manifestation of a range of interests outside his profession. Such a harmony is characteristic of extraordinary personalities, to which V.E. Paton certainly belongs.

A lot can be written about his contribution to development of welding equipment. government awards and state prizes, honorary titles and international recognition that he was granted. And quite a lot has already been written about it. But the main legacy of a teacher are his pupils. They are not always capable of taking the baton and carrying on his work in a fitting manner. Vladimir Paton was lucky in this respect, and today we are publishing the memoirs of one of his successors.

For the majority of colleagues, particularly for designers, directly contacting him at work, Vladimir Evgenievich Paton certainly set an example to follow. He had a unique combination of professional culture of a genuinely creative person with remarkable human charm. Those, who were lucky enough to interact with him beyond the scope of professional contacts, saw him as a great friend and idol. Hunting with his participation certainly left the most vivid, unforgettable memories. It was on these occasions that one could feel all his spontaneity and genuine friendliness mixed with caustic humour. This humour made everybody share the fun, and remained forever in the hearts of his comrades.

Yet the basis of our lives was cooperation in the professional sphere. His pioneering engineering solutions starting with single-motor TS-17 tractor, always provided guidance in the search for optimum designs. For me personally this example was the starting point in many of my developments.

So, I have set a challenge for myself — develop machines of an order of magnitude smaller weight and labour consumption in manufacturing compared to the known prototypes. One of such machines was OB1020 manipulator. At the start of 1960s I had to design a bench for TS-17 (suspended variant), which everybody liked calling overturned. Vladimir Paton liked the bench (Figure 1). Due to a rotary middle part it

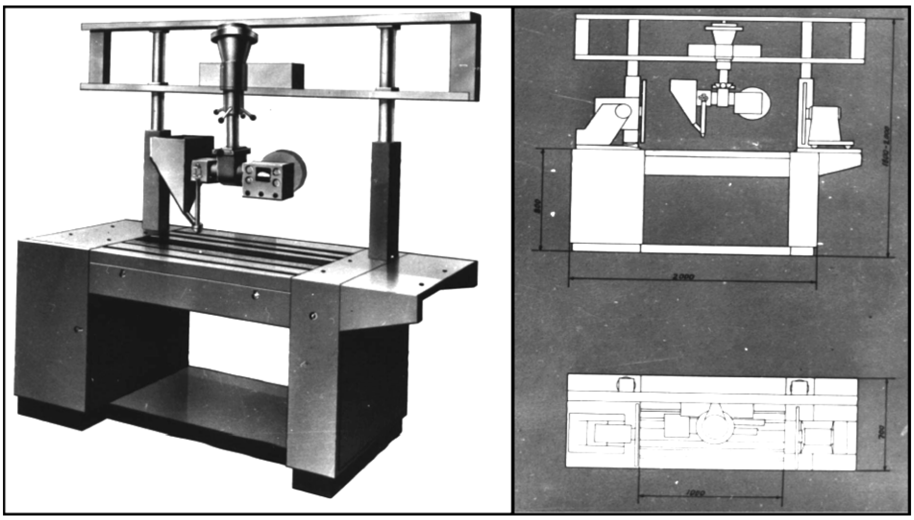

Figure 1. OB1003 facility for TS-17P tractor

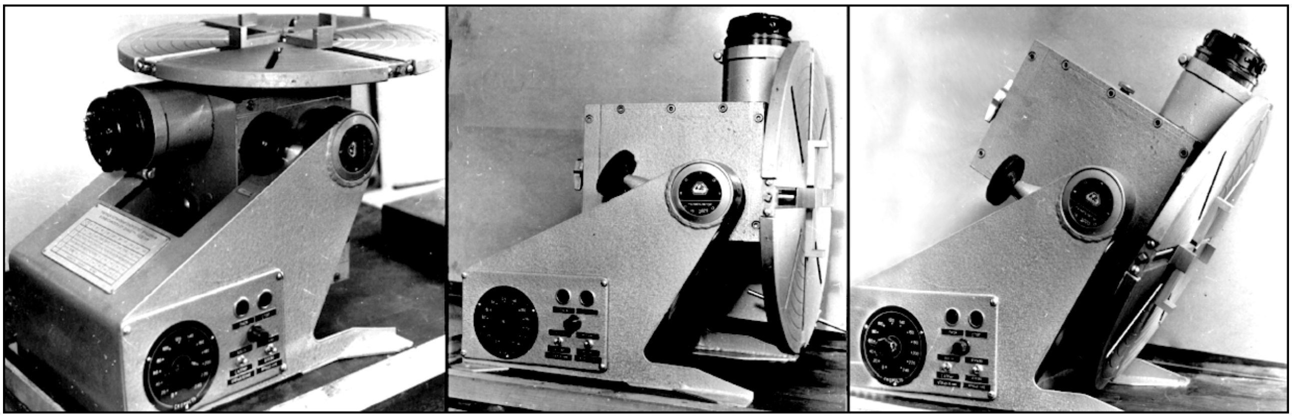

Figure 2. Bench-top manipulator OB1020

allowed «uphill-downhill» and «gravity» welding, but did not have any devices for welding of bodies of revolution. Then I had an idea to try and make a manipulator of 60 kg capacity (most often required) and also of 60 kg weight, so that it could be used as bench-top, and put away when not required. The weight of batch-produced manipulators of 60 kg capacity manufactured at that time, was 600 kg. Thorough calculation up to limit stresses, optimum design and assembly allowed making such a manipulator, which quickly found its advocates both at the institute and beyond it. Its special feature (Figure 2) was designing a four-speed transmission (without removable gears), which enabled welding circumferential welds in a broad range of speeds on diameters from 20 to 500 mm. It was possible to design a compact mechanism due to invention of an original device for speed changing and its manufacturing method. The manipulator was characterized by original design and appearance.

V.E. Paton was one of the first to continuously emphasize the need to develop aesthetically beautiful structures, making one conscious not only of the functional performance of the equipment, but also of its shape. This gave an impetus to searching for new solutions «without bolts or flanges, as in the previous century». And the machines changed, their appearance acquiring the features of machine architecture.

Beauty became a need that initiated formation of a new unit in the EDTB structure, namely the engineering aesthetics department. As in many of similar institutions established at that time, it mostly employed artists. But there were also professional designers among them, who were artists at heart, which, essentially, points to a connection between these two kinds of creativity. One of them was V.T. Mishel, a designer, who switched over to another profession — artistic design. Working with the architectural image of machines designed by other authors, he not only made them look beautiful, but at the same time improved their design and functional properties. And the developers always gratefully accepted the interesting solutions suggested by him.

Another of V.E. Paton's postulates was implemented in the Department: not only develop new products, but also pay attention to their advertising to achieve wide acceptance. This prompted us to publish the results of our developments and issue colourful posters for industrial exhibitions. I remember how the staff members from all over the Institute assembled to look at the poster made by Nadezhda Malinochka upon my request for promotion of valve surfacing machine tools. This was an impressive example of using artistic means to demonstrate the advantages of machines, which had an impact on the viewers similar to that of the actual work of art. The poster was only shown in two demonstrations, and then, unfortunately, it was purloined. It could have an appropriate place in the Institute's museum.

New equipment implementing the technological advantages of the Institute, in combination with technical perfection of the mechanisms and devices based on the inventions, led to a real avalanche of orders for our products.

At the end of 1960s– beginning of the 1970s the first in the world automatic machine tools and lines for manufacturing, carburetor and diesel engine valves clad by superalloys were created (Figure 3). Here also the following principle was implemented: reduce by an order of magnitude the labour consumption and metal content of the new equipment compared to the closest analogs. The first to be developed were automatic machine tools OB1099 with mechanical automatic operators, where assembly of the valve blank

Figure 3. V.E. Paton, M.G. Belfor, V.F. Moshkin and A.I. Chvertko near OB1038 unit for surfacing ICE valves in an international industrial exhibition

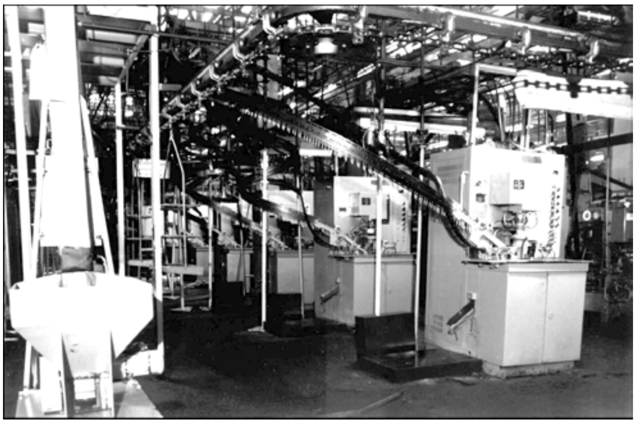

Figure 4. Automatic machine tools OB1099 in the valve surfacing line at AutoVAZ

with the superalloy ring, their orientation and feeding for surfacing into the inductor were all performed by one motion of the manipulator «arm». They ensured the surfacing productivity of 240 valves per hour at AutoVAZ (Figure 4), whereas with the Italian equipment welders of the highest qualification level were hardly able to manually surface 90 pieces per hour. Our six automatic machines with one elevator for ring feeding in the line (instead of 29 machine tools of Gustina, Italy, envisaged by the project), provided the annual output of 5 mln valves for Zhiguli car.

French Company Renault, Designer General of KamAZ, included only one Soviet item into the project of the KamAZ engine plant: OB1082 automatic line (Figure 5) for manufacturing surfaced diesel valves. The line included 8 automatic machine tools OB1100, elevator OB1081 for orientation and feeding of the surfaced rings to the machine tools, conveyor for ring feeding and other devices. Over the 10 years of this equipment operation, there was not a case of the mother conveyor stoppage because of it, whereas there

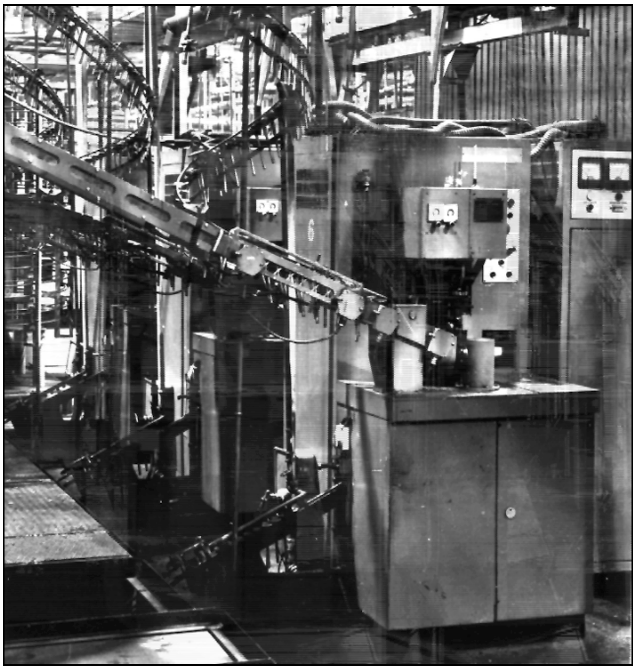

Figure 5. Automatic line OB1082 for manufacturing surfaced diesel valves at KamAZ

was not a single foreign company-supplier of equipment to this plant, because of which the mother conveyer would not stop. Nonetheless, we have been searching for new solutions all the time. Automatic machines with mechanical manipulators were replaced by machine tools with gravity automatic operators. Movement of valves and rings into the storage components up to clippers for their single-piece feeding, their further feeding to assembly and the assembly proper were performed under the impact of gravity force. Dozens of inventions were the basis of this qualitatively new equipment.

In this equipment the power units were completely made with contactless elements for the first time in the practice of PWI EDTB. Under the conditions of dustiness of plants under construction foreign-made equipment often developed malfunctions, because of contact relay failure. To great surprise of foreign specialists, our line operated without failures. The author of the electrical circuit design was V.L. Najda. L.S. Yazvinsky, A.D. Suchek, O.R. Kozhema, A.F. Marchenko, and others put is a lot of effort and inventiveness into this work.

It should be noted that when automatic machine tools and lines for production of surfaced valves were operating in our country in many plants of the automotive, tractor, heat locomotive, shipbuilding, and defense industries, specialists abroad were still «struggling» to develop their automatic machines for another 15 years.

At that time our products began attracting greater interest abroad. At construction of a car factory in the town of Belsko-Biala in Poland, Fiat, Italy — the General Contractor, included the valve surfacing machines into the plant project. They were designed not only for manufacturing valves of Polish cars, but also for many other foreign car models.

Starting from 1970s out equipment was part of license agreements for transfer abroad. Equipment for manufacturing the welding and surfacing consumables attracted a lot of interest. Mills for manufacturing flux-cored wires and strips of the type of OB1252, OB1367, OB2141 became widely accepted. I.P. Kaplienko, K.N. Minaev, I.E. Pavlovskaya, and others made a great contribution to these developments. Many original engineering solutions were based on these inventions. It is interesting to note that designers quite often were not only inventors of machines for material manufacturing, but themselves participated in invention of new designs of flux-cored wires and strips, and also performed their patent protection.

Licensed subjects also included equipment for explosion welding and treatment of products. Units of OB1087 and 2200 type (Figure 6) successfully produced explosion-welded steel-aluminium cathode pins of aluminium electrolyzers, which are currently operating in Siberia and in Africa. A large equipment complex was developed and supplied for welding missile cases, explosion treatment of items and for manufacture of specialized explosives. As Deputy Head of

Figure 6. OB2200 unit for explosion welding

EDTB, Vladimir E. Paton often conducted meetings, in which our projects were considered, and his remarks and advice quite often determined their further fate.

By the way, we learned from Vladimir Paton, not only to work, but also to relax. The range of staff hobbies was vast. Roaring cartings were created at PWI and given a test drive in the yard between the Institute's buildings. Tourists have covered the Urals, Siberia and reached the Far East. Scuba divers won underwater sports competitions in Kiev and swam in the Pacific, Bering and Japanese Seas, caught and resettled kalans in the Commandor Islands. At the same time, they wrote poems and songs, and participated in bards' competitions, popular at that time. And, certainly, shot films and showed them not only in the House of Scientists, but also in the competitions, where they were awarded Laureate Diplomas. One of the first amateur films was devoted to 10th anniversary of EDTB and was called «10th Spring». Shot on a 16-mm film with a magnetic sound track, it was a sound film and recorded our designers and their creations in the country's plants. The film also shows welding tractors in Zhdanovtyazhmash, the «father» of which was V.E. Paton, and pipe-welding mills in the Chelyabinsk Pipe-Rolling Plant, which made A.I. Chvertko and V.F. Moshkin work very hard, and our contribution to special electrometallurgy, which required a lot of efforts of A.I. Nekrasov, V.A. Pratkovsky, N.V. Rejda, and many other things. But, most important, it shows the people, many of whom are no longer with us.

It is impossible to describe in a short paper all the diversity of engineering embodiments of creative finds of the followers of Vladimir E. Paton and their further development. Hundreds of remarkable machines have been developed, which were manufactured in thousands by our and foreign plants, and were shipped to all the continents of the world. I only dwelled on those things, which I was directly involved in, during the life time of V.E. Paton, but still could not cover a great many subjects. This paper did not include chamber units for welding and surfacing in vacuum and shielding media (among which is the first machine for studying welding in «deep» vacuum), nor did it include the instruments and auxiliary welding equipment, equipment for application of strengthening and protective coatings, equipment for nondestructive testing, which I have been working on for the last ten years. But all the 45 years of my working at PWI I have followed Vladimir Paton's postulate: To design, while inventing.

CONSUMABLES AND ENERGY-SAVING CLADDING TECHNOLOGIES FOR RECONDITIONING AND MANUFACTURING PARTS OF MACHINES AND MECHANISMS

I.A. RYABTSEV, Yu.M. KUSKOV, I.A. KONDRATIEV, Ya.P. CHERNYAK and **I.I. RYABTSEV**
E.O. Paton Electric Welding Institute, NASU, Kiev, Ukraine

The experience gained at the E.O. Paton Electric Welding Institute in development of consumables and technologies for reconditioning and manufacturing of parts of different machines and mechanisms by arc cladding is described. The focus is on power-saving consumables and technologies, allowing cladding of carbon steel parts to be performed without or with minimum preheating.

Keywords: arc cladding, energy-saving technologies, cladding materials, flux-cored wires

Cladding is one of the most efficient and cost-effective methods of reconditioning worn parts or giving special properties to new ones. Deposition of specially alloyed metal layers on their damaged surfaces gives them a high resistance to different kinds of wear. Cladding is often used to join dissimilar metals, one of which usually has a satisfactory or poor weldability and a lower crack resistance. Deposition of an underalyer of ductile steels and preheating and concurrent heating are used to eliminate cracks, which should be followed by delayed cooling of a part. The above measures require additional material and energy consumption, moreover, increase of prices for energy carriers lowers the effectiveness of cladding application.

PWI developed cladding consumables with good welding-technological properties in particular, not requiring any preheating in cladding of carbon steel parts. The metal deposited with these materials, features high performance, heat, corrosion resistance, etc. Among the new cladding consumables, PP-AN202 flux-cored wire is widely applied for cladding parts from medium- and high-carbon steels without preheating. Deposited metal produced using this wire, corresponds to low-carbon high-alloyed chromium-manganese steel, which is characterized by a high wear resistance under the conditions of metal friction against metal with an abrasive interlayer. Deposited metal is strengthened as a result of impact of high contact loads, which increases its wear resistance even further.

New flux-cored wires PP-AN193 and PP-AN204 provide deposited metal of the type of maraging steels, featuring a high hardness, heat and wear resistance at friction of metal against metal at higher temperatures. These wires can be used for cladding without preheating of dies and die tooling from tool steels of 50KhNM, 25Kh5FMS type for hot and cold deformation of metals.

PP-AN198 flux-cored wire was developed for cladding large-sized casing parts from medium-alloyed steels without preheating. Deposited metal produced when using this wire has satisfactory crack resistance and strength properties on the level of structural steels of the type of steel 35, etc.

Sparsely-alloyed cladding consumables are being developed (total content of alloying elements is not more than 5 wt.%) with tribotechnical characteristics on the level of high-alloyed cladding consumables. Metal deposited with sparsely-alloyed flux-cored wire PP-AN194, has 2–3 times higher wear resistance than that of earlier developed cladding consumables with similar alloying level. Such wear resistance indices are achieved due to formation of microstructures following the Charpy principle in the deposited metal: individual hard inclusions with a low friction coefficient and low susceptibility to burrs are embedded in a ductile matrix.

Technologies of cladding critical parts of equipment of ore mining and processing enterprises of Ukraine have been developed with application of the above consumables. The work was conducted jointly with PKF «Ukrkomplekt», OJSC «Alians GRUP», DP «Krivbastekhmash» and other enterprises, where casing parts (bed frame and casing ring) of cone crushers (Figures 1, 2), shafts of crushing cones of cone crushers (Figure 3), ring gears of ball crushers for ore grinding (Figure 4), cases of carriages of calcining machines for pellet production, etc. [1, 2] were reconditioned.

Semi-automatic cladding with PP-AN198 flux-cored wire was used for reconditioning the bed and ring case from steel 35. The worn surfaces of the bed were surfaced in separate sectors in several layers. Tilting of the bed was performed if required, to move the surface to be treated into a position convenient for cladding. Total time of cladding one bed was 17 days, and more than 600 kg of flux-cored wire were used. Machining of the treated bed surfaces did not create any difficulties, which is particularly important

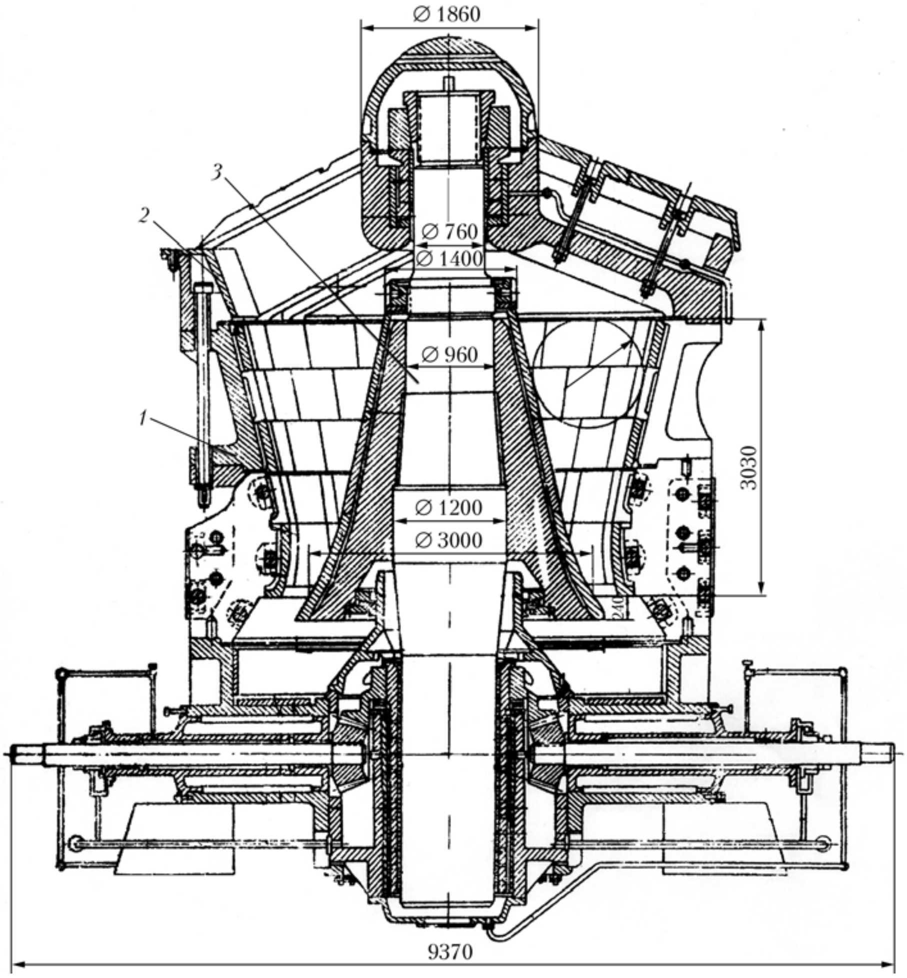

Figure 1. Schematic of a cone crusher: *1* – bed; *2* – ring case; *3* – shaft

in treatment of large-sized parts. No defects were found on the clad surfaces after machining.

Cladding of the casing ring was performed in a similar fashion: first along its end face in sectors in two layers, and then over the conical and vertical surfaces of the ring contacting the respective bed surfaces. Cladding of the worn or broken turns of the buttress thread was started from the turn horizontal portion by sectors. If required, partial forming of the deposited metal was performed in some thread sections using copper plates. Total weight of flux-cored wire used in cladding of the ring case was more than 500 kg. Quality and treatment of the deposited metal were similar to those achieved in bed surfacing.

Great difficulties were encountered in development of the technology of cladding the crushing cone shaft, made from steel 40 or low-alloyed steel of 34KhNM type (Figure 3). Wear (to 10–12 mm to a side) occurred in the zone of contact of the upper cylindrical part of the shaft with the bronze bushing as a result of penetration of dust with higher abrasive properties into the clearance between them. In operation part of the shaft with buttress thread, from which the cone is suspended, also failed. Cleavage of individual turns of the thread (thread module in the range of 40–50) or local fracture of several of its turns occurred as a result of fatigue processes.

Before cladding the reconditioned sections were subjected to ultrasonic testing. If fatigue cracks were found, they were always removed by machining with abrasive wheels. Self-shielded flux-cored wires of grades PP-AN198 and PP-AN202 were used for cladding. The worn cylindrical part of the cone was clad with PP-AN198 flux-cored wire, and more heavily-loaded thread — with high-alloyed PP-AN202 wire. Deposited metal hardness was not more than *HRC* 30, which does not lead to any difficulties in machining using special equipment. Quality of the treated surface of the deposited metal was assessed using ultrasonic testing. The cost of reconditioning the shaft cones did not exceed 30 % of new product cost at the same operating period.

Technology of cladding worn teeth of the gear of ball crusher rotary drive was developed in cooperation with «Ukrkomplekt»: teeth module — 20; teeth number — 268; teeth length — 800 mm; angle of teeth inclination — 5°15′; gear outer diameter — 5410 mm; number of sectors — 2; total weight of two gear sectors — 16.5 t (Figure 4). Semi-automatic cladding of the teeth was performed by flux-cored wire PP-AN198 in the continuous mode. Considering the gear teeth operating conditions, cladding was performed with local preheating up to 150–200 °C. First the teeth edges were clad, and then cladding was performed

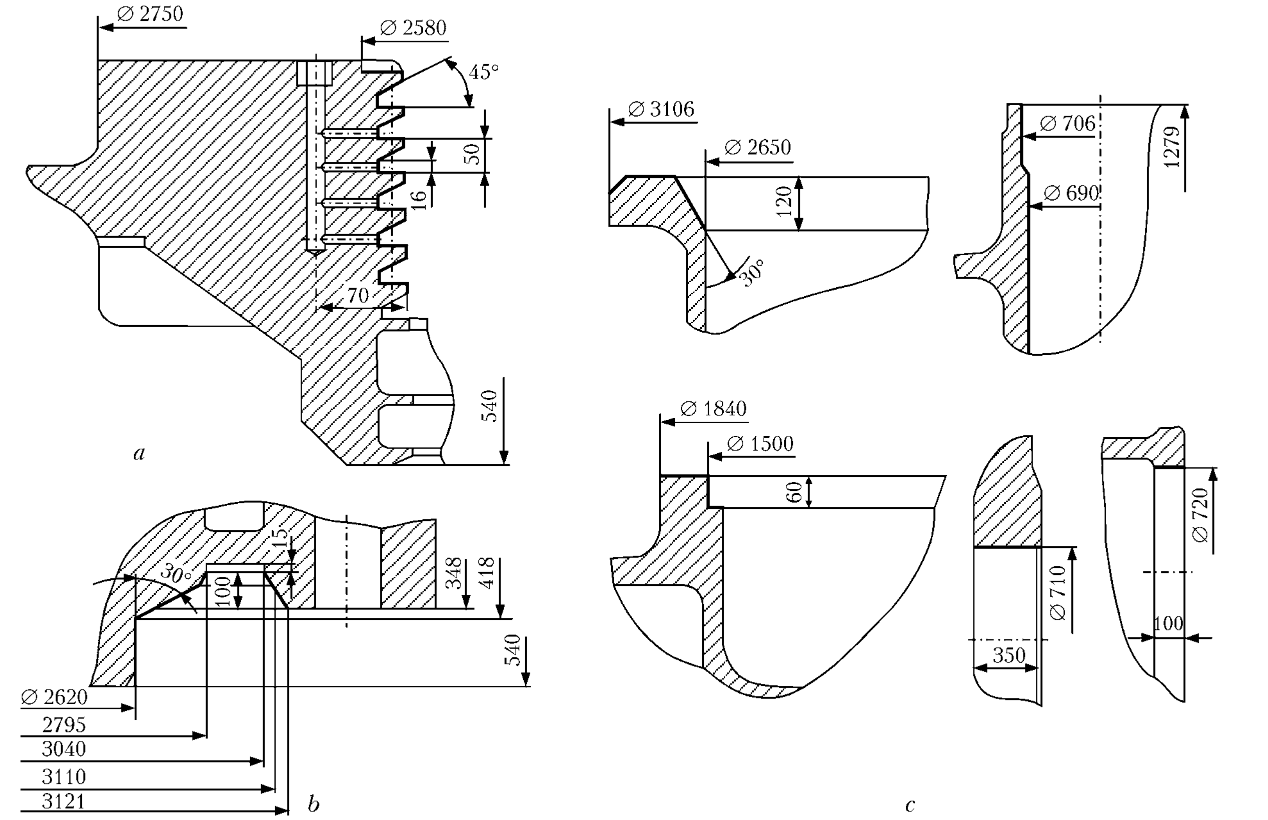

Figure 2. Clad surfaces (heavy lines) of ring case (*a*, *b*) and bed of cone crusher (*c*)

along the tooth generatrix by backstep procedure. Total time of cladding two sectors of the ring gear was 27 days, flux-cored wire consumption was 2350 kg. In total three ring gears were clad and machined.

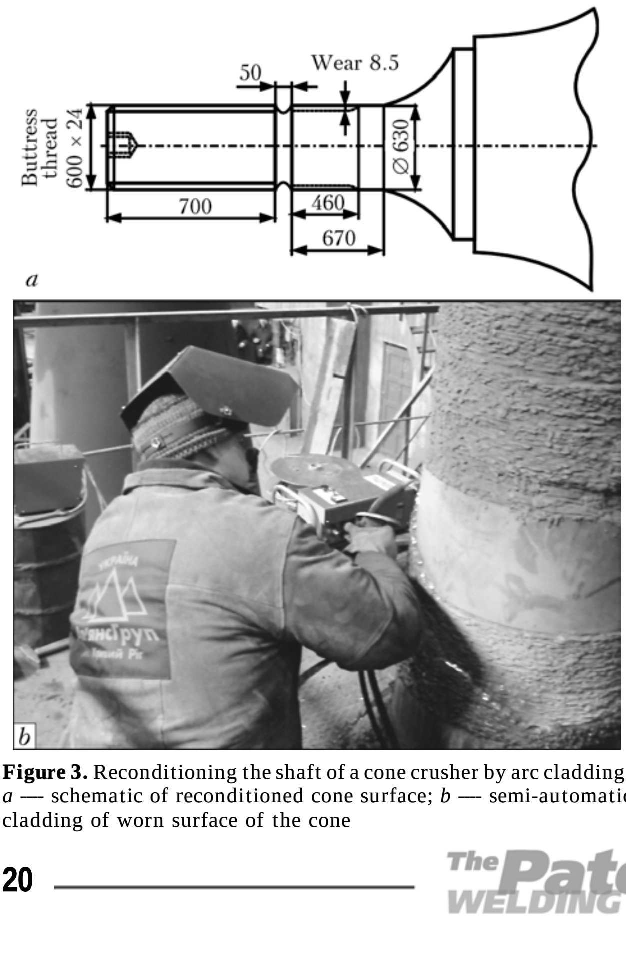

Figure 3. Reconditioning the shaft of a cone crusher by arc cladding: *a* — schematic of reconditioned cone surface; *b* — semi-automatic cladding of worn surface of the cone

Weight of the carriage case of calcinating machines from 14KhMTL steel is equal to approximately 5 t, its length being about 4 m. The carriages are assembled to form a closed agglomeration strip, carrying the sintered blast-furnace pellets. The main cause for carriage failure is deformation of their side beams as a result of non-uniform heating. External examination of failing cases of 70 carriages showed that they have practically no scale, and no fatigue cracks were found, either.

Considering the causes for carriage failure, self-shielded flux-cored PP-AN198 wire was used for their cladding. The number of deposited layers was selected depending on sagging. After deposition of each layer, mechanical scraping of the deposited surface was performed with abrasive wheels. After completion of cladding, the clad surface was mechanically scraped along the entire length of the beam, providing a clearance of not more than 1–2 mm between the clad surface and special template. Total amount of metal deposited on one carriage case was equal to 110–120 kg. More than 70 carriages were clad by the proposed technology.

Cladding of a rotary support of a unique MKT-250 crane (Figure 5) was performed together with OJSC «Tsentrstalkonstruktsiya» and GP SU-39. This crane allows mounting structures of up to 250 t weight at the height of 57 m [3]. As to its design, the rotary support is a large-sized radial-thrust bearing of a large weight (weight of the rotary support ring gear is up to 1.5 t with average diameter of 3 m). Rotary support parts are made from high-carbon low-alloyed steels of grades 50Kh and 50KhGM.

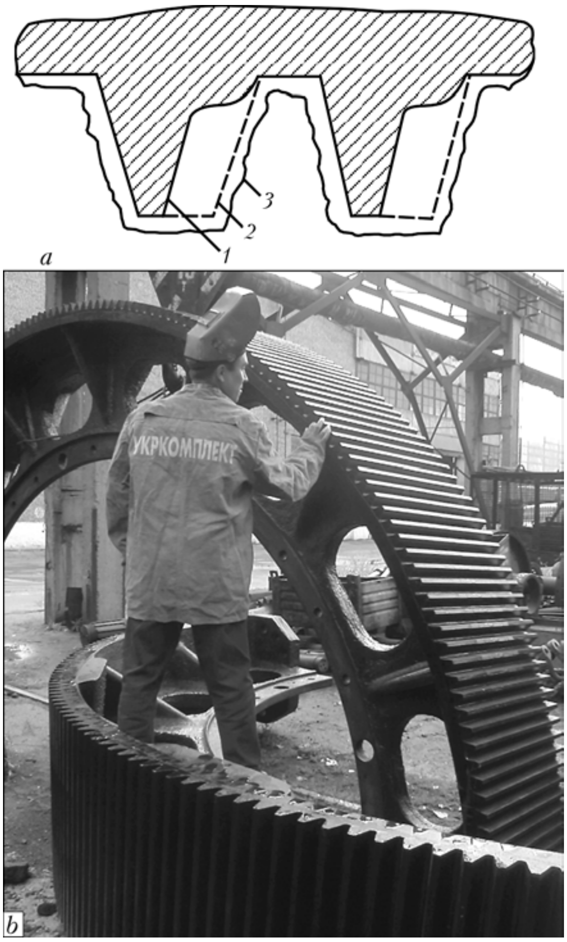

Figure 4. Schematic of reconditioning two sectors of ball mill ring gear (*a*) and appearance of reconditioned sectors (*b*): *1* — worn tooth profile; *2, 3* — clad tooth profiles after machining and cladding, respectively

External inspection and dye penetrant and ultrasonic testing were used to establish that the rolling surfaces of the gear and joint ring of the rotary support are prone to mechanical and fatigue wear of the race tracks because of multiple redeformation of the same metal volumes. Self-shielded flux-cored wire PP-AN202 of 2 mm diameter was used for cladding both the rings.

All the rolling surfaces to be clad were assessed using ultrasonic and dye penetrant testing; and the found defects were removed by machining. In view of the high content of carbon in the base metal, the ring sections to be clad were heated up to the temperature of 120–150 °C by gas burners before cladding. The surfaces being reconditioned were clad in sectors, the arc length (around the outer perimeter) being approximately 200–250 mm. Ring cladding was performed simultaneously by two welders (cladders) on diametrally opposite sections at a horizontal (or close to it) position of the treated surfaces convenient for cladding. Cladding was performed in two shifts for seven days, which was followed by delayed cooling of the clad rings. Then machining of the clad rings of the rotary support was performed. Ultrasonic and liquid-penetrant testing did not reveal any defects in the clad layer. Clad components of the rotary support

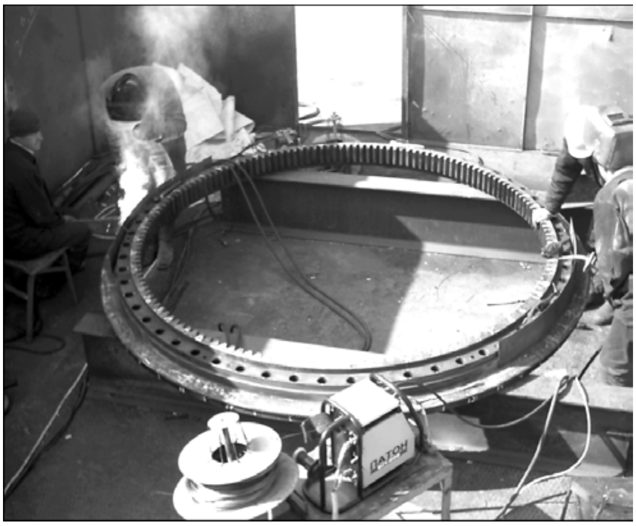

Figure 5. Semi-automatic cladding of ring gear of MKT-250 crane rotary support

were mounted on MKT-250 crane, which is successfully operating now.

For cladding the worn shafts of escalator drives in the Kiev metro without lifting them to the surface, a unit was developed, which allows performing automatic cladding and machining of the shafts before and after cladding (Figure 6). The shafts are made from structural carbon steels. Flux-cored wire PP-AN202 of 2 mm diameter is used for their cladding without preheating. Shaft wear is usually small, so that cladding is performed in one layer.

Using the new sparsely-alloyed flux-cored wire PP-AN194 providing deposited metal with higher tribotechnical characteristics [4], technologies of automatic cladding of parts operating under the conditions of dry friction of metal against metal were developed, namely of crane wheels (Figure 7), screw spools of diffusers for sugar-refineries, etc.

PP-Np-30Kh20MN flux-cored wire was developed for manufacturing and reconditioning cladding of mine hydro-support columns of tunneling machines, hydro-press plungers and other parts. Metal produced

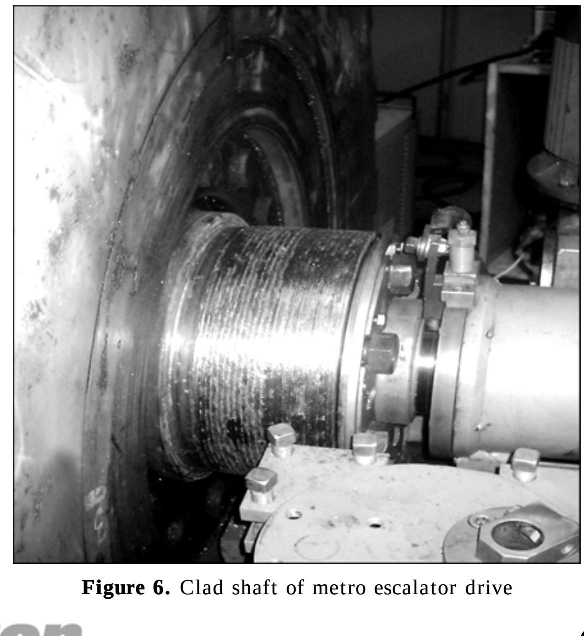

Figure 6. Clad shaft of metro escalator drive

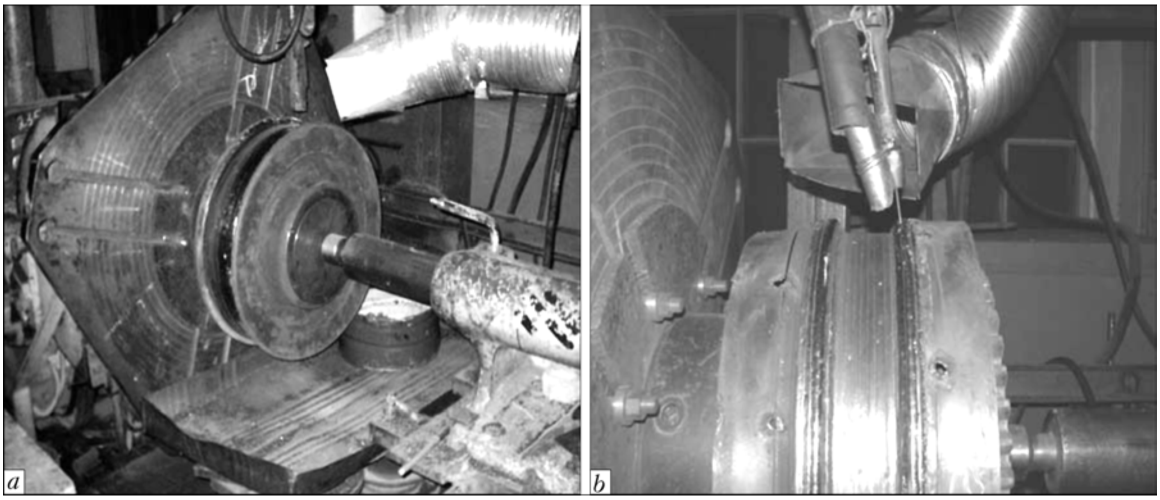

Figure 7. Automatic cladding with PP-AN194 flux-cored wire of rolling surface (*a*) and flange (*b*) of crane wheel

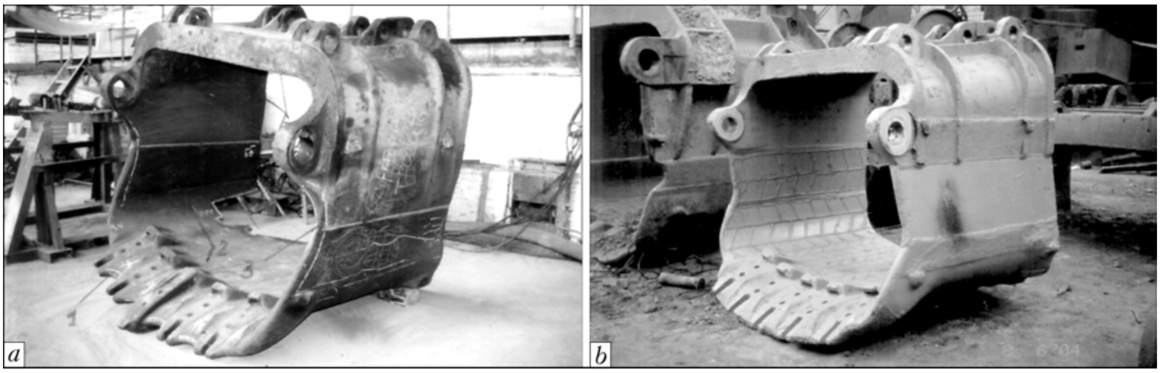

Figure 8. Appearance of worn excavator bucket of 5 m^3 capacity before (*a*) and after (*b*) cladding

in cladding with this wire, has a martensitic-ferritic structure and hardness *HRC* 42–45. It is characterized by a quite high corrosion resistance in the water-salt environment, as well as wear resistance at friction of metal against metal. Wear of hydro-support columns does not exceed several tens of millimeters. A technology of automatic single-pass arc cladding was developed for their reconditioning, the thickness of the deposited layer being equal to 0.5–1.0 mm. Cladding application allowed eliminating such an operation as column chromium-plating.

Earlier developed flux-cored wires were used for development of technologies of cladding parts operating under the conditions of impact-abrasive wear. In particular, self-shielded PP-AN105 wire was used to clad lifters and lining parts from G13L steel of a self-grinding mill. Technology of automatic submerged-arc cladding of cylindrical crusher shafts using AN-26 flux and PP-AN105 wire was developed. PP-AN105 flux-cored wire was also successfully used in reconditioning the buckets of open-mine excavators of 5, 8 and 10 m^3 capacity (Figure 8) [5].

Self-shielded flux-cored wire PP-AN192 was used for automatic open-arc cladding of parts exposed to intensive abrasive wear and moderate shocks, for instance, shares of ploughs and cultivators, blades of graders and bulldozers, as well as other products. Simultaneous cladding of two edges of grader blades is performed during their manufacture. Cladding is performed with oscillations, this allowing deposition of wear-resistant layers 2.0–2.5 mm thick and up to 30 mm wide on the two blade edges.

An automatic machine was produced for cladding new disc cutters of cultivators, in which cutters of different diameter are clad using flux-cored wire PP-AN192. Cladding is performed with oscillations, this ensuring the geometrical characteristics of the clad layer required for self-sharpening, namely 2.0–2.5 mm thickness and up to 20 mm width.

The list (although by far not a complete one) of parts (mostly large-sized) reconditioned and strengthened using cladding, given in this paper, is a convincing demonstration of the wide possibilities for application of advanced cladding consumables, as well as cladding technologies developed for them.

1. Ryabtsev, I.A., Kuskov, Yu.M., Makhovsky, Yu.A. et al. (2002) Reconditioning of large-sized parts of equipment of ore mining and processing enterprises by arc surfacing methods. *Svarshchik*, **1**, 6–8.
2. Ryabtsev, I.A., Kuskov, Yu.M., Poddubsky, A.I. (2004) Reconditioning of parts of cone crusher by arc surfacing. *Ibid.*, **1**, 16–17, 19.
3. Ryabtsev, I.A., Kuskov, Yu.M., Chernyak, Ya.P. et al. (2004) Reconditioning of rings of rotary support of crane MKT-250. *Ibid.*, **4**, 35–37.
4. Ryabtsev, I.I., Kuskov, Yu.M., Grabin, V.F. et al. (2003) Tribological properties of Fe–Cr–Si–Mn–P system deposited metal. *The Paton Welding J.*, **6**, 16–20.
5. Kuskov, Yu.M., Kondratiev, I.A., Bogachenko, A.G. et al. (2004) Reconditioning of quarry excavator buckets by surfacing with self-shielded wires. *Svarshchik*, **6**, 16–17.

CAUSES OF DEFECTS FORMED IN STEELS AND ALLOYS IN SURFACE HARDENING USING HIGH POWER DENSITY HEAT SOURCES

S.S. SAMOTUGIN and **V.A. MAZUR**
Priazovsky State Technical University, Mariupol, Ukraine

Causes of defects formed in surface layers of tool steels as a result of treatment of workpieces with high power density heat sources are considered. Peculiarities of formation of defects in laser and plasma treatment are noted. Methods for reducing the probability of formation of defects are suggested.

Keywords: heat hardening, heat sources, laser and electron beam, plasma jet, phase and structural transformations, defects

Methods of heat hardening using high power density (10^5–10^7 W / cm^2) heat sources, i.e. laser and electron beams and plasma jet, have received wide acceptance for increasing wear resistance of machine parts and tools. High values of power density of such heat sources provide qualitatively new properties of metal surfaces, which cannot be achieved with traditional methods of heat treatment. This effect is caused by a nanocrystalline metastable structure formed in the surface layer, having increased degree of dispersion of blocks and dislocation density. At the same time, parameters of super rapid (so-called «shock») hardening create conditions for initiation and propagation of defects (cracks, pores, inclusions), which are caused by a non-uniform and local thermal effect. In this case, the probability of formation and extent of propagation of defects depend both upon the composition of a material and its initial state, and upon the method and parameters of treatment.

In practice, laser hardening is performed in the majority of cases by melting the surface of workpieces. This is related to a number of peculiarities of interaction of laser radiation with metals, i.e. relatively small depth of the hardened layer (laser affected zone — LAZ) formed in treatment with heating to a temperature below the melting point, low efficiency of laser treatment (maximum 10 %) in hardening without surface melting and without the use of special absorbing coatings, achievement of the highest values of service properties (first of all, hardness) owing to super rapid solidification and quenching of the remelted layer. Because of a super high rate of solidification of the melt, and despite a high degree of dispersion of the crystalline structure, laser melting is characterised by a high probability of formation of solidification (hot) cracks [1–4]. High-carbon and alloyed tool steels [1, 3, 4], as well as cast irons [1, 5], are particularly sensitive to cracking in laser treatment.

One of the causes of cracking in laser melting is a high level and unfavourable distribution of internal residual stresses. Laser treatment of tool steels leads to almost complete dissolution of the carbide phase. Liquid solution is saturated with carbon and alloying elements. Austenite in the LAZ metal becomes resistant to $\gamma \rightarrow \alpha$ decomposition (temperature range of the beginning and end of martensitic transformation, M_s–M_f, is reduced) in super rapid cooling of the solidified metal. As a result, retained austenite becomes the main structural component of the LAZ metal, and residual tensile stresses [5] leading to cracking [4] are formed in the melted layer.

High sensitivity of grey cast iron to formation of solidification cracks in laser melting is also caused by the presence of substantial internal stresses. In this case, cracking is accompanied by formation of pores in the melted layers, which is related to incomplete dissolution of graphite in the melt because of a very high rate of heating and solidification. Microbubbles of gases evolved from deep layers of the melt are adsorbed on the remaining graphite particles. The biggest quantity of pores is formed at a high speed of treatment and high power density of laser radiation [6].

In addition to unfavourable residual stresses, the other important cause of formation of solidification cracks in laser melting of both steels and cast irons is the presence of a large quantity of non-metallic inclusions in the initial metal. The effect of inclusions on initiation and propagation of cracks in the LAZ metal was investigated in detail in study [6]. It was established that the energy of radiation is enough for melting refractory inclusions Cr_2O_3, Al_2O_3, TiN and SiO_2, as well as for development of diffusion processes through interfaces between the inclusions and matrix. As a result of diffusion, zones of the matrix surrounding the inclusions are saturated with the inclusion components, which are fixed in solid solution during rapid cooling. Therefore, local regions of the matrix around the inclusions are heavily saturated solid solutions. Substantial thermal stresses and, hence, solidification cracks are formed under these conditions at interfaces with the matrix. The character of microfracture depends upon the shape of the inclusions:

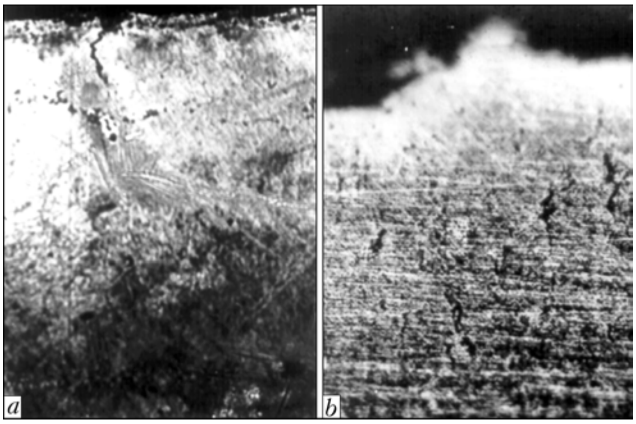

Figure 1. Microsections of melted layers with solidification crack and micropores formed in steel 150KhNM treated by the 1.2 kW laser beam (a — ×100), and with solidification cracks and inclusions formed in laser treatment of steel 45 (b — ×320)

cracks near compact inclusions are shorter, compared with those propagating along film-like inclusions. The centre of initiation of a crack shown in Figure 1, *a*, was a particle of lamellar cementite with spherical graphite inclusions. The microcrack surrounded by a chain of micropores and tears escapes to the surface of the melted layer and is gradually arrested at the interface between the melted and hardened layers in a solid state. Solidification cracks escaping to the surface of the melted layer can be easily detected visually.

Internal solidification microcracks that do not propagate to the surface and cannot be detected by such non-destructive test methods as ultrasonic, magnetic or beam methods are much more dangerous (Figure 1, *b*). Microcracks initiated by non-metallic inclusions propagate almost in a vertical direction corresponding to a direction of heat removal in rapid solidification. The cracks are very small, and only the cracks near inclusions located immediately under the surface escape to it.

Cracks of both types, escaping to the surface and internal ones, are very dangerous, as they may act as centres of microfracture of hardened parts during operation. It should be noted that solidification (hot) cracks do not usually propagate deep into a workpiece in laser treatment, but are arrested either at the interface between the melted and hardened layers (Figure 1, *a*) or at the interface between the hardened layer and initial metal.

Hardening (cold) cracks, which may propagate as early as at the hardening stage far deep into the initial metal of a workpiece up to its full fracture, are of a much higher danger.

Phase and structural transformations in plasma heating of metals share the mechanisms of transformations occurring in laser heating, and, at the same time, have their own specific mechanisms. In treatment without melting, i.e. solid-phase hardening, the transformation mechanisms and structure of the hardened zone in laser and plasma treatment are almost identical [1, 5, 7]. However, in treatment with melting, the character of rapid solidification and structure of the melted layer are substantially different for these treatment methods [8].

At a sufficient heat input, laser heating of steels and alloys causes local melting of surface microvolumes. The molten metal pool is retained almost completely due to the forces of surface tension. Some deterioration of quality of the surface (increase in roughness) is permitted for most types of parts or tools, and can be readily remedied by additional machining. In heating with a high-concentration plasma jet, the surface can be melted with preservation of the molten metal pool only in a narrow range of treatment parameters: in heating of the surface layer up to temperature $T_{\rm melt}$ – $T_{\rm melt}$ + 100 °C [8]. In this case, the depth of the melted zone is no more than 100 μm, i.e. it means that it is just a micromelting of the surface. Increase in heat input and, accordingly, heating temperature leads to melting of substantial volumes of metal, and to increase in volume of the molten pool and gas dynamic effect of the plasma jet over the forces of surface tension, thus resulting in splashing of part of the molten metal. The depth of the plasma macromelting zone may reach 1 mm. However, the recess formed after splashing out of metal has the same depth, which dramatically deteriorates quality of the surface and requires additional machining. Therefore, plasma hardening with macromelting of the surface can be applied only in limited cases, e.g. when it is necessary to increase depth of the hardened layer or provide special surface geometry.

The effect of plasma micro- and macromelting on mechanical properties and, in particular, on dynamic crack resistance is ambiguous and depends upon the composition of steels and alloys, as well as their initial state. For high-carbon and tool steels, grey cast iron and sintered hard alloys [7], plasma micro- and especially macromelting lead to dramatic embrittlement of the surface (decrease in impact toughness and dynamic fracture toughness). Fracture of metal of the melted zone occurs by the mechanism of intercrystalline cleavage. Even at the absence of defects (cracks, pores), the presence of such a brittle layer on the surfaces of parts and tools is undesirable. Therefore, plasma hardening without surface melting is indicated for parts of high-carbon and tool steels, cast iron and hard alloys. However, there are cases where treatment with plasma micromelting may hold higher promise [9]. For example, this is the use of plasma treatment with micro- and macromelting for low-carbon steels or deposited metal, where increase in wear resistance is accompanied by a substantial increase in impact toughness and dynamic fracture toughness, and fracture of the melted layer occurs by the microtough pit mechanism [7].

Potential sensitivity of a material being hardened to solidification cracking in plasma melting can be estimated from the character of fracture of the melted layer metal. No solidification cracks are usually formed in plasma melting in the case of formation of a high-dispersion structure with a characteristic quasi-

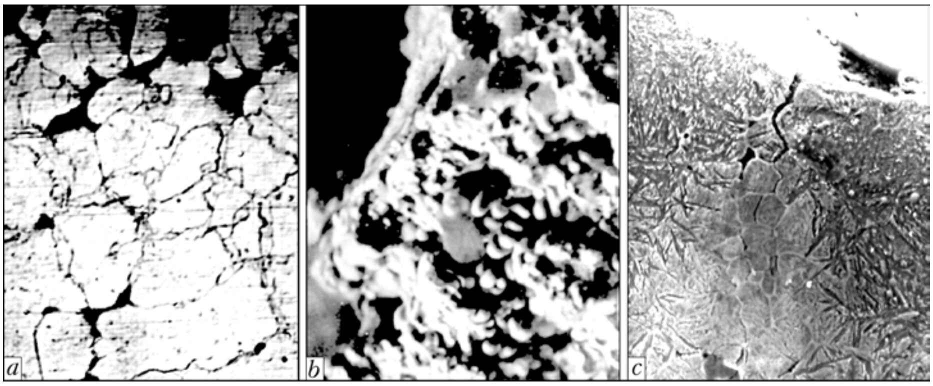

Figure 2. Microstructure (*a, c*) and character of fracture (*b*) of melted layer with solidification cracks formed in plasma macromelting of steels R6M5 (*a* — ×500; *b* — ×340) and 90KhF (*c* — ×320)

cleavage or microtough pit fracture mechanism. Hot cracks may occur in the case of formation of coarse-acicular martensite and fracture by the mechanism of intercrystalline cleavage. To illustrate, Figure 2, *a, b* shows a microstructure and fracture surface of steel R6M5 in plasma macromelting. Solidification microcracks are formed along the boundaries of melted grains, they have a chaotic location, are oriented mainly in a vertical direction, and may be both internal and escaping to the surface (Figure 2, *a*). Pores and non-metallic inclusions of compact and film morphology can be seen at the cracking centres (Figure 2, *b*). It should be noted that structure of the surface of a hot crack in a disk knife of steel Kh12M, formed during the process of plasma hardening of the cutting edge on the side surface (Figure 3, *b*), is similar on the whole to structure of hot cracks formed in welding [10], which is indicative of the common mechanisms of their initiation and propagation. A much higher (almost by an order of magnitude) degree of dispersion of the hardened zone metal promotes formation of a dispersed fracture with a large number of melted crystal grains, pores and inclusions (Figure 2, *b*). The similar character of propagation of hot cracks is seen also in plasma melting of low-alloy tool steel 90KhF (Figure 2, *c*).

As noted above, surface hardening using high power density heat sources may cause hardening (cold) cracking, in addition to solidification cracking. Cold cracks may be formed both in treatment with surface melting and in treatment (hardening) without melting. Loss of operational strength in this case is associated not so much with physical-metallurgical effect of the laser beam or plasma jet as with the stressed state of workpieces during treatment.

Figure 3, *a* shows the hardening crack formed in a sub-surface zone of the melted layer in plasma macromelting of rolls of the pipe welding mill made from steel 90KhF. Hardening cracks branch from the fracture centre, and one of them escapes to the surface.

Formation of hardening stresses in surface hardening is caused by a dramatic gradient of temperature across the section of a workpiece. Internal stresses may amount in value to yield stress of steel and cause hardening (cold) macrocracking. Parts and tools of complex configuration, especially annular one with design stress raisers (rolls (Figure 3, *a*), disk knives (Figure 3, *b*), mills, saws, dies, washers, etc.) are most sensitive to cracking during hardening. Radial through and non-through cracks may initiate and propagate either from the hardened surface or from the axial hole at a stress raiser, e.g. key slot. Cracking may occur directly during the hardening process or during natural cooling of a hardened part. In the majority of cases the hardened parts with hardening cracks (even non-through ones) are rejected. This leads to the need to take special measures for prevention of brittle fracture of parts and tools during hardening [11].

Therefore, total hardening stresses at the stage of cooling are determined by the composition of steel being hardened. Their most dangerous combination

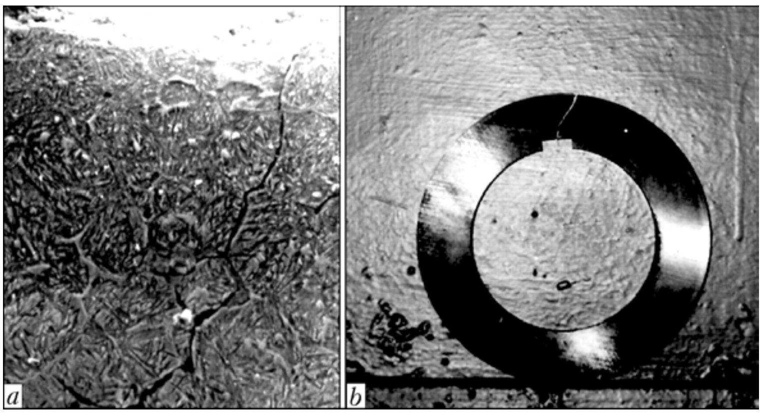

Figure 3. Microstructure of melted layer with hardening cracks formed in plasma treatment of steel 90KhF involving macromelting (*a* — ×320), and crack in disk knife of steel Kh12M for cutting of magnetic sheet (*b*)

for external layers occurs in hardening of parts and tools of alloyed steels, and for internal layers (near the axial hole) — in hardening of parts and tools of carbon steels. Design stress raisers are localised, thus facilitating brittle fracture of tools during hardening.

Proceeding from the established mechanisms of formation of hardening cracks, they can be prevented by two methods: relaxation of stresses due to volume hardening by increasing the temperature of intermediate volume tempering, and decrease in hardening stresses during hardening by regulating the thermal cycle of plasma heating.

Increase in the tempering temperature after preliminary volume hardening to 400–600 °C (depending upon the steel grade) must provide, firstly, relief of stresses due to volume hardening and, secondly, retaining of hardness of the core at a level of *HRC* 45–55 and, accordingly, high volume design strength of steel.

The thermal cycle of plasma heating must provide rapid cooling in a temperature range of the lowest stability of overcooled austenite (650–400 °C) and slow cooling in a temperature range below martensitic point M_s (for the majority of steels — 200–300 °C). This must allow thermal and structural (at the moment of formation of brittle phase, i.e. martensite) stresses to be decreased. In practice, this regulation of the thermal cycle can be readily achieved by using preliminary volume heating of workpieces immediately before plasma hardening to a temperature that is 20–30 °C below M_s for a given steel grade. Natural cooling of a preheated workpiece after plasma hardening does not only slow down in a temperature range of formation of hardening cracks, but also occurs uniformly in the entire volume of metal, which promotes decrease in a total level of hardening stresses. The recommended preheating temperature exerts almost no effect on values of heating rate, cooling rate and time of holding in a range of high temperatures, which determine the character of transformations and level of achieved mechanical properties after hardening using a high power density heat source.

Recommendations on regulation of the level of hardening stresses were implemented in development of the technology for plasma hardening of disk knives 203 mm in diameter and 12 mm thick, made from steel Kh12M, intended for cutting magnetic sheet (see Figure 3, *b*) [11].

It can be noted in conclusion that solidification (hot) cracks and micropores, as well as hardening (cold) cracks may be formed in surface hardening of parts using high power density heat sources both with and without surface melting. Careful selection of hardening parameters and application of additional technological arrangements allow prevention of cracks almost in all the cases.

Surface hardening using high power density heat sources does not involve extra addition of filler materials to the treatment zone (if it is not the case of laser and plasma surface alloying or coating). Therefore, laser or plasma hardening does not include any metallurgical factors affecting formation of non-metallic inclusions in the hardened zone metal. However, inclusions that are already contained in the initial metal may act as centres of initiation of cracks during the treatment process (particularly in treatment of alloyed steels, alloys and cast irons).

1. Leontiev, P.A., Chekanova, N.T., Khan, M.G. (1986) *Laser surface treatment of metals and alloys*. Moscow: Metallurgiya.
2. Pout, D. (1987) *Modification and alloying of surface by laser, ion and electron beams*. Moscow: Mashinostroenie.
3. Safonov, A.N., Tarasenko, V.M., Baskov, A.F. et al. (1985) Effect of initial structure on hardening of steel ShKh15 in treatment with CO_2-laser radiation. *Metallovedenie i Termich. Obrab. Metallov*, **4**, 5–9.
4. Kryanina, M.N., Bernshtejn, A.M., Chuprova, T.P. (1989) Heat treatment of high-speed steel using continuous-wave laser radiation. *Ibid*., **10**, 7–12.
5. Grigoriants, A.G., Safonov, A.N. (1987) *Methods for surface laser treatment*. Moscow: Vysshaya Shkola.
6. Gubenko, S.I., Egorov, V.V. (1984) Defects of hardened layer in laser hardening of steel. *Izvestiya Vuzov. Chyorn. Metallurgiya*, **6**, 91–96.
7. Samotugin, S.S., Leshchinsky, L.K. (2002) *Plasma hardening of tool materials*. Donetsk: Novy Mir.
8. Samotugin, S.S., Solyanik, N.Kh., Pujko, A.V. (1994) Properties of tool steels in plasma hardening with surface melting. *Svarochn. Proizvodstvo*, **11**, 20–24.
9. Samotugin, S.S. (1998) Plasma hardening of steel R6M5 after volume hardening. *Problemy Spets. Elektrometallurgii*, **3**, 35–42.
10. Royanov, V.A., Zusin, V.Ya., Samotugin, S.S. (2000) *Defects in welded joints and coatings*. Mariupol: PGTU.
11. Samotugin, S.S., Muratov, V.A., Kovalchuk, A.V. (1997) Plasma hardening of annular-shape tools. *Metallovedenie i Termich. Obrab. Metallov*, **10**, 2–4.

METHOD FOR IMPROVING LOCAL DAMAGE RESISTANCE OF WELDED JOINTS IN NPP PIPELINES*

O.G. KASATKIN[1], A.K. TSARYUK[1], V.Yu. SKULSKY[1], A.R. GAVRIK[1], S.I. MORAVETSKY[1], I.D. KLESHCHEVNIKOV[2], Yu.M. KOPYLOV[2] and A.G. MEDVEDEV[2]
[1]E.O. Paton Electric Welding Institute, NASU, Kiev, Ukraine
[2]Khmelnitskaya NPP, Ukraine

It is shown that the key factors causing corrosion cracking and fracture of composite welded joints in pipelines include chemical and structural heterogeneity of metal of a welded joint, formation of martensite and decarburised interlayers, stressed state and hydrogen-induced embrittlement of metal. The method is suggested for improving resistance of the welded joints to local corrosion damages.

Keywords: *pipelines, composite welded joints, structure, diffusible hydrogen, brittle interlayers, austenitic and carbon steels*

Experience of operation of power units of nuclear power plants (NPP) shows that their equipment comprises a number of assemblies, including different pipelines and welded joints on them, which are highly sensitive to damages. In particular, welded joints on pipes of dissimilar steels, i.e. low-alloyed and austenitic ones, in pipelines of the second loop are often damaged by corrosion. In repair, defective welded joints are usually removed, and inserts are welded into the pipes instead of them, the inserts being made under factory conditions from two sections of pipes of respective steel grades. However, they also have a limited service life, and require replacement in operation of a power unit.

According to the existing technology, welding of pipes of dissimilar steels is performed with an austenitic weld, the austenitic material being preliminarily deposited on the edge of a low-alloy steel pipe with wall thickness of more than 10 mm. Corrosion damages in dissimilar joints develop by the mechanism of intercrystalline corrosion, and they are localised in a narrow zone at interface between the austenitic weld and ferritic steel (Figure 1).

Characteristic feature of welded joints in dissimilar steels is a developed chemical, structural and mechanical heterogeneity [1]. Composite welded joints have the field of natural stresses, which are impossible to relieve by heat treatment. When performing welding, it is also necessary to take into account a different weldability of each of the steels joined.

Evaluation of performance of welded joints should be conducted with allowance for structure and properties of the fusion zone between dissimilar materials. Crystallisation interlayers of an intermediate composition, between the base and weld metal, are detected near the fusion line in the joints made by fusion welding.

The base metal on the side of the ferritic pipe has a ferritic-martensitic structure. The proportion of phases (content of martensite in structure) may vary depending upon the thermal welding cycle. Phase compositions of separate zones of the welded joints can be estimated from the Schaeffler diagram, which shows that interlayers with a martensitic structure will form in the weld in any case. This is related to the fact that near the fusion line, even at a low content of the deposited metal, the molten carbon steel is alloyed from the austenitic metal. As the proportion of the deposited metal increases, hardness of this zone dramatically grows with increase in the amount of

Figure 1. Microstructure of corrosion damage of the HAZ metal in welded joint between steel 20 and steel 08Kh18N10T (×25)

*The article is based on the results of accomplishment of the target integrated program of the NAS of Ukraine «Problems of Service Life and Safe Operation of Structures, Constructions and Machines» (2004--2006).

martensite, and then decreases mostly due to decrease in the concentration of carbon. Therefore, composite welded joints in low-alloy steels always comprise martensitic interlayers, which are formed in them independently of the type of austenitic filler metal.

Diffusion interlayers caused mostly by redistribution of carbon may be formed within the fusion zone in welding and heat treatment. At the same time, service temperature of the second-loop pipelines is not high, and the diffusion interlayers hardly develop there.

The diffusion interlayers formed in welding during the time of co-existence of the molten weld pool and base metal, as well as during the time of existence of solid phases in cooling after welding, are detected in composite welded joints. The cause of redistribution of carbon is, in particular, the presence of carbide-forming elements in austenite. These interlayers are located near the fusion line on the side of the austenitic weld, i.e. in the zone with the increased carbon content, whereas on the side of the ferritic steel a decarburised metal layer with coarse columnar grains of ferrite is formed (Figure 2). Note that because of a low carbon content this interlayer has low yield stress, and the concentration of impurities increases during the process of grain growth.

Residual stresses in composite welded joints greatly depend upon the thermal-physical and mechanical characteristics of the materials welded, in particular, upon the linear thermal expansion coefficient and thermal conductivity, as well as elasticity modulus and yield stress. The largest difference in thermal expansion coefficients (25–35 %) occurs between steels of the pearlitic and austenitic grades. It is especially pronounced if austenitic steel 08Kh18N10T is used in a composite welded joint.

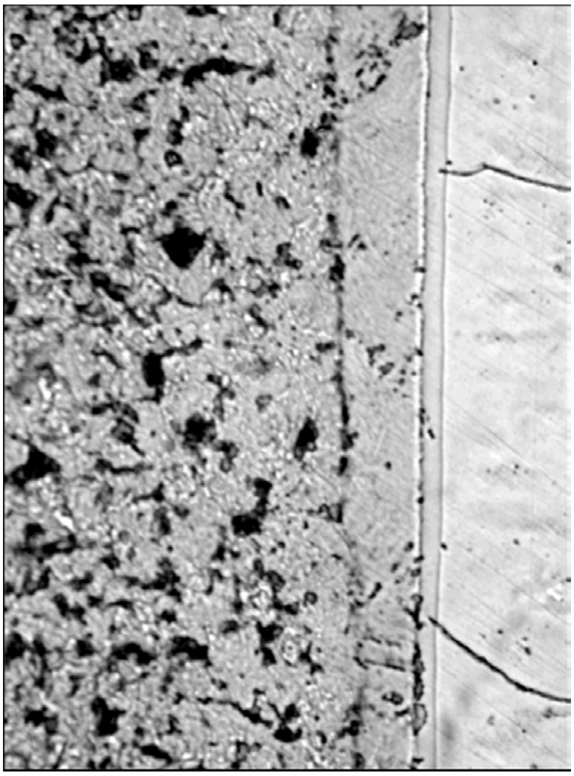

Figure 2. Microstructure of fusion zone between steel 20 and 08Kh18N10T (×1000)

Residual stresses in composite welded joints change to a substantial degree after heat treatment (tempering), which leads to growth of these stresses.

The important factor affecting performance of composite welded joints is hydrogen, which may lead to «static» fatigue of metal under certain conditions. Causing a decrease in bonding forces of the crystalline lattice at the locations of violation of its coherency, hydrogen leads to formation of microfracture centres at the boundaries with a high energy density. During welding, hydrogen enters into the weld metal mostly from the arc atmosphere during the arc–molten metal interaction [2].

Energy of the boundaries may substantially grow in martensitic transformation of austenite. The process of growth of martensite crystals induces structural stresses, microstrains and dislocation clusters, which are most pronounced near the austenite grains, whereto the coarsest martensite crystals migrate. A random stress field is formed at the boundary under the effect of growing martensite crystals. The coarser the initial austenite grains, the larger the size of the martensite crystals and the higher the local stresses and microstrains formed at their apexes. Embryos of microcracks may initiate in some of the weakest regions of boundaries with a considerable level of free energy under the combined effect of structural and welding stresses. The leading role in this process is played by structural stresses. Depending upon the stressed state, development of the crack embryos may lead to delayed (periodic jump-like growth of crack alternating in pauses with processes of microcreep and segregation of hydrogen at the boundaries near the crack apex) or brittle fracture. These processes develop most intensively near the fusion line between dissimilar steels.

Microfractures formed along the grain boundaries in the case of aggressive environment may develop into intergranular stress corrosion cracking of metal, and lead to fracture of a composite welded joint. The rate of this process grows with increase in the quantity and thickness of martensitic interlayers, growth of austenite grains, as well as contamination of the weld metal with impurities that increase the free energy of the grain boundaries.

To improve performance of a composite welded joint, it is necessary to use the welding technology that would provide decrease in chemical and structural heterogeneity, and formation of brittle and decarburised intarlayers. Addition of an interlayer with a low carbon content, e.g. armco-iron (commercially pure iron), to the welded joint between the austenitic and ferritic metals is an efficient method for handling this problem. This does not only exclude the probability of formation of alloyed martensite with a sufficiently high carbon content, but also substantially decreases diffusion redistribution of carbon.

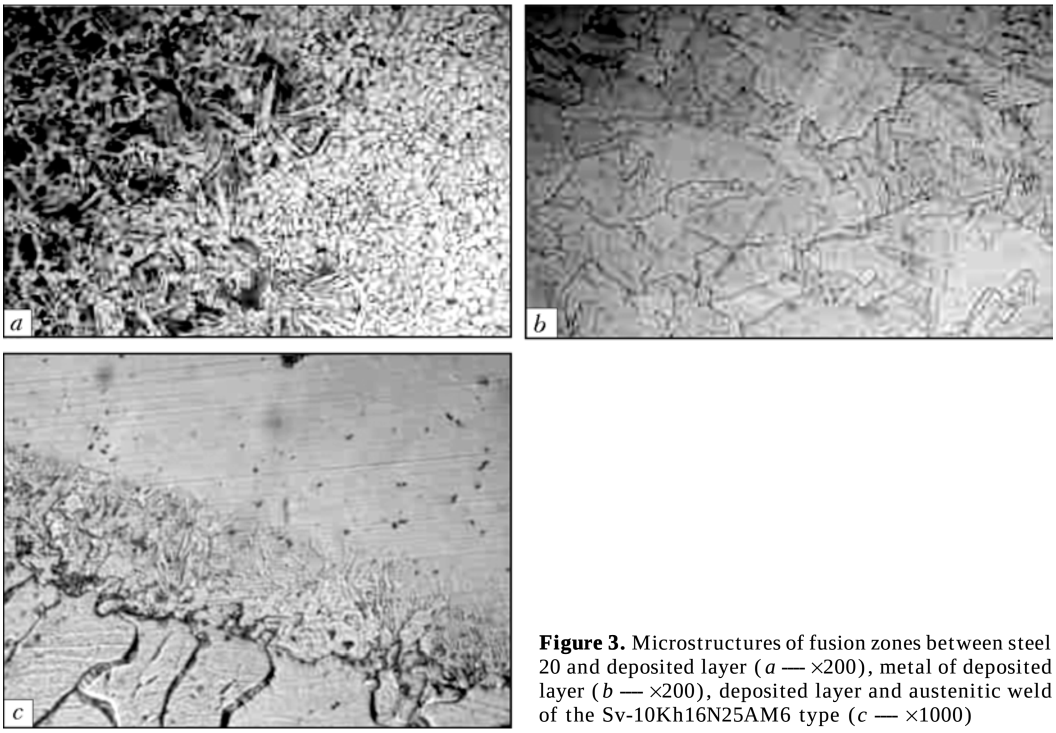

Figure 3. Microstructures of fusion zones between steel 20 and deposited layer (*a* — ×200), metal of deposited layer (*b* — ×200), deposited layer and austenitic weld of the Sv-10Kh16N25AM6 type (*c* — ×1000)

The intermediate layer can be deposited on the edge of the ferritic or austenitic pipe. However, the weld metal in this case should be austenitic or low-alloyed, respectively. The weld can also be made using metal with a low carbon content without preliminary deposition of the intermediate layer. However, this may cause difficulties with good weld formation.

Experiments were conducted on welded joints between steel 20 and austenitic steel 08Kh18N10T.

Deposition of low-alloyed metal on steel 20 results in the formation of:

• region of incomplete recrystallisation, where metal is heated to the temperatures of beginning of $\alpha \rightarrow \gamma$ phase transformation; here the structure is characterised by different grain sizes, i.e. coarse ferrite grains alternate with finer grains of ferrite and pearlite, which were formed as a result of partial transformation during heating of pearlitic regions;

• region of incomplete recrystallisation or normalisation, where metal acquires a fine-grained structure after phase recrystallisation (upper temperature limit of this region is about 1100 °C);

• coarse structure of large regions of ferrite and pearlite, called Widmanstatten structure, is formed in the overheated region near the deposited layer in steel 20;

• deposited layer near steel 20 has a fine-grained structure, and because of dilution with steel 20 this layer contains individual pearlitic regions (Figure 3, *a*);

• metal of the deposited layer has a pure ferritic structure with relatively coarse grains (Figure 3, *b*).

Depending upon the conditions of convective dilution of metal in the weld pool, transition from the deposited metal to weld of the Sv-10Kh16N25AM6 type may be of a sudden character, or there may be a layer with a finely dispersed structure (Figure 3, *c*). This layer is a metal formed as a result of incomplete melting of fragments of the deposited layer and its incomplete dilution with the austenitic weld metal. It is likely that formation of such interlayers in this case is affected by a higher melting temperature of the low-alloyed metal of the deposited layer (about 1530 °C, compared with 1380 °C of the austenitic metal) and narrow solidification range. No migration of carbon and no formation of decarburised interlayer in steel 20 were detected either.

Figure 4. Deposited layers of commercially pure iron on austenitic steel (×25)

Figure 5. Microstructure of the fusion zone between deposited layer and austenitic steel (×200)

As shown by the hardness measurement results, microregions with hardness close to that of the martensitic structure, as well as microregions with hardness characteristic of austenite are formed in the austenitic weld metal and deposited layer because of a different content of molten unalloyed and high-alloy deposited metals.

Figure 4 shows a variant of the composite welded joint with a layer of low-carbon metal deposited at a low level of heat input on the edge of austenitic steel, and the weld made by using a low-alloy filler metal. As more beads are deposited, etchability of the deposited metal increases as a result of decrease in the concentration of alloying elements coming from austenitic steel.

It should be noted that no zones with high hardness, which are characteristic of quenching structures, were formed with this steel–deposited layer combination. Variations in microhardness of the transition layer between the austenitic steel and deposited metal, observed in this case, are related to a non-uniform dilution of the materials being joined, and are in a range of HV 0.2-150–340. No substantial heterogeneity or defects were detected at the fusion line between austenitic steel and deposited layer (Figure 5). The similar situation was observed also at the fusion line between the low-alloy weld with the deposited layer and steel 20.

Results of mechanical tests of welded joints between dissimilar steels 20 and 08Kh18H10T, conducted according to GOST 6996–66, show that tensile strength of the GOST 6996–66 XIII type specimens ranges from 530 to 560 MPa and impact toughness KCU is 106–143 J / cm^2, and bending angle of the GOST 6996–66 XXVI type specimens is in a range of 160 to 180°. Fracture of the specimens in tensile tests in all the cases occurred in steel 20 at a distance of about 15 mm from the fusion line. These values meet requirements imposed on composite welded joints in NPP pipelines.

Evaluation of corrosion resistance of the suggested composite welded joints under service conditions is time-consuming. Accelerated tests of the specimens in chloride environments failed to reveal a clear intergranular fracture within the welded joint region. Corrosion in the weld metal develops more intensively than in the austenitic steel, but not faster than in the ferritic base metal.

Therefore, addition of an intermediate layer of low-carbon metal (commercial iron) to the welded joints between the austenitic and carbon steels allows elimination of formation of brittle alloyed martensite in the weld and decarburised interlayers in the HAZ metal. The welded joint with the above interlayer has increased corrosion resistance compared with the joint made according to the standard technology.

1. Zemzin, V.N. (1966) *Welded joints of dissimilar steels*. Moscow: Mashinostroenie.
2. Kasatkin, O.G. (1994) Peculiarities of hydrogen brittleness of high-strength steels in welding (Review). *Avtomatich. Svarka*, **1**, 3–7.

MECHANICAL PROPERTIES OF 1441 ALUMINIUM ALLOY JOINTS PRODUCES BY DIFFERENT WELDING PROCESSES

A.G. POKLYATSKY, A.Ya. ISHCHENKO, A.A. GRINYUK and **M.R. YAVORSKAYA**
E.O. Paton Electric Welding Institute, NASU, Kiev, Ukraine

Comparative analysis has been performed of the strength and hardness in joints of 1441 aluminium alloy produced by fusion and friction stir welding. It is shown that the process of producing the joint by metal plasticization without its melting allows avoiding formation of defects characteristic for the aluminium-lithium alloys and improving the tensile strength of welded joints. It is found that the welds made by friction stir welding are non-symmetrical relative to their longitudinal axis. It is established that fracture of samples at static testing occurs from the side, from which the metal is driven by the working tip of the tool.

Keywords: arc welding, friction stir welding, aluminium-lithium alloys, strength, hardness, mechanical properties

Special requirements are made of materials used in aerospace engineering welded structures in terms of providing minimum weight, high strength, long operating life and cost-effectiveness of welded structure operation. Meeting these requirements eventually defines the competitiveness of flying vehicles. Use of aluminium-lithium structural alloys with a low density and increased modulus of elasticity is the priority direction of improvement of modern flying vehicles [1, 2].

One of the most promising materials for manufacturing different components of such equipment is 1441 alloy of Al--Cu--Mg--Li alloying system that has the best adaptability at cold and hot deformation. The aluminium-base alloy has the following chemical composition, wt.%: 1.6 Cu; 1.1 Mg; 1.6 Li; 0.07 Zr; 0.04 Ti; 0.09 Fe; 0.03 Si; 0.05 Mn. A good proportion of the basic alloying element concentration with limited impurity content allows producing cold rolled sheets of up to 5 mm thickness by the technology similar to that which is used when manufacturing sheets from D16 alloy. The 1441 alloy sheets have high strength characteristics: tensile strength of 440 MPa, yield point of 330 MPa, relative elongation of 14.6 %, bending angle of 16°, alloy density of 2.6 g / cm^3, coefficient of elasticity of 78.4 GPa [2]. However, certain difficulties arise in fusion welding of this alloy promising for aircraft engineering.

Firstly, presence of lithium in its composition leads to formation of surface gas-saturated layer, promoting higher porosity formation in welded joints [3]. Secondly, in TIG welding it has high tendency of formation of extended oxide film inclusions in the welds [4], similar to all the lithium alloys. Thirdly, irreversibility of physicochemical processes occurring in weld pool under the influence of a high temperature heat source, leads to phase transformations and metal softening in welding zone [5]. As a result, 1441 alloy joints produced by fusion welding, have low mechanical properties. If heating of the joint zone to solidus temperature is removed from the technological process of alloy welding, it is possible to avoid these difficulties, eliminate the conditions for defect initiation and increase weld strength.

It is possible to produce permanent joints without melting the base metal by friction stir welding [6, 7]. The principle of weld formation with such a joining method is based on heating due to metal friction up to plastic state in welding zone, its stirring along the entire thickness of welded edges and plastic deformation as a result of pressing the work tool to the surfaces of parts being welded. The metal is not heated to melting temperature, so that the level of phase-structural transformations is much lower in the weld and in metal of HAZ than in fusion welding.

Sheets of 2 mm thickness were welded by the most widely accepted arc welding processes (Table 1), (namely, consumable electrode argon arc welding (MIG), nonconsumable electrode argon arc welding (TIG), nonconsumable electrode plasma arc welding (PAW) electron beam welding (EBW), as well as by friction stir welding (FSW) for comparative evaluation of mechanical properties, structure and hardness of 1441 alloy joints.

EBW was done at the current of 45 mA at accelerating voltage of 30 kV at the speed of 60 m / h. Filler wire of 1 mm diameter was fed at the rate of 180 m / h.

Table 1. Welding conditions for 2 mm sheets of 1441 alloy

Welding process	I_w, A	v_w, m / h	v_f, m / h	d_w, mm	Q_m, kg / min	U_a, V
MIG	55	30	105	1.6	--	17.2
TIG	150	14	75	1.6	--	–
PAW	165	36	110	1.6	0.3	–

Table 2. Mechanical properties of welded joints of 1441 alloy sheets 2 mm thick

Welding method	Filler wire	σ_t^{WJ}, MPa	σ_t^{WM}, MPa	δ, deg
MIG welding	SvAMg63	$\frac{320\text{--}309}{315}$	$\frac{280\text{--}269}{277}$	$\frac{70\text{--}64}{67}$
	Sv1201	$\frac{290\text{--}281}{284}$	$\frac{285\text{--}280}{284}$	$\frac{66\text{--}48}{57}$
TIG welding	SvAMg63	$\frac{315\text{--}312}{314}$	$\frac{288\text{--}280}{284}$	$\frac{136\text{--}132}{134}$
	1201 + 0.5 % Sc	$\frac{305\text{--}288}{293}$	$\frac{308\text{--}305}{304}$	$\frac{75\text{--}62}{68}$
PAW	SvAMg63	$\frac{306\text{--}303}{305}$	$\frac{267\text{--}263}{266}$	$\frac{170\text{--}140}{152}$
	Sv1201	$\frac{269\text{--}266}{267}$	$\frac{237\text{--}234}{235}$	$\frac{86\text{--}60}{73}$
EBW	SvAMg63	$\frac{288\text{--}285}{287}$	$\frac{257\text{--}254}{256}$	$\frac{86\text{--}77}{82}$
	Sv1201	$\frac{290\text{--}280}{285}$	$\frac{265\text{--}260}{262}$	$\frac{57\text{--}53}{55}$
FSW	–	$\frac{344\text{--}338}{341}$	$\frac{382\text{--}356}{366}$	$\frac{180\text{--}130}{155}$
	–	$\frac{417\text{--}415^*}{416}$	$\frac{439\text{--}436^*}{438}$	$\frac{58\text{--}54}{56}$

*Mechanical properties were obtained after artificial ageing of samples (150 °C for 24 h).

FSW was conducted at the speed of 14 m / h by a rotating with a frequency of 2880 rpm with shoulder diameter of 12 mm.

Standard samples for determination of ultimate strength and bending angle of welded joints were made from the produced butt joints. Weld metal strength was evaluated when testing samples of a reduced cross-section in the weld central part. In addition, the hardness distribution was determined in the welds and HAZ metal on some samples, and their structural peculiarities were also considered. The results of mechanical testing of samples produced by different welding processes are given in Table 2.

Analysis of the obtained results showed that in TIG and MIG welding using SvAMg63 filler wire, strength of welded joints of 1441 alloy sheets on the level of 315 MPa can be obtained, which is equal to about 72 % of base metal strength. Application of more concentrated heat sources shortens the time of welding pool existence, so that not all the gas bubbles have enough time to rise to its surface. Part of them in the form of fine pores stays in the zone of the weld fusion with the base metal, lowering the joint strength. Therefore, the welded joints produced with the same filler wire by PAW have the strength on the level of 305 MPa, and those made by the electron beam –– 287 MPa. Application of filler wire Sv1201 on the basis of copper alloying system gives lower strength values in the case of its modifying by scandium, although scandium positively influences the weld metal strength. In any case the weld has a cast structure in fusion welding and its strength values are lower than those of the welded joint.

Filler material is not used in FSW, and the weld is formed only from the base metal. Sample failure also runs along the zone of weld fusion with the base metal, but welded joints strength is on the level of 341 MPa and is equal to 78 % of welded sheet strength. The plasticized metal of the weld has the strength of about 366 MPa as a result of strain hardening, so that a certain weld depression, formed in FSW, does not influence the welded joint strength as a whole. Bend angle of such joints is on the level of that of the base metal and exceeds similar values obtained in fusion welding. Besides, artificial ageing of the produced joints after welding allows increasing their strength up to 416 MPa, which is equal to 95% of the sheet initial strength.

Higher strength of joints produced by FSW, is achieved due to the lower level of metal softening in the welding zone (Figure). Application of a high-temperature plasma jet leads to essential metal heating, as a result of which its hardness in the fusion zone changes from *HRB* 95 (from the side of the joint reinforcement) up to *HRB* 81 (in the root part). Cast weld metal has even lower hardness (*HRB* 76), but samples fail in the fusion zone, as the weld cross-section is increased due to reinforcement. No macroscopic metal melting occurs in FSW. It is heated only up to plastic state as a result of friction so that hardness distribution in the FS-welded samples made by FSW is indicative of a lower heat impact on all the sections of the welded joint. So, the minimum hardness is on the level of *HRB* 92 in the fusion zone of the weld with the base metal. Metal of the weld has higher hardness (*HRB* 95), as it is subjected to plastic deformation due to pressing of the tool to the surface of the welded sheets. As a result, sample fracture still runs along the zone of weld fusion with the base metal in any case despite a somewhat reduced working section of the weld.

In addition, the curve of hardness distribution shows that the weld produced by FSW is not symmetrical relative to its longitudinal axis. Such a shape of the weld results from that the plasticized metal from one (front) side is driven by the working tool tip to the other (rear) side. Fracture of welded samples at static testing occurs exactly from the front side.

After artificial ageing of the plasma-arc welded samples hardness of weld metal increases up to *HRB* 78, and in the zone of weld fusion with base metal up to *HRB* 95–99. Additional artificial ageing of the joints, produced by FSW, allows raising weld metal hardness up to *HRB* 104. Metal hardness in the zone of its fusion with the weld is on the level of *HRB* 103–107 that provides an essential increase of ultimate strength of the FS-welded joints.

CONCLUSIONS

1. Among the widely accepted fusion welding processes, the highest mechanical properties of lithium-containing aluminium 1441 alloy are achieved when using consumable and nonconsumable electrodes. The ultimate strength of such joints, produced using SvAMg63 filler wire, are on the level of 315 MPa, which is equal to about 72 % of the initial sheet strength. Application of high power density heat sources (electron beam and plasma jet) does not allow increasing this index because of high a tendency of 1441 alloy to porosity.

2. The level of the FS-welded joint softening decreases as weld formation occurs due to plastic deformation of the base metal without its melting. That is why the strength of welded joints increases up to 341 MPa and strength of strain-strengthened weld metal up to 366 MPa. The bend angle of welded joints is on the level of that of the base metal.

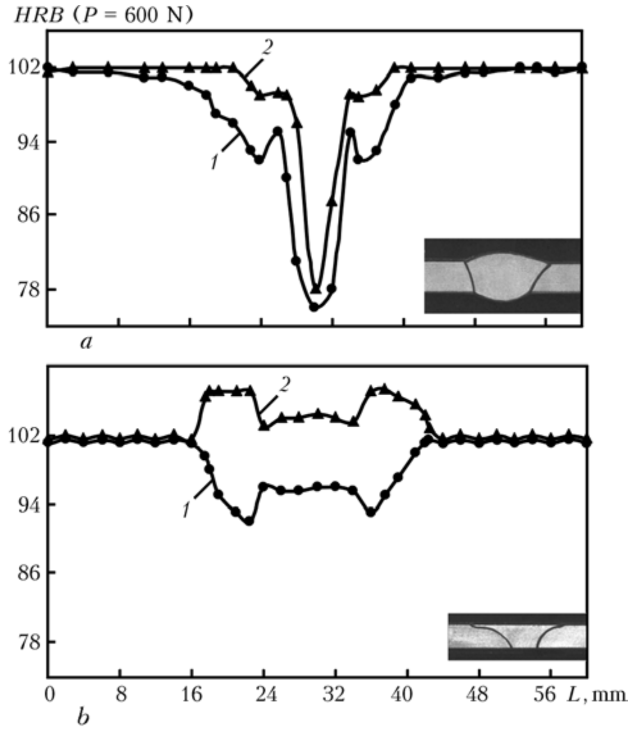

Hardness distribution in the 1441 alloy joints 2 mm thick produced by plasma-arc welding with different polarity asymmetrical current (*a*) and by FSW (*b*) after welding (*1*) and artificial aging (*2*)

1. Dmitriev, V.G., Zamula, G.N., Konovalov, V.V. et al. (2003) Priority trends of improvement of materials for structures of advanced aircraft. *Tekhnologiya Lyog. Splavov*, **1**, 3–8.
2. Fridlyander, I.N., Sadkov, V.V., Sandler, V.S. et al. (2002) Properties of semi-finished products of advanced Al–Li alloy 1441. *Ibid*., **4**, 24–26.
3. Ilyushenko, R.V. (1990) Influence of parameters of pulsed argon-arc welding on porosity of alloy 1420 joints. *Avtomatich. Svarka*, **9**, 27–30.
4. Poklyatsky, A.G., Lozovskaya, A.V., Grinyuk, A.A. (2002) Prevention of formation of oxide films in welds on Li-containing aluminium alloys. *The Paton Welding J*., **12**, 39–42.
5. Lozovskaya, A.V., Chajka, A.A., Bondarev, A.A. et al. (2001) Softening of high-strength aluminium alloys in different fusion welding processes. *The Paton Welding J*., **3**, 13–17.
6. Dawes, C.J., Thomas, W.M. (1996) Friction stir process welded aluminum alloys. *Welding J*., **3**, 41–45.
7. Stepanov, V.V., Konkevich, V.Yu., Frolov, V.A. (2003) Formation of joints in friction stir welding. *Tekhnologiya Lyog. Splavov*, **1**, 58–67.

NDT OF WELDED JOINTS

FLAW DETECTION IN WELDED JOINTS OF A TANK FOR LIQUID AMMONIA STORAGE

V.A. TROITSKY[1], **Yu.N. POSYPAJKO**[1], **I.Ya. SHEVCHENKO**[1], **V.I. KARMAZIN**[2] and **G.E. KOSTENKO**[2]
[1]E.O. Paton Electric Welding Institute, NASU, Kiev, Ukraine
[2]CJSC «Severodonetsk Obiedinenie «Azot», Severodonetsk, Ukraine

The paper presents the main kinds of diagnostics of welded joints at comprehensive technical examination of large-volume tanks for liquid ammonia storage with the purpose of extension of their service life, namely visual-optical inspection, including detection and evaluation of unevenness on the wall and bottom, more precise determination of the scope of application of other control techniques; NDT of welded joints and metal of the tank wall and bottom by ultrasonic, magnetic particle and liquid penetrant testing; determination of mechanical characteristics of the metal; metallographic examination and chemical analysis of the welded joint and base metal.

Keywords: nondestructive testing methods, flaw detection in welded joints, visual-optical, ultrasonic, magnetic-particle inspection, liquid penetrant testing, mechanical characteristics, metallographic examination, chemical analysis, welded tank

Technical diagnostics of large-capacity welded tanks, which are in long-term service, allows evaluation of their technical condition, possibility of further safe operation, as well as determination of the need for repair of individual components. An important stage of tank examination is flaw detection in their welded joints.

PWI Department of Nondestructive Testing of Welded Metal Structures together with the Research Laboratory of Metals and Technical Diagnostics of CJSC «Severodonetsk Obiedinenie «Azot» performed flaw detection of welded joints of inner tank of isothermal liquid ammonia storage in CJSC «Severodonetsk Obiedinenie «Azot», which included the following stages:

• visual-optical control of the tank inner surface, detection and assessment of unevenness (bulges, dents, delaminations, etc.) on the wall and bottom of the inner tank, and more precise determination of the scope of application of other kinds of control;

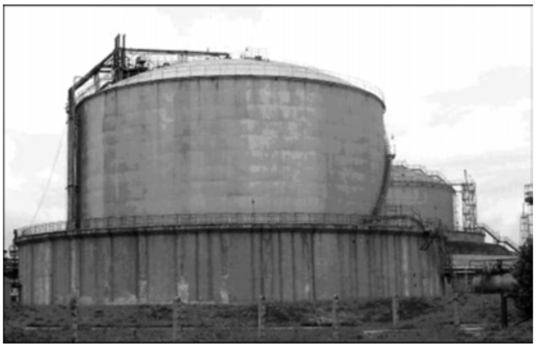

General view of the welded tank for liquid ammonia storage

• ultrasonic, magnetic-particle and liquid penetrant testing of welded joints of the bottom and wall of the inner tank at the height of the 1st girth;

• determination of mechanical characteristics of the metal on samples, cut out of the bottom;

• metallographic examination of welded joints on samples cut out of the bottom, as well as wall metal in the points of weld intersection between the 1st and 2nd girths by the replica method;

• chemical analysis of the metal, including quantitative analysis of hydrogen content in it.

The norms on which the integrated technical examination and flaw detection of tanks of isothermal liquid ammonia storage are based, are standards and instructions valid in chemical production [1, 2] and concerning individual inspection techniques.

The isothermal liquid ammonia storage is designed as a double-wall vertical cylindrical tank made by sheet-by-sheet method, which is located in a concrete casement (Figure).

Inner tank where liquid ammonia is directly stored, is made of low-alloyed steel and is designed for hydrostatic load of the stored product and external pressure of the bulk thermal insulation material. It is located inside the outer tank. The inner tank wall is assembled of large-sized (about 2×6 m) sheets of steel N-TVF33 (Japan), its local analog being 16GS steel, and the bottom is made of N-TVF30N steel (Japan), local analog being 09G2S steel. All the joints were butt welded.

The thickness of the tank inner wall is equal to 16–14–13–12–10–10–10–10–12–12 mm by girths with 10 girths altogether each of 2000–2050 mm height.

The interwall space between the outer and inner tanks is filled with thermal insulation from Circulite.

Manholes are envisaged in the wall lower part and on the roof to perform work inside the storage.

Inner tank specification

Bottom diameter, mm	30050
Wall height, mm	21000
Capacity, m^3	16846
Stored product weight, t	10000
Stored product temperature, °C	–33
Pressure in the tank, kPa	3–7

Isothermal liquid ammonia storage was manufactured element-by-element and mounted in 1973–1974.

Visual inspection of the inner tank was conducted in compliance with the requirements of DSTU ISO 17637–2003 [3], in order to determine the availability and dimensions of defects or damage in the base metal and welded joints, as well as reveal the inadmissible visible deformation of structural elements. Types and dimensions of inadmissible defects of the base and weld metal are specified in item 5.2.9 of DSTU 4046–2001 [1]. Geometrical dimensions of the welds (butt, overlap and fillet) were checked for compliance to the requirements of GOST 5264–80 [4].

Before testing, the surface of the welds and HAZ on the width of 100 mm from the weld was scraped using soft emery grinders. Roughness of the scraped surfaces was not more than *Ra* 12.5 (*Rz* 80).

The following auxiliary equipment was used at visual examination: examination magnifiers (two- and three-times magnification), measurement magnifiers, metal scale bars, slide calipers, versatile welder's templates UShS-3, metal and hair brushes for scraping, portable lamps, markers, binoculars for examination of the wall and roof metal structures.

As a result of thorough visual inspection, it was established that inadmissible defects in the base and weld metal were absent, and the geometrical dimensions of the latter did not always meet the requirements of GOST 5264–80 [4], however, their repair using welding was regarded to be impractical. Geometrical dimensions of the weld in one of the sections of about 100 mm length differed greatly from the requirements set forth in Table 53 of GOST 5264–80 [4] (horizontal leg of about 2 mm, penetration of 2–3 mm). The section was rejected and repaired by welding after mechanical removal of weld metal.

The bottom of the inner tank had bulges and delaminations of up to 100 mm height and 4–20 m^2 area, formed as a result of residual deformation after commissioning tests. 9th and 10th girths of the tank wall had two bulges of the size of approximately 1.5 × × 4.0 m and about 200 mm height, partially spreading to the cupola-shaped roof. The bulges did not have any rough bends, fractures or ruptures.

Magnetic-particle inspection was performed in keeping with the requirements of the norms [5–8] to reveal the surface and subsurface cracks of different origin, hairlines, tears, rolls, lacks-of-penetration and other defects of welded joints and HAZ. When developing the instructions [8], many-year experience of PWI activity in the magnetic-particle testing field [9] was used in addition to the norms [5–7].

Magnetic-particle inspection was performed on all the welded joints of the inner tank bottom and selective control was conducted on the vertical butt welded joints of the 1st girth and horizontal joints of the 1st and 2nd girths of the wall. Magnetic-particle inspection was performed using magnetization devices of flaw detectors Parker (USA) and PMD-70 (NPO «Volna», Moldova).

Method of control in the applied field was used. The longitudinal (pole) magnetizing was performed using an attached electric magnet. Intensity of the magnetic field between the poles was not less than 80 A / cm. Magnetic powder Ferromor of Ely Chemical, Great Britain, was applied onto the controlled surface by the «dry» process. White background contrasting with the magnetic powder was created by applying a white chalk suspension in an aerosol packing made by SPC «IFKh-Kolor», Kiev.

Operability of the magnetic-particle control system was checked using control samples, namely Berthold sample and factory control sample from the set of PMD-70 flaw detector. Results of magnetic-particle inspection confirmed the absence of inadmissible defects in the metal of the weld and HAZ.

Ultrasonic testing (UT) was conducted in keeping with the codes [10–12] to detect the inner plane and volume defects. When developing the instructions [12], many-year experience of PWI activity in UT field [13] was used in addition to the codes [10, 11].

All the welded joints of the bottom, as well as vertical and horizontal butt welded joints of the sheets of the 1st girth of the inner tank wall were subjected to UT, which was performed using flaw detectors USN-52 (Krautkramer, Germany) and UD2-12 (SPA «Volna», Moldova). Direct and inclined TR transducers with the working frequency of 2.5–5.0 MHz and angle of incidence of 45° were used for this method. Inclined transducers used to control overlap welds were specially manufactured at PWI. The main control parameters were checked on test blocks from KOU-2 kit [10].

Setting up of the flaw detector and control parameters was performed on test blocks with artificial reflectors of the specified dimensions and location.

The following techniques of control with the inclined transducer were used: direct beam (for revealing defects in weld root) and echo signal (for revealing defects in the weld middle and upper part).

Special gel-like couplant of MR-Chemie, Germany, was used to ensure acoustic contact of the transducer with the metal surface.

Flaw detector preparation included setting up the scanning speed, sensitivity, depth meter and setting the control zone. Quality was evaluated in keeping with SNiP 3.03.01–87 [14].

UT did not reveal any inadmissible defects in welded joints of inner tank wall (on 1st girth level) or in the chime welded joint, either.

A section of the bottom overlap joint of about 700 mm length was classified as an inadmissible defect. After mechanical cutting out of the weld metal this section was repaired using welding and checked by liquid penetrant testing and UT.

Liquid penetrant testing for revealing any defects visible or difficult to see by a naked eye of the type of material discontinuities coming to the surface (cracks, pores, lacks-of-penetration, etc.), was conducted in keeping with the requirements of GOST 18442–80 [15] and OST 26-5–88 [16]. Capillary control was performed on all the welded joints joining the nozzles and manholes and selective control — of overlap joints of the bottom, vertical butt welded joints of the wall, as well as the surface of the manhole ring, on which the plug is mounted.

Liquid penetrant testing was performed with flaw detection materials of MR-Chemie, Germany, in aerosol package — MR-68C penetrant, MR-85 cleaner, MR-70 developer. Testing method was luminous-colour using KD-33L luminous lamp (SPA «Volna», Moldova). Materials sensitivity was checked on a reference sample, made in keeping with the requirements of GOST 23349–78 [17].

No inadmissible defects were revealed in welded joints of the wall and bottom, as a result of liquid penetrant testing. Cavities were found in the lower part of the circumferential weld of inlet nozzles, which were revealed at weld scraping. Deposited weld metal in the cavity zone was removed by grinding with an abrasive wheel up to complete disappearance of the cavity traces, and then welding up of the weld, and subsequent capillary control were performed.

Mechanical characteristics of the metal were determined in the laboratory on samples cut out of the bottom sheets (GOST 6996–66 [18]). Tensile testing of the metal was performed on type I samples of 3 mm diameter using IM-4R testing machine, and impact toughness testing was performed on VII type samples with a V-shaped notch (at –20 °C temperature) with application of pendulum impact machine MK-30M. Yield point was 300–320 MPa, ultimate tensile strength was 440–445 MPa, relative elongation was 36–39 %, impact toughness — $(250–285)\cdot 10^6$ J / m^2.

Metallographic examination was conducted to study the macro- and microstructure of the weld and base metal under the laboratory conditions on six samples, cut out of the inner tank bottom. Samples were treated by grinding with diamond pastes and etching in 10 % alcohol solution of nitric acid.

No cracks, tears or other defects were found in the welded joints at weld metal macroanalysis. The gap between the plates in the overlap welded joint was equal to 0.2–1.5 mm, which met the requirements of GOST 5264–80 (Table 53, weld type N1).

Examination of welded joint microsections revealed whisker wormholes of up to 0.8 mm depth filled with corrosion products in the weld root in some samples. Their edges had a round shape without cracks. Such cavities formed, most probably, as a result of gases and metal vapours escaping from the weld pool in welding.

The structure of weld metal and HAZ is ferritic-pearlitic, fine-grained. Columnar crystals are visible in the section located in the weld upper part. Ferrite structure is acicular. In the weld root the weld structure is fine-grained.

Metallographic examination of the weld and base metal of the inner tank wall were conducted by the method of obtaining a surface imprint using polystyrol replicas or portable microscope «Neophot 21» (without cutting the samples out of the wall). Nine zones (sections) in the points of T-shaped intersections of vertical welds of the 1st and 2nd girths of the wall with the horizontal weld were prepared for examination.

Structure of the weld and base metal of the inner tank wall is ferritic-pearlitic. Grain size corresponded to 8–9 points (GOST 5639–82). Surface macrocracks were found in one of the sections, which disappeared at grinding to 0.2 mm depth, as well as micropore clusters.

Metallographic examination revealed that the microstructure, grain size, condition of intergranular boundaries in the weld and base metal of the inner tank bottom and wall, are typical for low-carbon steels and their welded joints. No signs of metal ageing were found.

Composition of samples cut out of the inner tank wall, showed that the metal corresponds to the local analog — 09G2S steel (GOST 5520–79) and has the following composition, wt.%: Fe 98; C 0.13; Si 0.29; Mn 1.35; Cr 0.001; Mo 0.014; Ni 0.065; Al 0.047; Co 0.065; Cu 0.02; Nb 0.0007; Ti 0.013; V 0.037.

Chemical analysis was used to establish the hydrogen content in the bottom metal, which is equal to 0.0005–0.0006 wt.%.

NDT technologies selected by us demonstrated their effectiveness during storage examination, this allowing performance of the required repair and extending the storage life for another five years.

1. *DSTU 4046–2001*: Technological petroleum refining, petrochemical and chemical plant equipment. Technical diagnostics. General technical requirements. Introd. 01.01.2002.
2. *RD 03-410–2001*: Instructions on carrying out complex technical examination of isothermal liquefied gas tanks. Introd. 01.01.2002.
3. *DSTU ISO 17637–2003*: Nondestructive testing of welds. Visual examination of joints made by fusion welding. Introd. 01.01.2004.
4. *GOST 5264–80*: Manual arc welding. Welded joints. Main types, structural elements and sizes. Introd. 01.01.81.
5. *GOST 21105–87*: Nondestructive testing. Magnetic-particle method. Introd. 01.01.88.
6. *DSTU 2954–94*: Steel. Methods of magnetic inspection. Introd. 01.01.96.
7. *OST 26-01–84*: Welds of steel pressure vessels and apparatuses. Procedure of magnetic-particle inspection method. Introd. 01.07.85.
8. (2003) *Technological instruction on magnetic-particle inspection of welded joints of isothermal tank bottoms*. Kiev: PWI.
9. Troitsky, V.A. (2002) *Magnetic-particle inspection of welded joints and machine parts*. Kiev: Feniks.
10. *GOST 14782–86*: Nondestructive testing. Welds. Ultrasonic methods. Introd. 01.01.88.
11. *GSTU 3-057–2003*: Pressure vessels and apparatuses. Procedure of ultrasonic testing of welded joints. Introd. 01.01.2004.
12. (2003) *Technological instruction on ultrasonic testing of overlap and fillet welded joints of isothermal tank bottoms*. Kiev: PWI.
13. Troitsky, V.A. (1997) *Concise manual on quality control of welded joints*. Kiev: PWI.
14. *SNiP 3.03.01–87*: Load-carrying structures and enclosures. Introd. 01.07.88.
15. *GOST 18442–80*: Nondestructive testing. Liquid penetrant methods. General requirements. Introd. 01.07.81.
16. *OST 26-5–88*: Nondestructive testing. Color method of testing of welded joints, deposited and parent metal. Introd. 01.07.89.
17. *GOST 23349–78*: Nondestructive testing. Capillary detectors. General technical requirements and testing methods. Introd. 01.01.81.
18. *GOST 6996–66*: Welded joints. Methods of determination of mechanical properties. Introd. 01.01.67.

METHOD FOR INCREASING CYCLIC AND SERVICE LIFE OF WELDED STEEL STRUCTURES

V.S. KOVALCHUK, V.V. KNYSH, V.D. POZNYAKOV and **S.B. KASATKIN**
E.O. Paton Electric Welding Institute, NASU, Kiev, Ukraine

A method for increasing fatigue resistance of welded joints of plate steel in initial state and after repair welding of remote fatigue cracks according to standard technology, using recommended consumables with subsequent facing of the welds by austenite-martensite wire Kh10N10 that induces favorable residual compressive stresses, is suggested. It is determined that cyclic life of welded joints in steel 09G2S, made and repaired according to the suggested technology, increases 5–7 times in comparison with that achieved in case of using standard technology.

K e y w o r d s : cyclic life, welded joints, facing welds, residual compressive stresses

In the elements of railway and motor-road bridges, crane girders, ships, drilling platforms, other industrial structures, and in components of machines of transport and energy engineering industry fatigue cracks occur after a certain period of operation under conditions of complex cyclic loads. One may assume that main reasons of their premature origination and accelerated development in metal structures are additional local vibrations of certain elements, which are imposed on the main variable loads, and residual welding stresses that are not taken into account when designing the structures. Confirmation of this may be span structures of railway bridges [1], built in 1950–1980s. In the bridges, built in the earlier period, mainly attachments of cross and longitudinal linkages are affected by fatigue cracks because of their vibration during passage of the rolling stock. In the bridges, built in the second half of mentioned period according to the standard designs, in which freeing of the chords of main girders from welding to them of centering plates, stiffening ribs, and linkages in the walls of girders was envisaged, had place significant additional bending stresses, which were caused by side shifting and vibrations. As a result focuses of origination of fatigues cracks became ends of the welds near cut-outs of vertical stiffening ribs, where welding tensile residual stresses achieved yield strength values of the base metal. Such cracks usually propagate along walls of main girders, but in case of their turn and propagation across the girders they represent even greater hazard, especially in winter, when under conditions of low temperatures even relatively small fatigue cracks in the span structures may initiate brittle failure at low rated stresses. At present in many countries, including Ukraine, many bridges, having fatigue cracks, are in operation. In the same state is the rolling stock, which has exhausted to significant degree its design service life.

In this connection an actual issue is increase of fatigue resistance of welded structures at the stages of their designing, manufacturing, and after their repair, in the course of which metal around a fatigue crack is removed for extension of the service life of the items, and welding-up of the damages is performed.

Different methods of increasing cyclic life of welded joints exist. As a rule they are based on removal of tensile residual stresses or artificial induction of favorable compressive stresses after termination of welding works, which worsens adaptability to manufacture and increases time and cost of manufacturing and repairing metal structures. Mentioned shortcomings are removed by the method of increasing fatigue resistance by induction of compressive stresses in the process of welding, suggested by Japanese researchers [2].

They made assumption that application of a welding wire with low temperature of interphase transformation (re-solidification) can enable efficient reduction of residual tensile stresses.

It is known [3] that in the Fe–Ni–Cr triple system temperature of phase transformations in solid state, connected with transformation of one class of solid solutions into the other one, depends upon the weight share of these metals (Figure 1). If the solid solution consists of 10 wt.% Cr, 10 wt.% Ni and 80 wt.% Fe, re-solidification of such metal occurs within the range of low (200–50 °C) temperatures. In welding by the wire of mentioned composition process of interphase transformation of austenite into martensite ($\gamma \rightarrow \alpha$) causes expansion of the weld metal at the final stage of cooling and, as a result, occurrence of favorable residual compression stresses in the welded joint zone.

According to [4], fulfillment of welding with application of wire of mentioned composition allows increasing fatigue resistance of steel joints almost twofold. However, wide application of this wire for welding of steels of different classes of strength has certain shortcomings. Mechanical characteristics of the weld metal are determined to a significant degree by the filler material and may significantly differ from those of the base metal, which often causes occurrence of cold cracks in the joints, especially in welding of the weld root [5], and reduction of resistance to brittle

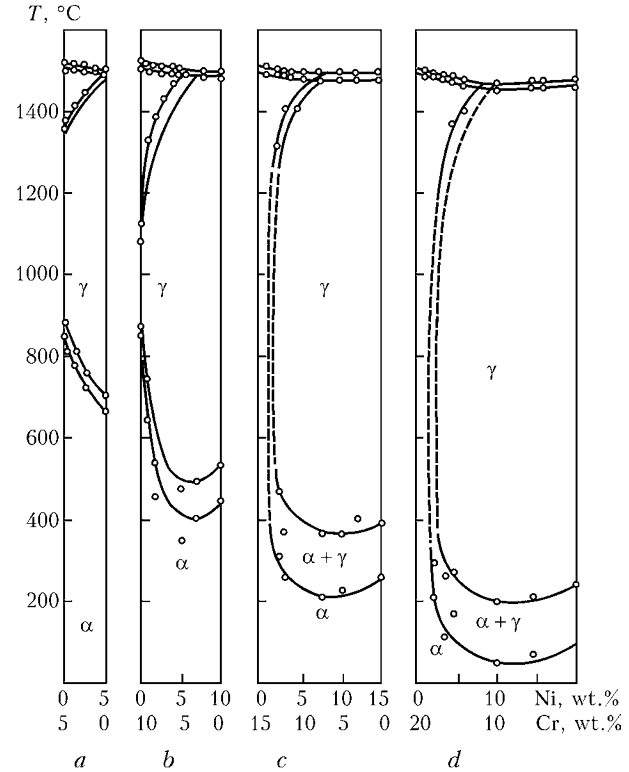

Figure 1. Polythermal sections of Fe–Ni--Cr triple system alloys: *a* — 95; *b* — 90; *c* — 85; *d* — 80 wt.% Fe

failure. It should be also noted that high cost of the welding wire reduces economical efficiency of manufacturing and repairing plate structures.

Taking into account mentioned above it is assumed that for increasing fatigue resistance of the welded joints one should not make all layers of a multilayer weld by chromium-nickel consumables. It is suggested to make welding of the multilayer welds and welding-up of the zone with remote fatigue cracks according to the standard technology, using recommended consumables, and the last (facing) welds — by austenite-martensite wire.

For estimating fatigue resistance of welded joints, made according to suggested in this work technology, specimens of cruciform shape from plate steel 09G2S were manufactured (Figure 2), which had high concentration of stresses and tensile residual stresses in initial state in case of using standard technology of production. All welds on longitudinal ribs of the specimens on the left side of axis OO' and internal welds on its right side (Figure 2, *a*) were made by manual welding with complete penetration, using stick electrodes UONI-13 / 55, and facing welds on the ribs on right side of the axis OO' — by austenite-martensite wire Kh10N10 of 1.6 mm diameter in CO_2 with application of a semi-automatic welding machine.

Such structure of the specimen and technology of manufacturing allowed determining fatigue resistance of the joints in initial state and after facing, as well as after repair welding and repair welding and facing on the same specimens and under the same conditions of loading. Fatigue tests of the specimens were performed under soft conditions from zero single-frequency axial tension on servo-hydraulic machine URS 200 / 20. A developing fatigue crack of 20 mm length was used as a criterion for termination of the test. In the process of tests the fatigue cracks originated over the line of fusion of the weld with the base metal in the joints, produced with application of electrodes UONI-13 / 55. After the crack achieved critical length the tests were stopped, metal with the fatigue crack was removed by the finger-type cutter, and formed recess was welded-up by the electrodes UONI-13 / 55.

In the specimens, designated for obtaining data on fatigue resistance of joints after repair welding according to the standard technology, full welding-up of the prepared cracks was performed by electrodes UONI-13 / 55. In all other specimens welding-up by the electrodes was performed flush with plane of the specimen, and the last (facing) weld was performed

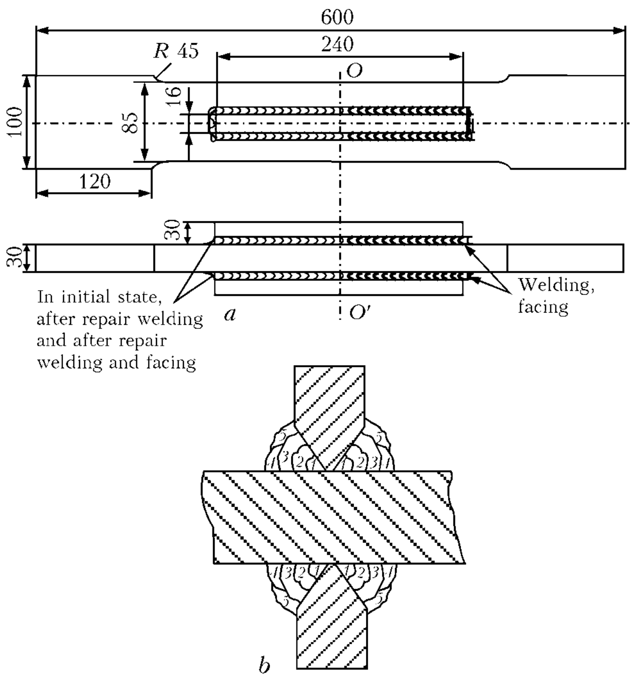

Figure 2. Scheme of specimen for estimating fatigue resistance efficiency of facing welds by wire Kh10N10 of new and repaired welded joints in case of single-frequency loading (*a*), and scheme of welding (*b*): *1* — first pass (weld root); *2* — center part; *3* — welding-up of groove using electrodes UONI-13 / 55; *4, 5* — facing welds made using wire Kh10N10 in CO_2

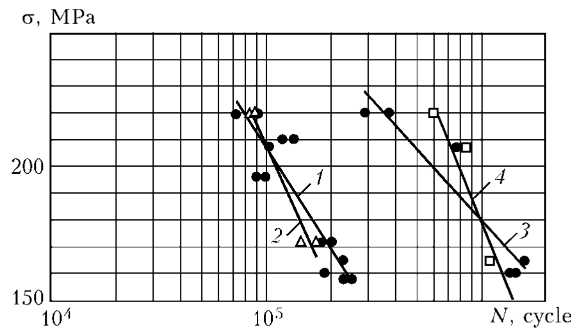

Figure 3. Fatigue resistance of welded joints of steel 09G2S with longitudinal stiffening ribs (see Figure 2): *1* — initial welding technology; *2* — after first repair welding according to initial technology; *3* — welding with facing welds; *4* — after first repair welding with facing by wire Kh10N10; *N* — number of loading cycles; σ — maximal stresses

by austenite-martensite wire, whereby facing welds started and terminated on longitudinal part of the ribs.

Subsequent tests after the repair were continued under the originally assigned conditions of loading till formation of fatigue cracks of assigned critical dimensions in the repaired and initially strengthened by the facing joints. Obtained fatigue test results of the specimens, presented in Figure 3, showed that repair welding according to the standard technology allowed practically restoring initial cyclic life of the welded joints with high level of tensile residual welding stresses and peculiar for this type of joints concentration of stresses. In case if welding in fabrication or repair of metal structures is performed in combination with facing of the produced joints by austenite-martensite wire, cyclic life of the metal structures with such joints may be increased 5–7 times.

CONCLUSIONS

1. Application of austenite-martensite wire with low temperature of interphase $\gamma \to \alpha$ transformation in welding of low-alloyed steels allows significant increasing fatigue resistance of the joints.

2. Proposed technology of welding joints from plate steel, using standard consumables and facing of the welds by austenite-martensite wire, in contrast to the welding with only austenite-martensite wire, excludes occurrence of internal cracks and, therefore, increases cyclic life of the joints and reduces expenses, connected with production and repair of welded metal structures.

3. Cyclic life of welded joints of steel 09G2S with high level of residual welding stresses, made and repaired according to the suggested technology, increases 5–7 times in comparison with that, achieved in case of using standard welding technology.

1. Mirolyubov, Yu.P., Panin, E.I., Frolov, V.V. et al. (1983) Fatigue cracks in welded continuous wall spans. In: *Problems of design and service of artificial buildings*. Leningrad: LIIZhT.
2. Ohta, A., Suzuki, N., Maeda, Y. (1996) Effective means for improving the fatigue strength of welded structures. *Welding in the World*, **37**, 84–89.
3. Kornilov, I.I. (1956) *Ferroalloys*. Vol. 1: Alloys of iron–chrome–nickel system. Moscow: AN SSSR.
4. Ohta, A., Maeda, Y., Suzuki, N. (2000) Fatigue life extension by repairing fatigue cracks initiated around box welds with low transformation temperature welding wire. *IIW Doc. XIII-1835–2000*.
5. Mazel, Yu.A. (2002) 10 % Cr–10 % Ni martensitic welding wires with a low temperature of the $\gamma \to \alpha$ transformation. *Svarochn. Proizvodstvo*, 49(**12**), 10–13.

CONTROLLER OF METAL POOL LEVEL IN ESW

Yu.N. LANKIN

E.O. Paton Electric Welding Institute, NASU, Kiev, Ukraine

Structural scheme is presented and a system for the metal pool level control in ESW with application of the inductive sensor, containing a measuring fast-response transducer, is described. The system has passed laboratory tests that confirmed its design characteristics.

Keywords: electroslag welding, molten metal pool, pool level, automatic control

According to the adopted classification electroslag welding (ESW) machines relate to the automatic welding machines. However, during welding some ESW parameters require for constant manual correction. To the mentioned parameters relate, first of all, speed of movement of the carriage, on which the machine is installed, or electrode wire feed rate. It is caused by the fact that it is very difficult to coordinate these parameters in such way that the resulting speed of movement of the welding pool surface to be in exact correspondence with the speed of movement of the forming sliders. Even if one manages to coordinates these speeds, equality of speeds of the sliders and the welding pool surface will be violated and manual correction of the welding parameters will be required because of excitations, which act on the welding process. The list of excitations is rather big — change of the welding gap width because of inaccurate assembly and welding deformations, fluctuations of voltage in the mains, instability of fit of the sliders, etc. Maladjustment of the movement speeds of the welding machine and speed of movement of the welding pool surface may cause in extreme cases pouring of the slag pool from above or the metal pool from below of the forming sliders. Difficulties of manual correction of the welding machine movement increase together with increase of the welding speed. At welding speeds above 5 m / h manual maintenance of the metal pool level relative a moving slider becomes practically impossible.

Several systems of the metal pool level control in ESW are known from the literature sources, which differ by types of the level sensors and the controller. Control systems with electric contact sensors, thermocouple, radioisotope, and different induction sensors are proposed [1–3]. In practice systems for controlling the pool level with an electric contact sensor and a linear controller [1] and with an induction sensor and a relay two-position controller [2, 3] were implemented.

In the described system for controlling the metal pool level (Figure 1) an inductive sensor, containing a new measuring transducer, was used. The sensor is supplied by sinusoidal voltage with frequency above

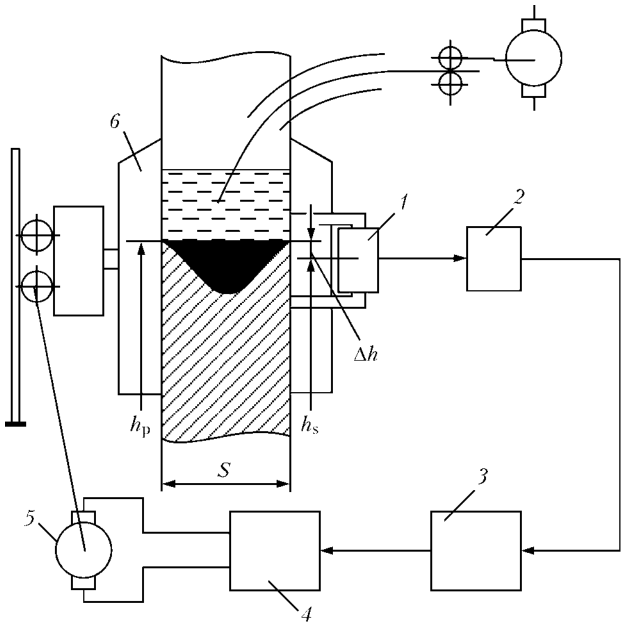

Figure 1. Functional scheme of system for automatic stabilization of metal pool level in ESW: *1* — sensor; *2* — measuring transducer; *3* — controller; *4* — engine control unit; *5* — engine for movement of welding carriage; *6* — slider; h_p — level of metal pool; h_s — position of slider (level sensor); Δh — error of pool level control

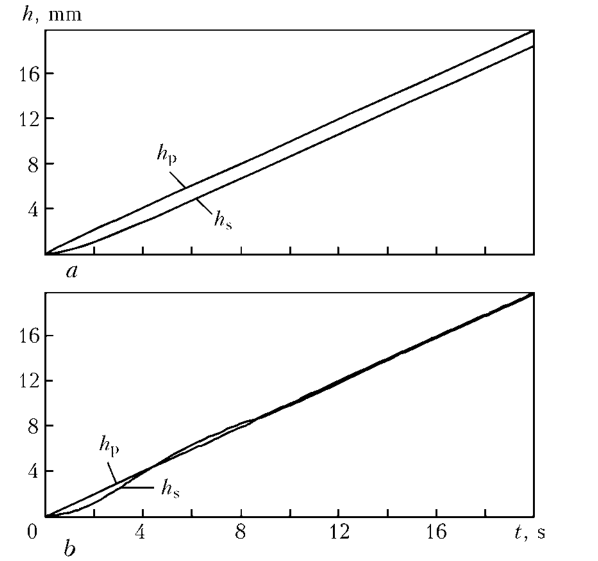

Figure 3. Tracking curves of system for controlling change of metal pool level: *a* — P-controller (K_c = 10); *b* — PI-controller (K_c = = 10, T_c = 10 s)

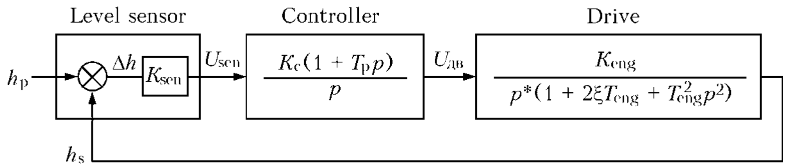

Figure 2. Structural scheme of control system

10 kHz, and frequency of output voltage pulses of the measuring transducer is more than 20 kHz. For efficient suppression of such pulsations it is sufficient to have the simplest filter with the time constant not more than 5 ms, that's why one may consider this sensor with the measuring transducer a fast-response one. In the real working measurement range linear characteristic of the sensor with the transducer has transfer factor K_{sen} = 0.1 V / mm.

As a drive for movement of the carriage, the drive, described in [4], was used. Analysis of transition processes in the drive speed allows approximating it by the fluctuation element with the transfer factor K_{eng} = = 0.5 mm / (s·V), time constant T_{eng} = 0.025 s, and attenuation factor ξ = 0.35.

Structural scheme of the level control system is presented in Figure 2. For generality the proportional-integral (PI) controller is presented on the scheme. Due to presence of the carriage engine in the control loop, the object of control has astatism of first order. So, even in case of using the simplest proportional (P) controller (T_c = 0), the system ensures zero error of stabilization of the metal pool level and excellent dynamic characteristics of control. However, during welding the metal pool level continuously increases because of melting of the electrodes, i.e. the system should work as a tracking one. In this case the tracking error occurs, which is directly proportional to the rate of change of the metal pool level and inversely proportional to the transfer factor of the controller K_c (Figure 3, *a*). The tracking error can be brought to zero by using the PI-controller. In Figure 3, *b* tracking curves of the pool level for the PI-controller with K_c = = 10 and T_c = 10 s are presented. Implementation of the analogue integrator with the integration constant not less than 10 s is rather difficult task. It is much simpler to increase transfer factor of the P-controller up to the value, at which a tracking error is reduced down to the acceptable level. Parameters of the control system are such that the transfer factor may be increased up to a significant level without loss of the system stability. As one can see from Figure 3, *a*, at K_c = 10 error of tracking level of the pool Δh, which moves at speed 1 mm / s (3.6 m / h), is 1.3 mm. Increase of K_c up to 50 reduces error of the pool level tracking down to 0.23 mm, which is more than sufficient for ESW. As transfer factor of the P-controller increases, proportionally reduces response time of excitations and controlling actions.

System of control of the metal pool level has passed laboratory tests, which confirmed its design characteristics.

1. (1959) *Electroslag welding*. Ed. by B.E. Paton. Kiev: Mashgiz.
2. (1986) *Automation of welding processes*. Ed. by V.K. Lebedev, V.P. Chernysh. Kiev: Vyshcha Shkola.
3. Bondarenko, O.P., Popovsky, V.Yu. (1988) Control of metal level in processes of electroslag technology. In: *Automatic control of processes of welding and coating deposition*. Kiev: PWI, 65–72.
4. Lankin, Yu.N., Masalov, Yu.A., Bajshtruk, E.N. (2006) Schematic for control of welding machine drives. *The Paton Welding J.*, **7**, 50–51.

NEWS

NKMZ SUMMED UP RESULTS OF ITS ACTIVITY IN 2006

Novo-Kramatorsk Machine-Building Plant (NKMZ), Kramatorsk, Donetsk region, as said at the press-conference on 26th of January President of the Company G.M. Skudar, finished the year 2006 with growth of the commodity production relative the year 2005 by 29.5 %. Average salary increased up to UAH 2212. Personnel of the plant were reduced by 480 employees.

Power inputs in the absolute values reduced within the year, which means that the whole growth of industrial production was achieved due to introduction of new efficient technologies and programs of conservation of the resourses. Owing to introduction of the efficiency programs, saving in the year 2006 constituted UAH 81 mln.

In 2006 in workshops of NKMZ 43 new machine tools with PNC and processing centers were installed. This allows increasing within one year productivity of the machine works by 15 %.

At present NKMZ numbers about 3.5 thou automated working places.

In 2006 NKMZ commissioned such important objects as TLS 3000 at Alchevsk Metallurgical Works (plate mill was at once brought to the design capacity), 64 ore mills, a ladle-furnace and a vacuumator were installed at EMSS (Kramatorsk, Donetsk region), a ladle-furnace and a machine for continuous casting of billets (MCCB) were installed at Omutninsk metallurgical plant in Kirov region (Russia). For the first time in practice of the enterprise, the installation for direct reduction of iron was developed and fabricated jointly with Dnepropetrovsk scientists. This invention was patented.

In 2007 NKMZ sets the task to produce products at UAH 2.5 bln and bring average salary up to UAH 2500. While in the year 2006 into development of the enterprise UAH 240 mln were invested, investments in the year 2007 will achieve UAH 380 mln. In the year 2007 NKMZ is going to purchase 26 new machine tools.

In the year 2007 two MCCB will be fabricated at NKMZ for the Novolipetsk Metallurgical Works, mill 2000 of the Magnitogorsk Metallurgical Works will be redesigned, three mixers of 600 t capacity for transportation of cast iron and six excavators will be produced. All this corresponds to strategic plan of the plant development till the year 2011.

Goal of the NKMZ strategy is to bring volume of production up to USD 1 bln and level of salary up to USD 1000.

MEASURING-DIAGNOSTIC COMPLEX «RESURS» FOR THERMAL INVESTIGATIONS OF BOILERS, BOILER EQUIPMENT AND PIPELINES

Proceeding from the state of economy of Ukraine and its energy resourses, prolongation of the service life of the operating energy equipment and reduction of heat losses through its heat-insulation structures is an actual issue. For timely detection of the heat loss places, operative control of heat-insulation characteristics of the materials, used in the repair-renovation works, and establishing correspondence of their actual values to the advertised ones the equipment for measuring heat losses and thermal resistance is necessary. For solution of this task scientists of the Institute of Engineering Thermophysics of the NAS of Ukraine, developed the universal measuring complex «Resurs». This development is based on the 50-year experience of designing instruments for direct measurements of the heat flux density, temperature, and thermal physical properties.

The computerized measuring complex «Resurs» is designed for determining heat losses of the energy

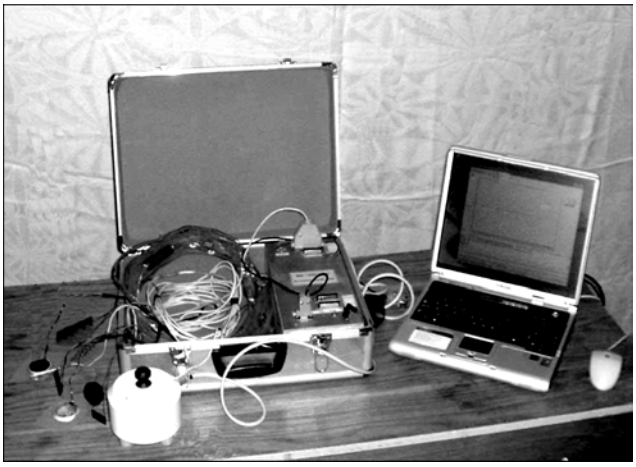

objects and thermal resistance and heat-conductivity factor of heat-insulation materials and coatings. It allows filling the instrumental niche of energy auditing. It is advisable to determine new normative values of heat losses of new hot-water boilers from external cooling.

EXPERT SYSTEM FOR CONTINUOUS MONITORING OF REAL STATE AND ENSURING INTEGRITY OF PIPELINES FOR THE PURPOSE OF PROLONGATION OF THEIR SERVICE LIFE

Main pipelines, which are linearly elongated decentralized industrial objects, experience in the process of their operation long repetitive-static loads, technogenic effect, and influence of the environment. Exactly these conditions of operation cause technological failures and in some cases serous accidents at the pipelines. Ensuring of reliable and efficient operation of the main pipeline system requires from the operator, in addition to increased industrial information, efficient and quality solution of both current and prospective tasks. In this connection many enterprises use in their operation technologies of geographic information systems. However, they fulfill information role and are not the tool for issue of the managerial decisions.

Scientists of the G.S. Pisarenko Institute for Problems of Strength of the NAS of Ukraine, have developed methodology and expert system for continuous monitoring of real state of the pipelines with application of the technology of risk-analysis as the most efficient strategy of ensuring reliability. The developed expert information-analytical system is designed for fulfillment of three main functions: integration of data (collection and storing of information on objects of the pipeline system, conditions of loading, calculations of pressure, etc.), calculation of risks (calculations of stressed-strained state of the pipelines, estimation of danger of the defects, calculation of probability of the defect failure, determination of social and economic aftereffects of the pipeline failure), and control of the risks (reduction of the risk by certain operation means). At present the system is being introduced in SC «Ukrtransgaz».

ESTIMATION OF STRENGTH OF THE NPP PIPELINES TAKING INTO ACCOUNT THEIR ACTUAL STATE, BY MEANS OF SOFTWARE COMPLEX «3D PipeMaster»

In analysis of the state of equipment of nuclear power plants (NPP) special attention is paid to performance of strength verification calculations of the pipelines, subjected to the complex loading (internal pressure, weight, temperature, and compensation loads). Complicated special configuration of the pipeline axis in combination with high degree of static indefinability makes this task rather complex. Presence of friction

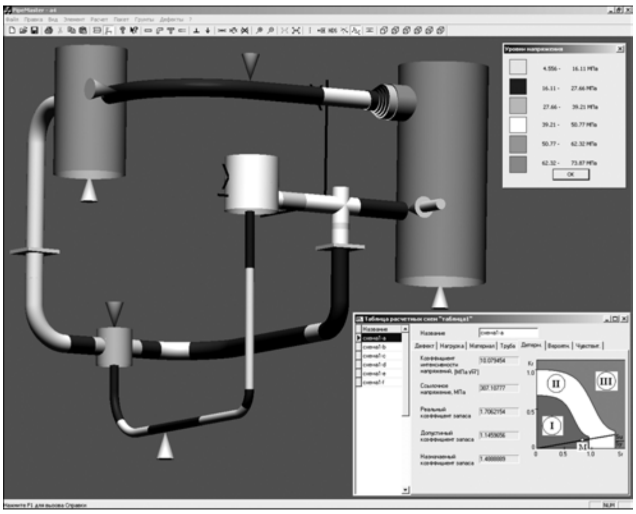

in the supports, which has to be taken into account according to the valid norms, brings us to the nonlinear problem that increases complexity of the calculations at least by one order.

In case of presence of a defect in the pipeline, further strength analysis is performed by considering the pipeline section as an envelope, located in the assigned global field of loading. State-of-the-art requirements to analysis of state of the NPP equipment assume availability of the computer programs, within the framework of which are envisaged:

- visualization of the computer portrait of the pipeline system;
- operative fulfillment of strength calculations in case of change of the operation conditions or the pipeline system;
- individual estimation of danger of the detected defects under real conditions of loading;
- storage and processing of these calculation results for making well-reasoned decisions relative residual service life of the pipeline, diagnostics volumes, periodicity and priority of the repair works.

Scientists of the G.S. Pisarenko Institute for Problems of Strength of the NAS of Ukraine, have developed methodological basis for design of the computer system for estimating real state, residual strength, and service life of complex special pipeline systems of the operating NPP.

Computer system and software complex «3D Pipe-Master» have been developed for estimating real state, residual strength, and service life of complex special pipeline systems, taking into account main loading factors and presence of defects. The method of initial parameters is used for calculation of the global stressed state of the pipeline system. Estimation of the defects is performed with application of the double-criterion approach, in which developed by the authors decisions are used for finding the calculated parameters. For storing the whole information on the pipeline special attention in the program is paid to creation of the general database.

ATLAS OF OPERATION DEFECTS IN HEAT EXCHANGE PIPES OF STEAM GENERATORS OF NPP POWER UNITS WITH REACTORS OF WWER TYPE

Group of scientists of NSC «Kharkov Physical-Technical Institute» of the NAS of Ukraine, have developed atlas of operation defects in heat exchange pipes of steam generators, detected and checked on the dismantled steam generator of South-Ukrainian NPP at various stages (in the steam generator, after cutting out, after decontamination). The defects were detected by the eddy-current check, systematized, and then investigated using metallographic method. Four types of the defects were established: corrosion pits, cracking, single cracks, corrosion spots. Physical nature of all types of the defects is determined as stress corrosion cracking. The difference is only in quantitative share of participation of the corrosion and the stresses. Such distribution of the defects by their types, which gives idea about their danger, is advisable when performing checking and plugging of defective pipes.

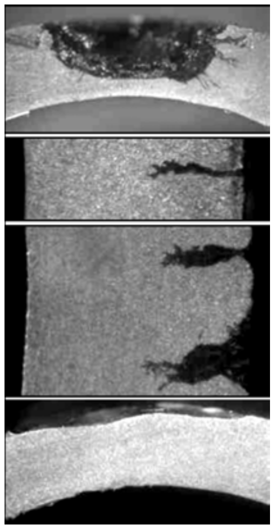

TV SENSOR SYSTEM FOR ESTIMATING GEOMETRIC PARAMETERS OF RAILWAY RAIL PROFILE

The basis for prolonging service life of railway tracks may be the results of the metrological measurements and non-destructive control of the rails. The complex of measures for determining state of the tracks includes separate measurements of geometry of each rail and distance between the rails. For quantitative measurement of geometry the rails are simulated in the form of lines in 3D space, which are then projected on 2D planes. After termination of the measurements each result, which represents interest or causes anxiety, is localized according to its actual position.

Technical means, used at present, most frequently represent sensors with mobile contacts, which are in constant contact with the rails. Geometric parameters of the track are determined by movement of the contacts. Such systems represent a significant progress in comparison with the manual measurement means. However, systems, in which contact sensors are used, have general disadvantage — they can not ensure sufficient accuracy of measurements when the track-test car moves at high speed, because under such con-

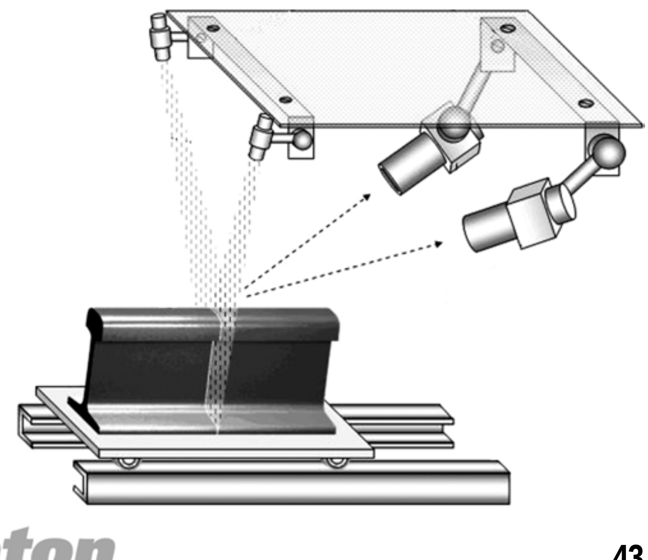

ditions constant contact of the sensors with the track is not preserved. That's why for obtaining required parameters of the track geometry it is most advisable to use means of the technical vision.

Specialists of the E.O. Paton Electric Welding Institute of the NAS of Ukraine, developed hardware and software means of the TV sensor system for automatic estimation of the profile geometry of the railway rails. Design solutions are suggested for sensor unit of the system, which includes two measurement optical channels, based on the method of laser triangulation. Methodology for calibration of the sensor unit by means of the flat rail gauge template, and software for presenting profile of the rails by two digital images have been developed.

Developed hardware and software means for the TV sensor system mockup may be used for designing commercial models of the system for automatic diagnostics of the railway track parameters.

ECOWELD SYSTEM

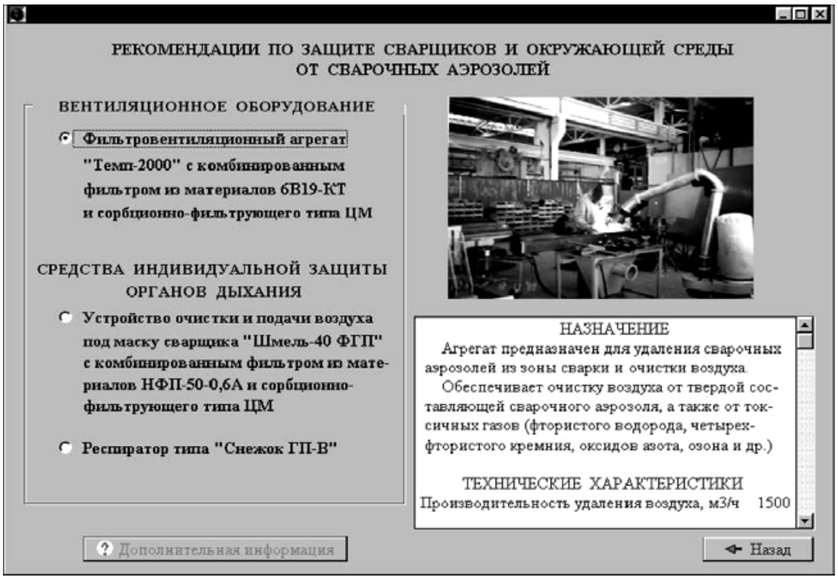

For presenting and processing the results of primary hygienic estimation of welding consumables and methods of welding in the E.O. Paton Electric Welding Institute the computer and information-search system of databases of hygienic characteristics of the welding aerosols (WA) ECOWELD has been developed, which consists of three databases: for coated electrodes, welding consumables for mechanized welding, and welding fluxes. In each database its peculiarities and characteristic factors, which effect the level, chemical composition, and toxicity of WA, are taken into account. Initial data, which are entered into this system, are the level of emissions and chemical composition of WA; the rest necessary for comprehensive environmental-hygienic estimation indices are displayed on the monitor screen and printed out in the form of a document. In addition, depending upon a grade of the welding consumable the information system issues recommendations on necessary protection means for the welders and the environment, based on hygienic and chemical classification of WA and methods of welding, in which they are formed.

THESIS FOR A SCIENTIFIC DEGREE

Priazovsky State Technical University (Mariupol)

V.A. Volkov defended on 20th of October 2006 candidate's thesis on topic «Development of Plasmatrons with Long Service Life for Processing of Disperse Materials».

The thesis is devoted to development of plasmatrons with long service life for processing of disperse materials. Plasma-technological processes with disperse substances acquire ever growing significance. Spraying, spheroidization, production of ultra-disperse powders of micron and sub-micron size, growing of single crystals, formation of condensation films — this is far from being complete list of their application. However, application in the plasmatrons of the plasma gas (air) and the mixture of air with oxygen and hydrocarbon gases caused, on one hand, increase of their power, and, on the other hand, sharp reduction of their service life.

Review of the known results of theoretical and experimental investigations, directed at application of plasmatrons for processing of the disperse materials, showed that their common disadvantages are short service life (up to 50 h), low thermal efficiency of a substance heating (30–40 %), low productivity (10–15 kg / h), and high power consumption (25–27 kW·h / kg). Proceeding from these shortcomings, the main directions of increasing efficiency of plasmatrons for processing of the disperse materials were determined. Search of the ways for solution of these issues allowed finding design solutions and conditions, enabling increase of the service life and efficiency of plasmatrons, and creating the latter with a hollow copper cylindrical cathode of 36 kW capacity, with the end thermochemical insert, the elongated inter-electrode insert (IEI) of 60 kW capacity, and the low-erosion cathode unit of 350 kW capacity. In the developed designs the methods for increasing service life and efficiency, due to forced distribution of the cathode and the anode tie of the arcs, the elongated IEI, and the low-erosion sectioned cathode unit, have been used for the first time, which allowed achieving in the plasmatron with a hollow cylindrical cathode service life more than 90 h at the arc current 300 A, and achieving at the arc current 600 A service life above 500 h in the plasmatron with the low-erosion cathode unit. In addition, in the plasmatrons of 36 and 60 kW capacity efficiency of processing of the disperse materials was increased due to superimposition of external electric disturbance on positive column of the arc. On the basis of known theoretical investigations theoretic basis of calculation of the plasmatrons was developed.

Significant part of experimental investigations is generalized in the form of diagrams and criteria dependencies, convenient for application in the engineering practice. For the purpose of practical demonstrating usefulness of the developed plasmatrons, plasma complexes for treating refractory surfaces of chemical-metallurgical equipment, strengthening of oxygen lances, and producing oxygen and oxygen-free powders were developed. The mathematical model and the algorithm for calculation of plasma dispersion of a powder were developed, which are the simplest of all known models, concerning heating of particles in active zone of the jet, and describe sufficiently well process of a particle heating up to the melting point of the material. Developed plasmatrons are used in treatment of refractory materials, renovation of the worn automotive units and components, removal of defects from surface of the roll necks, and in a number of other production processes.

CONFERENCE ON PROBLEMS OF RESIDUAL SERVICE LIFE AND SAFE OPERATION OF STRUCTURES, CONSTRUCTIONS AND MACHINES

Summing-up Scientific Conference dedicated to analysis of scientific and applied results received during 2004--2006 when performing projects under the Integrated National Program «Problems of the Residual Service Life and Safe Operation of Structures, Constructions and Machines», took place at PWI on January 12, 2007. Scientific leaders and performers of the projects, as well as representatives from interested ministries, departments, educational and branch institutions, industrial enterprises and organizations participated in the work of the Conference.

The Conference opened by academician B.E. Paton, President of the National Academy of Sciences of Ukraine, who noted the importance of the residual service life problem and determination of scientifically based terms of extension of safe operation for critical objects. Emphasizing the comprehensive nature of the Program, which consists of 8 sections and 107 projects, academician B.E. Paton said that 22 institutions from 8 divisions of NASU participated in its realization.

Scientific leaders of Program Sections addressed the plenary session.

Academician V.I. Makhnenko, scientific leader of the Section «Development of methodological basis of technical condition evaluation and validity of safe term of operation for structural elements of high-risk objects in the territory of Ukraine», reported in his presentation, that urgent studies on risk-analysis of violation of the main functions of nuclear power engineering equipment, main pipelines, metallurgical equipment and constructions, operated under complex mining and geological conditions, were done in the Section.

Academician Z.T. Nazarchuk, scientific leader of the Section «Development of methods and new technical means of nondestructive testing and diagnostics of the condition of materials and products in long-term operation», noted in his speech that an effective system of monitoring, new tools of nondestructive quality control for a number of vitally important objects were created, and a new diagnostic equipment was prepared for serial production.

V.I. Pokhmursky, Corresp. Member of the NAS of Ukraine, scientific leader of the Section «Development of corrosion protection methods for structural elements of long-term operation objects», noted that new domestically produced primer inhibited by modified pigments, was developed for pipeline protection at the outlet from gas compressor stations, which application increases the operating time 1.5--1.8 times, and new sparsely-alloyed alloys were developed on the basis of commercial purity aluminium for protection from corrosion and for extension of the service life of the equipment of heat- and hydro PP, and main pipelines.

In the report by academician I.M. Neklyudov, scientific leader of the Section «Development of effective methods of evaluation and extension of service life of nuclear power engineering objects», it was emphasized that the main part of the Section projects was carried out with participation of NPP of Ukraine. The system of monitoring the properties of reactor body metal in power unit No.4 the of the Rovno NPP in the process of operation by reference samples was designed and realized within the framework of the Section. Fundamental technology of mechanized welding of the main circuit pipe elements was designed at replacement of PGV-1000M type steam generator to extend the NPP residual service life, and normative documents were approved and validation of the technology was carried out.

Academician B.S. Stogny, summing up the investigations in the Section «Increase of reliability and extension of service life of power equipment and systems», noted that important results were obtained that will be used for increasing the reliability and extension of service life of turbines, generators, gas pumping unit equipment, as well as in upgrading boiler equipment of municipal power engineering and coal power units. The main measures for extension of the service life of boiler equipment elements for decentralized thermal power engineering were formulated and substantiated due to the conducted investigations.

A.Ya. Krasovsky, Corresp. Member of the NAS of Ukraine, scientific leader of the Section «Creation of systems for monitoring the technical condition of pipelines and objects of gas and petroleum refining industry», informed about the scientific results received in the Section. He mentioned creation of procedural approaches to evaluation of probable parameters of defects in pipelines and their use in risk-analysis problems, mathematical model of fatigue failure of materials at biaxial and bicyclic loadings, expert system of monitoring the technical condition of the main pipelines, taking into account their actual operating conditions, as the most important achievements. It was noted that the developed electrochemical methods of active monitoring of the corrosion state were tried out when surveying the main gas pipeline «Urengoj–Pamary–Uzhgorod».

Academician L.M. Lobanov presentation was dedicated to the results obtained in the Program Section «Increase of reliability and extension of service life of bridges, building, industrial and transport constructions». In particular, the main factors of early damage accumulation in welded components and metal structure joints of bridge spans were found, and high efficiency of high-frequency mechanical peening application for extension of their service life was determined.

Modern methods of investigation were used to establish the peculiarities of technological factors influence on residual stresses formation in welded joints, their resistance to delayed and brittle fracture.

Application of local high-density current pulse for stress relaxation in the joint by electron speckle-interferometry method allows creating a new nondestructive technology for effective determination of residual stresses in different metallic materials.

Micro-alloyed steel was designed and found its application in industry for manufacturing high-strength railway wheels, their maintenance tests demonstrating their high wear resistance.

Technology that provided high water and cold resistance of reinforced concrete structures and, hence, extension of their service life was designed on the basis of polymer and polymer mineral materials.

Results obtained under the projects of the Section «Development of technologies for repair and reconditioning of structural elements of higher-risk objects to extend the term of their operation» were presented by academician K.A. Yushchenko. He noted that new materials and technologies were developed for repair welding and surfacing of equipment and parts of oil and gas transportation systems, for metallurgical, mining and shipbuilding industries and power engineering. Many developments have already found their industrial application. In particular, the technology of gas turbine blade repair, providing a 40–70 % increase of their service life, was created and implemented in «Ukrtransgaz» facilities. The developed new welding consumables were used in repair of tanks for storage of concentrated sulphuric acid at the East Ore Mining and Processing Enterprise.

Academician V.V. Panasyuk, scientific leader of the Program Section «Preparation and issuing of normative documents and scientific-engineering manuals on evaluation of the residual life of long-term operating objects», noted in his speech that during 2004–2006 modern scientific-engineering reference manuals were prepared and published to assist the engineers and technicians of design and industrial enterprises in evaluation of the fatigue life and reliability (residual service life) of elements of long-term operating constructions, in particular, bridge and building structures, heat and nuclear PPs, pipelines and so on. Five new standards and normative documents for evaluation of the reliability and residual life of structures were developed, as well as instruments for non-destructive testing and diagnostics of metal products and welded joints.

Discussion of the received scientific results described in the reports of Program Section scientific leaders took place in the plenary session. P.I. Krivosheev, V.N. Gordeev, I.M. Dmitrakh, Doctors of Sci. (Eng.), and A.Ya. Krasovsky, Corresp. Member of NAS of the Ukraine, and others participated in the discussion.

Conference participants, noting the urgency of the received results for solving the problem of service life of long-term operating objects, expressed their opinion about the rationality of continuing fulfillment of the Program «Problems of residual service life and safe operation of structures, constructions and machines» in 2007–2009.

The following directions were named as priorities:

• development of the processes of mathematical modeling of deformation and degradation of properties of structural materials and welded joints during their long-term operation with the aim of prediction of the residual service life of structures with damage;

• creation of effective methods, technical procedures, technologies for diagnostics and extension of service life of heat and nuclear power plant equipment, oil and gas pipelines, gas and petroleum processing facilities, bridges, building, industrial and transportation, in particular, aircraft structures;

• effective application of nondestructive methods and techniques for evaluation of structure stressed states and physical-mechanical properties of materials in service;

• creation of continuous monitoring systems of critical objects in long-term operation using modern information technologies;

• development of modern technologies and materials for the repair of objects in long-term operation and corrosion protection of metal structures;

• preparation of normative documents on evaluation and extension of service life of long-term operating objects.

When forming the projects for the following period, it is rational to include into this Program integrated large-scale projects on priority directions of studies of the problems of extension of service life of important and ecologically dangerous objects.

During the work of the Conference, an exhibition of the instruments and equipment, designed when carrying out the Program projects was organized, and summary collection of papers containing the basic scientific and applied results of the work over the reporting period was presented.

A.V. Babaev, Dr. of Eng. Sci., PWI
A.T. Zelnichenko, Dr of PhMath. Sci., PWI

TO CENTENARY OF S.P. KOROLYOV'S BIRTH

January 2007 marked 100th anniversary of the birth of S.P. Korolyov — the scientist, designer of space rocket systems, academician, twice Hero of Socialist Labour, Lenin Prize laureate. His name is written forever in the history of mankind. S.P. Korolyov led the development and launching of ballistic and geophysical rockets, rocket-carriers and space vehicles «Vostok», «Voskhod», satellites of «Elektron», «Molniya», and «Kosmos» series, the first automatic interplanetary stations «Zond». Space rocket systems created under his supervision enabled making flights to the Moon, Venus, Mars.

The ceremony of S.P. Korolyov's monument opening (designed by N.A. Olejnik, Merited Artist and Sculptor of Ukraine) took place in Museum Square of NTUU «Kiev Polytechnic Institute» campus. It was at KPI that the future scientist gained theoretical knowledge and applied it in his first engineering developments during two years (1924–1926). Inauguration of the monument was entrusted to S.P. Korolyov's daughter — Nataliya S. Korolyova. Prof. B.E. Paton, President of the NAS of Ukraine, director of the E.O. Paton Electric Welding Institute, who worked in close and effective collaboration with S.P. Korolyov for many years, as well as D.I. Tabachnik, vice-Premier of Ukraine, S.N. Nikolaenko, Minister of education and science of Ukraine; M.Z. Zgurovsky, Rector of NTUU «KPI»; A.A. Zinchenko, Assistant of the President of Ukraine; A.I. Martynyuk, the first Deputy Speaker of Verkhovna Rada of Ukraine; V.S. Chernomyrdin, Ambassador of the Russian Federation in Ukraine; P.R. Popovich, USSR space pilot, pupil of S.P. Korolyov, twice Hero of the Soviet Union, Hero of Labour; Yu. Alekseev, General Director of the National Space Agency of Ukraine; scientists, lecturers and students of NTUU «KPI», as well as grandsons and great-grandsons of S.P. Korolyov, took part in the opening ceremony. At the opening of the monu-

ment the speakers marked S.P Korolyov's outstanding achievements in the field of space exploration, expressing their deep respect and admiration of his great talent.

When the opening ceremony was over, official meeting dedicated to S.P. Korolyov's memory was held in the palace of culture and arts of NTUU «KPI», where Viktor A. Yushchenko, President of Ukraine; A.A. Moroz, Head of Verkhovna Rada of Ukraine; V.F. Yanukovich, Prime Minister of Ukraine; friends and companions of S.P. Korolyov made their speeches. N.S. Korolyova told about the hard life and great achievements of her father. It is remarkable that carrier rocket «Soyuz-U» with cargo transport ship «Progress-M59» was launched on the same day from Bajkonur space-launching site. The launching was dedicated to the centenary of academician S.P. Korolyov birth.

At the end of the evening N.S. Korolyova thanked the National Academy of Sciences, Verkhovna Rada of Ukraine, administration of NTUU «KPI» for remembering her father, and noted that she believes that the greatest demonstration of respect for S.P. Korolyov is continuation of space research, and suggested that there maybe other great future scientists among the NTUU «KPI» students who will right new pages in the history of cosmonautics.

E. Lopatkina, Master of Sci.

MATERIALS, TECHNOLOGIES AND EQUIPMENT FOR PLASMA POWDER CLADDING

Iron-, nickel-, cobalt- and copper-base powders, as well as technologies and equipment were developed for plasma powder cladding of parts of different machines and mechanisms.

Nickel- and cobalt-base powders are applied for cladding of parts of different-application fixtures, internal combustion engine valves and seats, etc. High-carbon powders of iron-base alloys of the PG-S1 and PG-AN1 grades are intended for cladding of parts operating under conditions of intensive abrasive wear, e.g. tools of cultivating and earth-moving machines and components of fittings for pulp feed lines. Powder PR-10R6M5 is intended for cladding of cutting tool billets, dies and different process fixtures. Powders PR-17Kh5V3MF5S and PR-22Kh6VMF8S are applied for cladding of die tools for hot and cold forming, and powders PR-25Kh5FMS and PR-30Kh4V2M2FS ---- for hot rolls, dies and knives for cutting hot metal. Powder PR-22Kh16N3M is successfully used instead of powders of nickel- and cobalt-base alloys for cladding different-application fitting components. Copper-base alloys serve for cladding of friction pair components and repair of marine fixture parts made from non-ferrous alloys.

Specifications of plasma powder cladding machines

Parameter	Type of machine	
	Ob-2184	UP-142
Application	Versatile	Cladding of fixture components
Cladding current, duty-cycle 100 %, A, not more than	400	300
Additive powder feed speed, kg/h	0.35--15	0.35--15
Device travel speed, m/h	3--6	--
Chuck plate rotation speed, rpm	0.1--5	0.08--5
Plasmatron oscillation amplitude, mm	25	25
Plasmatron oscillation frequency, 1/min	20--120	20--120
Gas flow rate, l/min, not more than	20	20
Plasmatron cooling	Water	Water, independent
Dimensions, mm	1800 × 1160 × 1850	1500 × 1000 × 1200
Weight, kg	800	400

Plasma powder cladding is performed using versatile machine Ob-2184 and specialised machine UD-142, the latter being intended for cladding fixture components.

Application. Cladding of power generation, petrochemical and general-engineering fixture components, internal combustion engine valves and seats, metal cutting tools, etc.

Proposals for co-operation. Application of the plasma powder cladding technology and equipment at a customer's.

Dr. Ryabtsev I.A.
E-mail: ryabtsev@paton.kiev.ua